



QA: NA

LSA-AR-037 REV 00

May 2009

## **Inputs to Jason Associates Corporation in Support of the Postclosure Repository Supplemental Environmental Impact Statement**

LSN DETERMINATION HAS BEEN CHANGED TO LSN-RELEVANT ON 6/5/09.

Prepared for:  
U.S. Department of Energy  
Office of Civilian Radioactive Waste Management  
Office of Repository Development  
1551 Hillshire Drive  
Las Vegas, Nevada 89134-6321

Prepared by:  
Sandia National Laboratories  
OCRWM Lead Laboratory for Repository Systems  
1180 Town Center Drive  
Las Vegas, Nevada 89144

Under Contract Number  
DE-AC04-94AL85000





# Postclosure Analysis Report Signature Page/Change History

QA: NA  
Page 1 of 106

*Complete only applicable items.*

1. Document Title  
Inputs to Jason Associates Corporation in Support of the Postclosure Repository Supplemental Environmental Impact Statement

2. Identifying Number (Including Revision No.)  
LSA-AR-037 REV 00

3. Analysis Type:      Diagnostic Analysis      Interim Analysis

	Printed Name	Signature	Date
4. Originator	Ming Zhu	<i>Robert MacKinnon for</i>	<i>05-18-09</i>
5. Checker	Teklu Hadgu	<i>Teklu Hadgu</i>	<i>05/18/09</i>
	Elena Kalinina	<i>Ramuncea</i>	<i>05/19/09</i>
	N/A		
6. Responsible Manager	Robert MacKinnon	<i>Robert MacKinnon</i>	<i>05-18-09</i>

7. Remarks

### Change History

8. Revision No.	9. Description of Change
REV 00	Initial Issue

SCI-PRO-009.2-R2

INTENTIONALLY LEFT BLANK

# CONTENTS

	<b>Page</b>
1 INTRODUCTION .....	1
2 INPUT AND SOFTWARE .....	1
3 EVALUATION .....	3
3.1 MODIFICATION OF THE DEATH VALLEY REGIONAL GROUNDWATER FLOW MODEL .....	6
3.2 ESTIMATION OF RADIONUCLIDE PLUME AT THE ACCESSIBLE ENVIRONMENT .....	10
3.3 PARTICLE TRACKING ANALYSIS FOR CURRENT CONDITIONS .....	11
3.4 ESTIMATION OF SPECIFIC DISCHARGE AND FLOW PATHS FOR FUTURE CLIMATIC CONDITIONS .....	12
3.5 CALCULATION OF RADIONUCLIDE MASS RELEASE RATES FROM THE TSPA-LA .....	12
3.6 EVALUATION OF BREAKTHROUGH CURVES FOR NONRADIOLOGICAL CONTAMINANTS .....	17
3.7 NOTE ON ANALYSIS FOR COMPARISON TO GROUNDWATER PROTECTION STANDARD .....	17
4 ANALYSIS RESULTS AND CONCLUSIONS .....	18
4.1 SIMULATED FLOW FIELDS .....	18
4.2 ESTIMATED RADIONUCLIDE PLUME AT THE ACCESSIBLE ENVIRONMENT .....	38
4.3 RESULTS OF PARTICLE TRACKING ANALYSIS FOR PRESENT-DAY CONDITIONS .....	38
4.4 ESTIMATED SPECIFIC DISCHARGE AND FLOW PATHS FOR FUTURE CLIMATIC CONDITIONS .....	51
4.5 CALCULATED RADIONUCLIDE MASS RELEASE RATES FROM THE TSPA-LA .....	58
4.6 SELECTED BREAKTHROUGH CURVES FOR NONRADIOLOGICAL CONTAMINANTS .....	60
4.7 RESULTS OF ANALYSIS TO COMPARE TO GROUNDWATER PROTECTION STANDARD .....	65
5 REFERENCES .....	69
5.1 DOCUMENTS CITED .....	69
5.2 REGULATIONS CITED .....	72

INTENTIONALLY LEFT BLANK

## FIGURES

	<b>Page</b>
1a. Geographic and Prominent Topographic Features of the Death Valley Regional Groundwater Flow System .....	5
1b. Measured Water Levels in Devils Hole (AM-4).....	9
2. Cumulative releases of <sup>14</sup> C from the Unsaturated Zone: (a) Expected Values Calculated by EXDOC_LA; and (b) Unweighted Values Calculated by GoldSim.....	16
3. Layer 1 Hydraulic Heads for (a) Case 1 (pre-pumping) and (b) Case 2 (pumping).....	19
4. Layer 2 Hydraulic Heads for (a) Case 1 (pre-pumping) and (b) Case 2 (pumping).....	20
5. Layer 3 Hydraulic Heads for (a) Case 1 (pre-pumping) and (b) Case 2 (pumping).....	21
6. Layer 4 Hydraulic Heads for (a) Case 1 (pre-pumping) and (b) Case 2 (pumping).....	22
7. Simulated Layer 1 Hydraulic Heads for Case 3 (reduced pumping conditions) .....	24
8. Simulated Hydraulic Heads and Drawdowns at the Devils Hole “Copper Washer” Datum: (a) Case 4 Hydraulic Head; (b) Case 4 Drawdown; (c) Case 5 Hydraulic Head; and (d) Case 5 Drawdown .....	25
9a. Simulated Vertical Hydraulic Gradient between the Carbonate Aquifer (or Deeper Crystalline Units) and the Water Table for Case 5 for Year 2016.....	28
9b. Simulated Vertical Hydraulic Gradient between the Carbonate Aquifer (or Deeper Crystalline Units) and the Overlying Volcanic Aquifer for Case 5 for Year 2016 .....	29
9c. Simulated Vertical Hydraulic Gradient between the Carbonate Aquifer (or Deeper Crystalline Units) and the Water Table for the Pre-pumping Condition (Stress Period 1 from Case 5) .....	30
9d. Simulated Vertical Hydraulic Gradient between the Carbonate Aquifer (or Deeper Crystalline Units) and the Overlying Volcanic Aquifer for the Pre-pumping Condition (Stress Period 1 from Case 5) .....	31
9e. Simulated Vertical Hydraulic Gradient between the Carbonate Aquifer (or Deeper Crystalline Units) and the Water Table for Case 5 for Year 2453.....	32
9f. Simulated Vertical Hydraulic Gradient between the Carbonate Aquifer (or Deeper Crystalline Units) and the Overlying Volcanic Aquifer for Case 5 for Year 2453 .....	33
9g. Vertical Hydraulic Gradient between the Carbonate Aquifer (or Deeper Crystalline Units) and the Water Table as a Function of Time (Case 5) .....	34
10. Locations of Particles Released from below the Repository and Tracked with FEHM’s SPTR Routine at the Accessible Environment Boundary.....	38
11a. Simulated Hydraulic Heads and Groundwater Flow Paths for the Pre-pumping Case (Case 1).....	42
11b. Simulated Horizontal and Vertical Groundwater Flow Paths for the Pre-pumping Case (Case 1) .....	43
12. Histogram of Specific Discharges for the 8,024 Particles Released at the Accessible Environment Boundary for the Pre-pumping Case (Case 1) .....	44
13a. Simulated Hydraulic Heads and Groundwater Flow Paths for the 2003 Estimate of Long-Term Pumping Rates (Case 2) .....	46
13b. Simulated Horizontal and Vertical Groundwater Flow Paths for the 2003 Estimate of Long-Term Pumping Rates (Case 2).....	47
14. Histogram of Specific Discharges for the 8,024 Particles Released at the Accessible Environment Boundary for the 2003 Estimate of Long-Term Pumping Rates (Case 2) .....	48

15a. Simulated Hydraulic Heads and Groundwater Flow Paths for the Reduced Estimate of Long-Term Pumping Rates (Case 3).....	50
15b. Histogram of Specific Discharges for the 8,024 Particles Released at the Accessible Environment Boundary for the Reduced Estimate of Long-Term Pumping Rates (Case 3).....	51
16. Locations of Lakes and Regional Springs from D’Agnese et al. (1998 [DIRS 103006]) .....	54
17. Locations of Lakes and Regional Springs from Belcher (2004 [DIRS 173179]).....	55
18. Paleodischarge Deposits and Active Springs in the Yucca Mountain Region, Nevada .....	57
19. Distribution of Drains and Constant Head Cells Simulated as Discharging during Past Climate Conditions in the DVRFS Model .....	58
20. Fraction of Mean Cumulative Unsaturated Zone Release in 1,000,000 Years by Radionuclide .....	60
21. Cumulative Distribution Function of Sampled $K_d$ for Selenium in Volcanic Rocks and Alluvium .....	62
22. Cumulative Distribution Function of Sampled $K_d$ for Uranium in Volcanic Rocks and Alluvium from the Saturated Zone Flow and Transport Abstraction Model.....	63
23. Simulated Breakthrough Curves in the Saturated Zone for Molybdenum, Vanadium, and Nickel .....	64

## TABLES

	<b>Page</b>
1. Inputs Used in this Analysis .....	1
2. Software Used in this Analysis.....	2
3. Summary of Nomenclature and File Names Used.....	7
4. Local and UTM Coordinates for the DVRFS Model .....	11
5. TSPA-LA Model Time-Step Schedule for the Ground Motion, Drip Shield Early Failure and Waste Package Early Failure Modeling Cases .....	13
6. Simulated Hydraulic Head at the Approximate Locations of Well UE-25 p#1 and Well NC-EWDP-19D .....	35
7. Simulated Drawdown Relative to Pre-pumping Conditions at the Approximate Locations of Well UE-25 p#1 and Well NC-EWDP-19D.....	35
8. Simulated Hydraulic Gradients at the Approximate Location of Well UE-25 p#1 and Between the Location of Well UE-25 p#1 and Well NC-EWDP-19D.....	35
9. Average Flow Path Lengths and Expected Transport Model Parameter Values in Hydrogeologic Units (Pre-pumping Case) .....	44
10. Average Flow Path Lengths and Expected Transport Model Parameter Values in Hydrogeologic Units (Long-Term Pumping Case) .....	48
11. Specific Discharge Estimates.....	51
12. Estimates of Mean Annual Ground-Water Discharge from Major Evapotranspiration-Dominated Discharge Areas in Death Valley Regional Ground-Water Flow System Model Domain .....	56
13. Radioelements Transported as Solutes in the Saturated Zone Flow and Transport Abstraction Model .....	61
14. Groundwater Protection Regulation Limits and Radionuclides Used in Analyses .....	65

INTENTIONALLY LEFT BLANK

## ACRONYMS

DIRS	Document Input Reference System
DVRFS	Death Valley Regional Flow System
DTN	Data Tracking Number
EBS	Engineered Barrier System
NRC	U.S. Nuclear Regulatory Commission
TSPA	total system performance assessment
TSPA-LA	total system performance assessment for the license application
UTM	Universal Transverse Mercator
SEIS	Supplemental Environmental Impact Statement
SNL	Sandia National Laboratories
SNWA	Southern Nevada Water Authority

## ABBREVIATIONS

ft	feet
g	gram
gpm	gallons per minute
L	liter
mL	milliliter
m	meter
mrem	millirems
yr	year

INTENTIONALLY LEFT BLANK

## ACNOWLEDGEMENT

The following individuals contributed to the modeling analyses and documentation of this report: Ming Zhu (overall technical lead and MODFLOW and MODPATH model development), Scott James (radionuclide plume at the accessible environment, flow simulations, and particle tracking analyses), Bill Arnold (nonradiological contaminants, paleosprings discharge data, and groundwater protection standard), Pat Lee (TSPA source release rates for radionuclides), and Susan Altman (paleosprings discharge data and report preparation). Tim Vogt and Jeff Gromney assisted with the preparation of the base maps and the scaling of MODPATH-generated DXF files for Figures 3 through 7.

Elena Kalinina performed the checking of earlier drafts of the report. Teklu Hadgu completed the checking of the breakthrough curves for nonradiological materials, files for MODFLOW simulation Cases 3 through 5, and the final report.

Claudia Faunt of the U.S. Geological Survey San Diego provided input files *mnw\_dvrf pub\_03.txt* and *wel\_irr\_ret\_pub\_03.txt* for the simulation of the pumping case, and performed a review of the MODFLOW and MODPATH files for simulation Cases 1 and 2. Her contribution to this analysis is documented in Appendix A.

Wayne Belcher of the U.S. Department of Energy provided technical guidance to the development of this product.

INTENTIONALLY LEFT BLANK

# 1 INTRODUCTION

This report presents a summary of the inputs provided to Jason Associates Corporation in support of the Postclosure Repository Supplemental Environmental Impact Statement (SEIS-3). In September 2008, the U.S. Nuclear Regulatory Commission (NRC) released *U.S. Nuclear Regulatory Commission Staff's Adoption Determination Report for the U.S. Department of Energy's Environmental Impact Statements for the Proposed Geologic Repository at Yucca Mountain* (NRC 2008 [DIRS 186113]). Jason Associates Corporation, the organization primarily responsible for preparation of SEIS-3, has requested assistance from the Lead Laboratory. Ten tasks, including a final report, were conducted to provide Jason Associates Corporation with: (1) information regarding groundwater flow paths and discharges in the central and southern Death Valley subregions beyond the 18-km accessible environment, (2) information from TSPA-LA results regarding radionuclide mass release rates, (3) breakthrough curves that will assist the nonradiological contaminant modeling, (4) an estimate of the cross section of the plume at the 18-km accessible environment, and (5) an explanation of the total system performance analysis for the license application (TSPA-LA) groundwater protection analysis.

This report has been prepared in accordance with SCI-PRO-009, *Postclosure Analysis Reports* and the analysis outline *Work in Support of the Postclosure Repository Supplemental Environmental Impact Statement (SEIS-3)* (AO-037). During the execution of AO-037, additional groundwater flow simulations, as noted in Section 3.1, have been performed as directed by the U.S. Department of Energy (DOE). Model files generated as part of this work are archived in the AO-037 folder of the Lead Laboratory SharePoint site.

# 2 INPUT AND SOFTWARE

This analysis uses data from the TSPA-LA (including its supporting process and component models) and the Death Valley regional groundwater flow model (Belcher 2004 [DIRS 173179]).

Table 1 lists inputs used in this analysis and provides explanations for appropriate use of unqualified data.

Table 1. Inputs Used in this Analysis

Section	Input	DIRS Number
3.1	Death Valley Regional Groundwater Flow System Model	173179
3.2	Site-scale Saturated Zone Transport Model	184806
3.3	Results from Sections 4.1 and 4.2	—
3.4	Results from Section 4.3.and Saturated Zone Flow and Transport Abstraction Model	183750
3.5	TSPA Model	183478, 183751, 183752
3.6	Saturated Zone Flow and Transport Abstraction Model	183750
3.7	NA	—

NOTE: DIRS = Document Input Reference System.

Table 2 lists software used for this analysis. In addition, post-processing codes were written in Intel Visual Fortran version 11.0.066 to extract heads and particle-track information from flow models as described in Sections 3.2, 3.3, and 4.1. Furthermore, off-the-shelf software products Microsoft Excel 2007 and SURFER 8 were also used for post-processing model outputs described in Sections 3.1, 3.2, and 4.1.

Table 2. Software Used in this Analysis

Section	Software Name and Version	DIRS Number	Software Tracking Number	Platform Used
3.1	MODFLOW 2000 V.1.13.00	NA	NA	Windows XP
3.1	MODFLOW 2000 V.1.18.00	NA	NA	Windows XP
3.1	MODFLOW 2005 V1.5.00	NA	NA	Windows XP
3.2	18km.F90 18km-spdis.F90	NA	NA	Windows XP
3.3	MODPATH V. 5.0	NA	232	Windows XP
3.4	Not Applicable	—	—	—
3.5	CWD v2.0	162809 181037	10363-2.0-00 10363-2.0-01	Windows 2000 Windows 2003
3.5	EXDOC_LA v2.0	182102	11193-2.0-00	Windows 2000 Windows 2003
3.5	FEHM v2.26	185792	10086-2.26-00	Windows 2000 Windows 2003
3.5	GetThk_LA v1.0	181040	11229-1.0-00	Windows 2000 Windows 2003
3.5	GoldSim v9.60.300	184387	10344-9.60-03	Windows 2000 Windows 2003
3.5	InterpZdll_LA v1.0	167885 181043	11107-1.0-00 11107-1.0-01	Windows 2000 Windows 2003
3.5	MFCP_LA v1.0	167884 181045	11071-1.0-00 11071-1.0-01	Windows 2000 Windows 2003
3.5	MkTable_LA v1.0	181047 181048	11217-1.0-00 11217-1.0-01	Windows 2000 Windows 2003
3.5	PassTable1D_LA v2.0	181051	11142-2.0-00	Windows 2000 Windows 2003
3.5	SCCD v2.01	181157 181054	10343-2.01-00 10343-2.01-01	Windows 2000 Windows 2003
3.5	SEEPAGEDLL_LA v1.3	180318 181058	11076-1.3-00 11076-1.3-01	Windows 2000 Windows 2003

Table 2. Software Used in this Analysis (continued)

Section	Software Name and Version	DIRS Number	Software Tracking Number	Platform Used
3.5	SZ_Convolute v3.10.01	181060	10207-3.10.01-00	Windows 2000 Windows 2003
3.5	TSPA_Input_DB v2.2	181061 181062	10931-2.2-00 10931-2.2-01	Windows 2000 Windows 2003
3.5	WAPDEG v4.07	181774 181064	10000-4.07-00 10000-4.07-01	Windows 2000 Windows 2003
3.6	NA	—	—	—
4.1	DVRFS-vgrad.F90 DH_head.F90	—	—	Windows XP
4.3	xtract_path_LCA.for	NA	NA	Windows XP
4.3	xtract_path_LCA_count.for	NA	NA	Windows XP
4.3	HGUloc.F90 HGU_name.F90	NA	NA	Windows XP

NOTE: DIRS = Document Input Reference System.

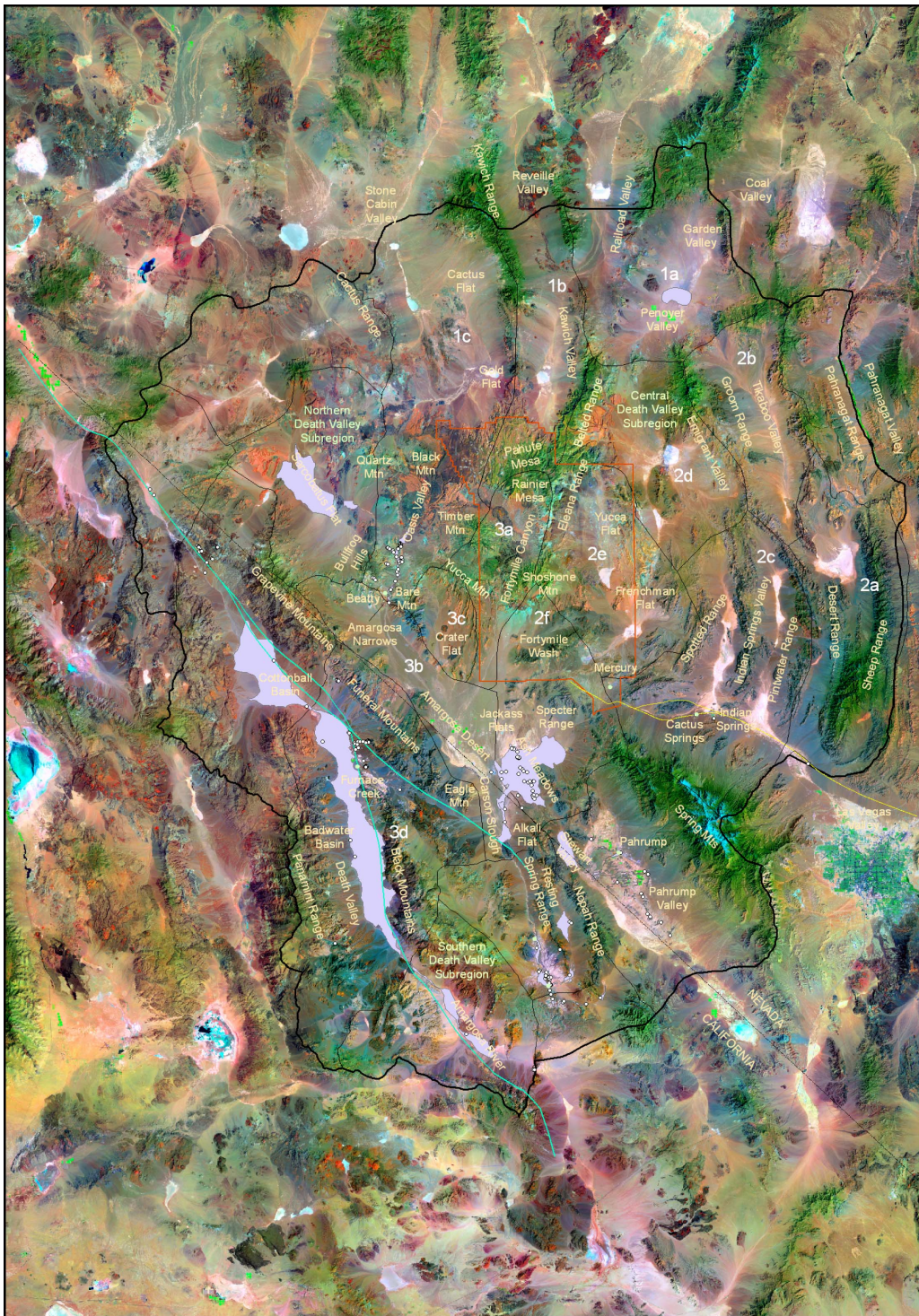
### 3 EVALUATION

This report documents the development of the inputs that have been transmitted to Jason Associates Corporation for the purpose of developing responses to NRC requests for SEIS supplementations (SEIS-3). This section describes the methodologies used for developing these inputs, followed by a summary of the results in Section 4. The analyses include the development of the steady-state flow fields between the accessible environment and points of interest to groundwater discharge (Section 3.1), the estimated radionuclide plume at the accessible environment (Section 3.2), the analysis of groundwater flow paths and flow rates for the present-day climatic condition (Section 3.3), and the estimated flow paths and flow rates for future wetter climates (Section 3.4). In addition, Section 3.5 describes the calculation of radionuclide mass release rates from the TSPA-LA, Section 3.6 discusses a qualitative assessment of breakthrough characteristics of nonradiological contaminants based on similar radionuclide breakthroughs simulated with TSPA-LA, and Section 3.7 documents the methods used in TSPA-LA for calculating groundwater quality parameters for comparison to the groundwater protection standard.

To facilitate the discussion of results from this analysis, Figure 1a shows the subbasins, sections, and geographic and prominent topographic features of the Death Valley regional groundwater flow system (DVRFS). The DVRFS region encompasses approximately 100,000 km<sup>2</sup> in Nevada and California and is bounded by latitudes 35°00'N and 38°15'N and by longitudes 115°00'W and 118°00'W. The DVRFS region is in the southern Great Basin, a subprovince of the Basin and Range physiographic province. The region includes several large valleys, including the Amargosa Desert, Pahrump Valley, and Death Valley; and also includes several major mountain ranges (Belcher 2004 [DIRS 173179], pp. 9 and 11).

The DVRFS region is underlain by a sequence of basin fill, volcanic rocks, and a principal carbonate aquifer. The thick sequence of Paleozoic carbonate rock extends throughout the subsurface of much of central and southeastern Nevada and crops out in the eastern one-half of the region. Fractured Cenozoic volcanic rocks in the vicinity of the Nevada Test Site (NTS) and permeable Cenozoic basin fill throughout the region locally are important aquifers that interact with the regional flow through the underlying Paleozoic carbonate rocks. Stratigraphic units in the region are disrupted by large-magnitude offset thrust, strike-slip, and normal faults (Belcher 2004 [DIRS 173179], p. 27).

The DVRFS is divided into the northern, central, and southern subregions and a number of basins and sections within each basin (Belcher 2004 [DIRS 173179], Figure D-5). The region receives recharge through precipitation in the mountains and lateral flow through the carbonate aquifer, and discharges through seeps and springs, evapotranspiration, groundwater pumpage, and lateral flow (Belcher 2004 [DIRS 173179], p. 142). Most of the basins seldom contain perennial streams or other surface-water bodies (Belcher 2004 [DIRS 173179], p. 11). The Amargosa River drains Yucca Mountain and surrounding areas to Death Valley. The nearest impoundments to Yucca Mountain are Ash Meadows, which drains to the Amargosa River through Carson Slough (DOE 2008 [DIRS 180751], p.3-26).



NOTES: For illustration purpose only. Thick black line represents the boundary of the DVRFS model. Thin black lines are the boundary between the subbasins and subbasin sections within the DVRFS. White numerical and alphabetical labels are subbasin sections. Cyan lines are fault zones. Orange line is the boundary of the Nevada Test Site. Yellow labels are prominent topographic features and locations of interest. Open circles represent springs and discharge locations.

Figure 1a. Geographic and Prominent Topographic Features of the Death Valley Regional Groundwater Flow System

### 3.1 MODIFICATION OF THE DEATH VALLEY REGIONAL GROUNDWATER FLOW MODEL

To support the groundwater transport calculations to be performed by Jason Associates Corporation, five sets of simulations were run, three of which were to determine steady-state hydraulic heads and particle paths from the edge of the accessible environment down gradient. These simulations were run for:

- No groundwater pumping (Case 1)
- Initial estimate of long-term groundwater pumping conditions and return rates (Case 2)
- More realistic estimate long-term groundwater pumping conditions and return rates (Case 3).
- Transient simulation of current pumping into the future (Case 4)
- Transient simulation of pumping including proposed additional pumping to the east of the Nevada Test Site (Case 5)

Case 4 considers the continuation of the current (year 2003) level of pumping for another 500 years, and Case 5 includes additional groundwater withdrawal from carbonate and alluvial aquifers east of the Nevada Test Site as proposed by the Southern Nevada Water Authority. Cases 3 through 5 were added to the original work scope for this report under the direction of the U.S. Department of Energy.

Cases 1 through 5 were performed using a modified version of the DVRFS model published by Belcher (2004 [DIRS 173179]). The simulations were run as forward simulations using the hydraulic properties calibrated by Belcher (2004 [DIRS 173179]). Changes were made to the DVRFS model (Belcher 2004) for the present-day climate to conduct the simulations described above. The Belcher (2004 [DIRS 173179]) DVRFS model was developed with MODFLOW 2000 (Harbaugh et al. 2000 [DIRS 155197]) for simulation of transient flow conditions for the period of 1913 to 1998 (DTN: MO0602SPAMODAR.000). The model simulates a pre-pumping condition for prior to 1913 and pumping for the period of 1913 to 1998. Updated versions of the DVRFS model have been provided by the USGS for transient simulation of the period from 1912 to 2003 and for simulation using MODFLOW 2005 (Harbaugh 2005 [DIRS 186106]) (Appendix A). Years 1998 and 2003 were chosen for these simulations because they represented the last period of time for which published groundwater withdrawal data were available during the development of the 2004 and 2005 versions of the DVRFS model. The double precision version of MODFLOW 2000, version 1.13.00 was used for the simulations for Cases 1 to 3. MODFLOW 2005 was used for Cases 4 and 5. Nomenclature and files names for the five cases are included in Table 3.

Note that the USGS has updated the model input files used in this modeling exercise twice since its original release. These updates are described in the memo from Claudia Faunt (Appendix A). First, the drain observation file (*drob\_tr.txt*, Appendix A, Table 1) was updated to include 787 entries, the total number of drain observations used in the updated DVRFS model (2005).

Second, scale factors for the storage parameters were updated. An error was identified in the scale factors for the storage parameters in the report documenting the 2004 DVRFS model (Belcher 2004 [DIRS 173179]). A relatively large value for a storage scale factor (1) was identified in the model input files after the report was published. A significantly smaller value ( $10^{-10}$ ) is considered more reasonable. Since publication of the report, the values were updated by the USGS in the archived 2004 DVRFS model files (Appendix A). Updates are for values used during parameter estimation and sensitivity analyses, hence these changes are not part of forward runs discussed here.

Table 3. Summary of Nomenclature and File Names Used

Case	Description	Model Run Name	Input and Output Files	MNW File	WEL File	Particle Tracking Files
1	Pre-pumping	pdss1	<i>pdss1_mf2k.zip</i> [originally called <i>Pre-pumping.zip</i> ]	NA	NA	<i>pdss1_mpath.zip</i>
2	2003 estimate of long-term pumping rates	pdss5	<i>pdss5_mf2k.zip</i> [originally called <i>Pumping.zip</i> ]	<i>test5.MNW</i>	<i>test5.wel</i>	<i>pdss5_mpath5.zip</i>
3	Reduced estimate of long-term pumping rates	pdss6	<i>pdss6.zip</i>	<i>scaled.MNW</i>	<i>scaled.WEL</i>	<i>Pdss6_mpath-mplot.zip</i>
4	Transient	pdt1	<i>pdt1_mf2005_inp.zip</i>	<i>mnw_dvrfs_2503.txt</i>	<i>wel_irr_ret_2503.txt</i>	N/A
5	Transient with additional groundwater withdrawal	pdt2	<i>pdt2_mf2005_inp.zip</i>	<i>mnw_dvrfs_2503_snwa.txt</i>	<i>wel_irr_ret_2503_snwa.txt</i>	N/A

NOTE: MNW and WEL files are MODFLOW input files prepared in using the Multi-Node-Well package (Halford and Hanson 2002) and the WEL package (Harbaugh et al 2000), respectively.

The first step for running Cases 1 through 3 was to convert the original transient model to steady-state. For Case 1, this was done per the instructions of Blainey et al. (2006 [DIRS 186071], pp. 20 to 22). Files *BAS\_active.txt*, *CHOB\_15reg.txt*, *CHD\_15reg\_tr.txt*, *DIS\_WT\_CONFINED.txt*, *DRN\_tr.txt*, *DROB\_tr.txt*, *HFB\_final\_tr.txt*, *HUF2\_CONFINED.txt*, *HOBS\_sstr.hyd*, *MULT.txt*, *OBS.txt*, *OC.txt*, *PCG.txt*, *RES.txt*, *RCH\_tr.txt*, *SENSITIVITY.txt*, and *ZONE.txt* from the 2004 DVRFS model (as contained in the publicly released file *archive\_model\_tr.zip*) were modified where appropriate and renamed as shown in Appendix A, Table 1.

Cases 2 and 3 were developed on the basis of Case 1. For these cases, both pumping and return flow were modeled. The pumping data are simulated using the Multi-Node-Well option of MODFLOW (Halford and Hanson 2002 [DIRS 186107]). Pumping rates for the year 2003 were used for the initial estimate of long-term pumping conditions (Moreo and Justet 2008

[DIRS 185968]) for Case 2. For Case 2, file *MNW\_withdrawal\_1\_7\_20.txt* from the 2004 DVRFS model was modified and renamed *test5.mnw*, and a new file, *test5.wel*, was added for the return flow (Table 3).

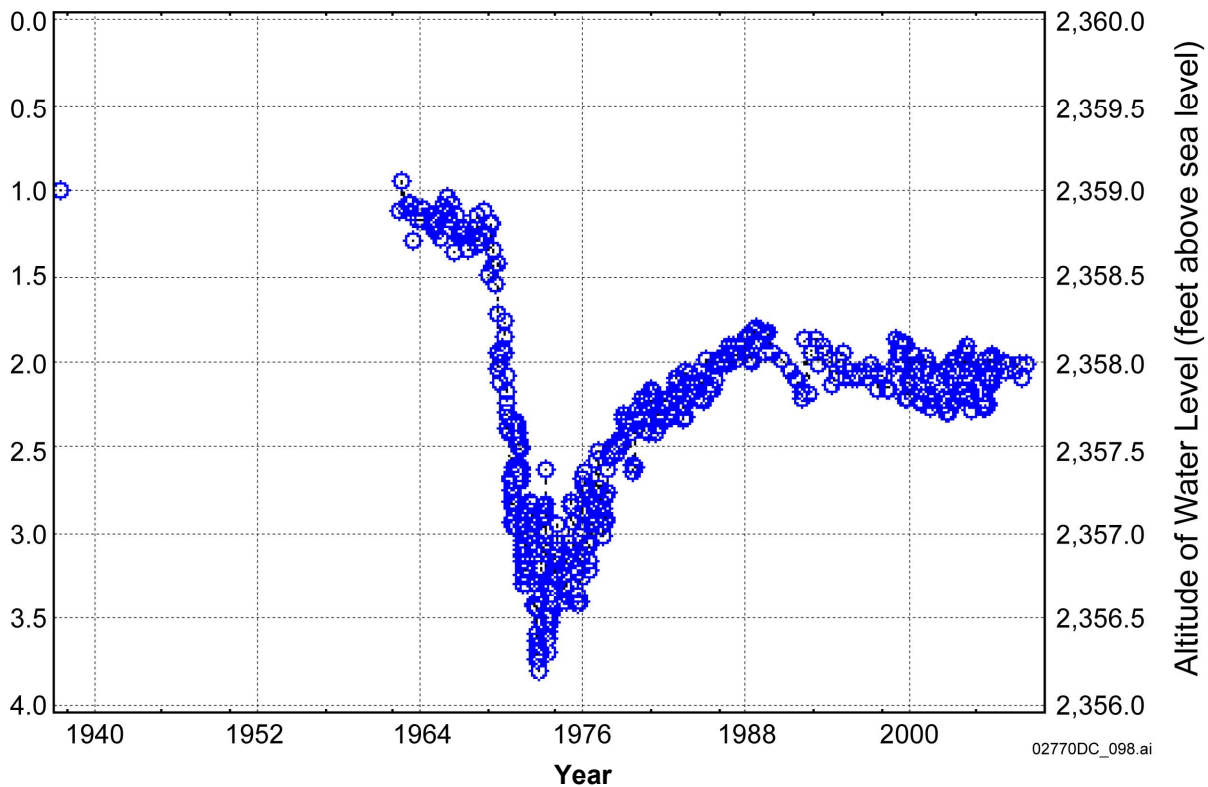
Many difficulties are associated with estimating return flows. These include uncertainties in the magnitude and timing of pumping, in the hydraulic properties of unsaturated zone sediment, and delineating the actual areas where water is or was returned to the environment. In the 2004 DVRFS model (Belcher 2004 [DIRS 173179]), for each withdrawal point, return flow was estimated to be 20% of the estimated annual pumpage, lagged by seven years (Appendix A) and returned to the top model layer. The same method of calculation and values were used for the updated DVRFS model (2005) (Appendix A). To more easily distinguish pumping and return flow, a separate WEL Package (Harbaugh 2005 [DIRS 186100]) input file was developed to apply the irrigation return flow. Separating the pumping and irrigation return flow allows for future updates to pumping and return flow separately. The separation also aids in varying the percentage of return flow and the lag time through automated parameter estimation methods.

The pumping data for the period of 1913 to 2003 were provided in MNW file *new\_mnw\_03.txt* and the corresponding irrigation return data were provided in WEL file *new\_irr\_ret\_03.txt* by Claudia Faunt of the USGS (Appendix A). The pumping rates contained in these files are consistent with 2003 groundwater withdrawal data published in USGS Data Series 340 (Moreo and Justet 2008 [DIRS 185968]). The data files provided by the USGS were modified such that they only contain the 2003 pumping data.

For Case 3 pumping and return flow rates were uniformly reduced by a factor of 0.023 such that they result in a drawdown of 0.2 m (0.7 ft) from the copper washer reference elevation in Devils Hole from the current conditions. The copper washer was installed on a wall of Devils Hole by the USGS to measure the water level in the pool in 1962, and has since been replaced by an ordinary bolt. The minimum pool level in Devils Hole has been set forth by the U.S. Supreme Court at 2.7 ft (0.82 m) below the datum (Cappaert v. United States 1976; United States v. Cappaert 1978). Currently the pool level is at about 2 ft (0.6 m) below the datum (Figure 1b). Therefore, the maximum future drawdown that is allowed at this location is  $2.7 - 2 = 0.7$  ft or 0.2 m. Case 3 also incorporated the planned groundwater withdrawal from well J-13 to support repository operations. The assumed pumping rate from well J-13 is 1,452 m<sup>3</sup>/day (266 gpm) and no return flow was assumed. Table 3 lists MNW and WEL files used in Case 3.

The transient model (Case 4) was constructed on the basis of the 2005 DVRFS model using the 1913 to 2003 pumping rates by Claudia Faunt (Appendix A). The 2005 DVRFS model was an extension of the 2004 DVRFS model (Belcher 2004 [DIRS 173179]), which modeled the DVRFS for the period of 1912 to 1998, to incorporate pumping rates between 1999 and 2003. The 2005 DVRFS model was developed to run with MODFLOW 2005. In Case 4, the 2005 DVRFS model was modified to simulate effects of continued pumping at the 2003 level of groundwater withdrawals for another 500 years (2003 to 2503). This modification resulted in the new MNW and WEL files *mnw\_dvrfs\_2503.txt* and *wel\_irr\_ret\_2503.txt*. In addition, MODFLOW input files *DIS\_WT\_CONFINED.txt*, *OC.txt*, *DRN\_tr.txt*, *RCH\_tr.txt*, and *CHD\_15reg.txt* were modified. The complete set of input files are saved in *pdt1\_mf2005\_inp.zip*.

USGS 36253211617200 230 S17 E50 36DC 1 Devils Hole (AM-4)



Source: [http://nevada.usgs.gov/doi%5Fenv/sitepage\\_temp.cfm?site\\_id=362532116172700](http://nevada.usgs.gov/doi%5Fenv/sitepage_temp.cfm?site_id=362532116172700) (accessed on 2/19/09).

NOTES: Although displayed as “Ground-water Level, in feet below land surface” in the USGS GWSI database on the above website, the left vertical axis actually shows the depth of water level in the pool below the datum (i.e., the copper washer which was replaced with a regular bolt in 2002. The datum was reset from 2359.9 to 2360 m in 2002) (Personal communication between Glenn Locke of USGS and Wayne Belcher of DOE, March 2, 2009).

Figure 1b. Measured Water Levels in Devils Hole (AM-4)

Finally, Case 5 was conducted to evaluate the additional impact on Devils Hole water level and upward hydraulic gradient between the carbonate aquifer and overlying aquifers as a result of proposed groundwater pumping for water supply in Indian Springs, Three Lakes, and Tikaboo Valleys east of the Nevada Test Site by the Southern Nevada Water Authority (SNWA). This case simulates additional groundwater withdrawal from the carbonate aquifer at Tikaboo Valley North well 53948TVN (Layers 1 to 3, Row 52, Column 136) at a rate of 2,587 acre-ft/yr and another 8,018 acre-ft/yr from seven other wells along U.S. Highway 95. The cluster of new wells along U.S. Highway 95 includes one from the carbonate aquifer (Layers 1 to 4, Row 114, Column 126, rate 5,400 acre-ft/yr), and 6 others from the alluvial aquifer (Row 115, Column 125; Row 116, Column 126; Row 117, Column 127; Row 119, Column 130; Row 120, Column 131; and Row 120, Column 132, all screened in layers 1 to 4, each with a total rate of 2,618 acre-ft/yr). These well locations and pumping rates are based on a May 17, 2005 application to the Nevada State Engineer's Office by SNWA and a subsequent ruling on June 15, 2006 by the Nevada State Engineer (<http://water.nv.gov/scans/rulings/5621r.pdf>). Locations of the permitted wells are obtained from the permits available at the State's Water Rights database (<http://water.nv.gov/water%20Rights/permitdb/permit.cfm>) and were converted into Universal

Transverse Mercator (UTM) coordinates and model cell indices by the USGS (Wayne Belcher, personal communication, February 25, 2009). This case simulates the increased level of pumping assuming this pumping started in year 2003 and continues for another 500 years. Table 3 lists MNW and WEL files used in Case 5. The complete set of input and output files for Case 5 can be found in *pdt2\_mf2005\_inp.zip*.

### **3.2 ESTIMATION OF RADIONUCLIDE PLUME AT THE ACCESSIBLE ENVIRONMENT**

Particle tracks using the DVRF model, which has heads calculated with MODFLOW, are conducted with MODPATH and visualized with MODPLOT. The start points of the particle tracks for this modeling effort are derived from the base-case site-scale saturated zone (SZ) transport model (SNL 2007 [DIRS 184806]). In the base-case site-scale SZ transport model, 10,000 particles are released from random locations below the footprint of the repository and uniformly distributed with depth throughout the top layer of this model. Particles are tracked in the base-case site-scale SZ transport model subject to the effects of advection and dispersion until they exit the model boundary. These particle tracks are analyzed to determine the location where they cross a plane defined at the 18-km compliance boundary at UTM Northing 4,058,256 m to define the starting location for MODPATH particle tracking using results from the Death Valley regional groundwater flow model as described in Section 3.3. Subsequent transport calculations will be performed by Jason Associates Corporation. There were three steps involved in determining these locations:

- Run a transport simulation using the base-case site-scale SZ transport model (SNL 2007 [DIRS 184806]); in this simulation, the expected value for dispersivity, 100 m (SNL 2008 [DIRS 183750], Table 6-8), was used
- Establish particle starting locations as the positions where they cross the accessible environment boundary from output file
- Translate particle tracks from UTM coordinates used in the base-case site-scale SZ transport model (SNL 2007 [DIRS 184806]) to local coordinates used in the Death Valley regional groundwater flow model (Belcher 2004 [DIRS 173179]) to establish starting locations.

The FEHM v. 2.26 (Table 2) SPTR particle-tracking routine was used to model the particle tracks from below the Yucca Mountain repository to the accessible environment at 4,058,256 m UTM Northing in the site-scale SZ transport model (SNL 2007 [DIRS 184806]). Ten thousand particles were distributed randomly below the repository footprint. Dispersion was included in the particle tracking. The results of this simulation are in output file *sz06\_sptr.sptr2*. Particle tracks at the accessible environment boundary were extracted from the FEHM SPTR output using utility code *18km.F90* (Table 2). All particle tracks were read into a FORTRAN array, which was searched until the *y*-location (Northing) of the particle was less than 4,058,256 m (the location of the accessible environment boundary). Then, the corresponding spatial *x*-locations (Easting) and *z*-locations (elevation) are calculated through linear interpolation between the locations at the time step that the particle crossed the 18-km compliance boundary and the

particle locations at the previous time step. A total of 8,024 particles crosses the accessible environment boundary within the time period of the simulation.

Initial particle tracks were extracted by translating the FEHM coordinates, which are in UTM Zone 11 coordinates, to local coordinates in the DVRFS model. To do so, UTM northing coordinates had 3,928,000 m subtracted from them and UTM easting coordinates had 437,000 m subtracted from them. This translation was performed within utility code *18km.F90*. Table 4 lists DVRFS coordinates data.

Table 4. Local and UTM Coordinates for the DVRFS Model

Corner	Grid Node (row, column)	UTM Northing (m)	UTM Easting (m)	Local (Model) Northing (m)	Local (Model) Easting (m)
Northwest	1, 1	4,219,000	437,000	291,000	0
Northeast	1, 160	4,219,000	677,000	291,000	240,000
Southeast	194, 160	3,928,000	677,000	0	240,000
Southwest	194, 1	3,928,000	437,000	0	0

NOTE: All values are in the units of meters.

The FEHM SPTR particle-tracking routine has the output format ordered by time such that all particles that are active at a given time step are listed sequentially. When a particle exits the model domain, it is no longer listed in the data table for any subsequent time step. Particle starting locations and positions where they cross the accessible environment boundary are extracted; 8,024 particles were found.

### 3.3 PARTICLE TRACKING ANALYSIS FOR CURRENT CONDITIONS

The particle tracking analysis was conducted to provide:

- Predominant groundwater flow paths in the central and southern Death Valley subregions beyond the accessible environment
- Major discharge locations
- Specific discharge estimates along the predominant flow path.

The particle tracking analysis was performed for Cases 1 to 3 described in Section 3.1 (pre-pumping and two different pumping conditions) using MODPATH V5.0 (11/6/08 release). Table 3 includes pertinent file names. Particle starting positions were those determined from the analysis described in Section 3.2. These starting locations are consistent with the “plume” started at the accessible environment as simulated with representative base-case parameter values with the site-scale transport model (as described in Section 3.2). The MODPATH option of particles passing through weak sinks was used. The porosity for all model cells was set equal to 1 for the calculation of specific discharge described below.

Specific discharges were calculated for each particle track by summing the path segments for each particle (i.e., calculate the path length) and dividing the path length by the travel time. A

utility code *18km-spdis.F90* was used for these calculations. The code outputs particle number, path length, and specific discharge. Excel 2007 was used to develop the histogram and cumulative distribution plots. Note that the travel time estimates from these simulations are not realistic because the actual porosity is less than unity (on the order of 0.1). Specific discharges were only calculated for Cases 1 and 2.

### **3.4 ESTIMATION OF SPECIFIC DISCHARGE AND FLOW PATHS FOR FUTURE CLIMATIC CONDITIONS**

Specific discharge for the wetter future climate was estimated using the specific discharge values obtained for the present-day climatic conditions (Sections 3.3 and 4.3) and a linear scale factor (the same approach as in the TSPA-LA, see SNL 2008 [DIRS 183750], Section 6.5[a]). A higher water table is expected in the Yucca Mountain and surrounding areas under future wetter climatic conditions. In the TSPA-LA, a scaling factor was used to increase groundwater specific discharge from the present-day conditions to account for the effect of water table rise under future wetter climates. This approach assumes that the flow paths are similar under the future wetter climatic conditions based on the fact that simulations with a previous version of the Death Valley regional flow model under wetter glacial climatic conditions indicate that the groundwater flow paths from below Yucca Mountain do not significantly change (D'Agnese et al. 1999 [DIRS 120425]). However, the flow paths in the Death Valley groundwater basin may be shortened based on reviews of additional paleospring discharge data. The scaling factor was chosen to be the same as the factor developed for the site-scale SZ model for the glacial-transition climate, 3.9 (see SNL 2008 [DIRS183750], Table 6-4[a]). The increase in groundwater specific discharge will result in an increase in groundwater flow rates and in rates of contaminant transport in the saturated zone.

A literature review was conducted to estimate present and paleodischarge areas as well as discharge rates. This information was used in comparison to the modeling results described in Sections 4.3 to better evaluate potential flow paths south of the accessible environment.

### **3.5 CALCULATION OF RADIONUCLIDE MASS RELEASE RATES FROM THE TSPA-LA**

Jason Associates Corporation requested the mean, median, 95th percentile, and 5th percentile values of annual radionuclide mass release rate and cumulative release for the 300 realizations in TSPA-LA. The annual mass release rates and cumulative releases were requested for sum of the 1,000,000-year groundwater dose modeling cases (Drip Shield Early Failure, Waste Package Early Failure, Igneous Intrusion, Seismic Ground Motion, and Seismic Fault Displacement) and for the 1,000,000-year Nominal Modeling case alone. This information was provided at the boundary between the unsaturated zone and the saturated zone and at the accessible environment for the 49 radionuclide species, including multiple colloidal forms, tracked in the TSPA-LA Model.

As the data at the unsaturated zone and saturated zone boundary were not saved when running the TSPA-LA Model for the license application documentation, the simulations had to be re-run for this analysis. The TSPA-LA Model v5.005 was updated to automatically export the unsaturated zone and saturated zone release information. Specifically, time history results

elements that export calculated results to text files were added for the mass flux rates and cumulative releases from the Engineered Barrier System (EBS), unsaturated zone, and saturated zone. Time history elements were added for the 49 radionuclide species tracked in the TSPA-LA Model. In addition, release rates for dissolved and colloidal isotopes (“Ic,” “If,” and “Ifcp”) were added together to yield one release history per isotope. For each of the five 1,000,000-yr groundwater dose modeling cases, the models were re-run to export the time history results. Dose comparisons were made to confirm that the calculations agree with the compliance runs. The results were then processed through EXDOC\_LA v2.0 (Table 2) to yield expected quantities for each epistemic realization. Once the expected quantities for each epistemic realization were calculated, the values were summed together over all modeling cases to yield a total release history. The summation files are *Read\_Histories\_Calc\_RN\_Total\_UZ\_Flux\_2021.gsm* and *Read\_Histories\_Calc\_RN\_Total\_SZ\_Flux\_2021.gsm*. Mean, 5th-percentile, median, and 95th-percentile values were then reported at selected time steps for the annual mass release rates and cumulative releases at the unsaturated zone/saturated zone boundary and at the accessible environment. The Nominal Modeling Case was also re-run to export release histories at the unsaturated zone/saturated zone boundary and at the accessible environment.

To reduce the computational burden of the downstream calculations to be run, Jason Associates Corporation requested a time-step schedule of “no more than 20.” This schedule is much coarser than the time steps produced by the TSPA-LA Model runs. The Drip Shield Early Failure, Waste Package Early Failure, and Seismic Ground Motion cases used a time step schedule with 470 variable length time steps (Table 5). The Igneous Intrusion and Fault Displacement modeling cases used a 500-year time step length over the 1 million year analysis period resulting in 2,000 time steps. In order to capture short duration spikes in the calculated histories, the release data for the five modeling cases were added together using a time step schedule that included the smallest time step length from any of the five modeling cases. Therefore, a total of 2,020 time steps were used to sum the data from the five modeling cases. This schedule applies a 250-year time step length up to 10,000 years and a 500-year time step length thereafter up to 1,000,000 years.

Table 5. TSPA-LA Model Time-Step Schedule for the Ground Motion, Drip Shield Early Failure, and Waste Package Early Failure Modeling Cases

<b>Time Range (years)</b>	<b>#Steps</b>	<b>Length (years)</b>
0 to 10,000	40	250
10,000 to 100,000	180	500
100,000 to 120,000	20	1,000
120,000 to 160,000	20	2,000
160,000 to 1,000,000	210	4,000

The identification of 20 suitable time steps from the 2,020 time steps to characterize the curves over a 1,000,000 year period is subjective and was determined by observing trends in the cumulative release data. This analysis considers the mean cumulative release for 49 different species, which are each released from the unsaturated zone and saturated zone at different rates. Thus it is possible that the reduced time step schedule selected for one species may not be the

optimal selection for another species. Because downstream calculations are not expected to process the different radionuclides together, it is not necessary to output the same time step schedule for each species.

To determine the optimal schedule, first the mean cumulative release from the unsaturated zone was determined using the time step schedule with 2,020 time steps. The cumulative release value at 1,000,000 years for each species was used to normalize the release histories to fractional cumulative release histories according to Equation 1:

$$f_{CR,RN}(t_i) = \frac{CR_{RN}(t_i)}{CR_{RN}(t_{1,000,000-yr})} \quad (\text{Eq. 1})$$

where  $f_{CR,RN}(t_i)$  = fraction of 1,000,000-yr cumulative release at time  $t_i$

$CR_{RN}(t_i)$  = cumulative release (g) at current time step

$CR_{RN}(t_{1,000,000-yr})$  = cumulative release (g) at 1,000,000 years

$t_i$  = time (yr) of current time step.

Using the cumulative release results calculated above, the calculations also compute the corresponding release rates for the same time step schedule. To compute average release rates over the specified time period, the total release during a time step, calculated as the difference between the cumulative release at the end of the current time step and the cumulative release at the end of the previous time step, is divided by the time step length:

$$rate_{RN}(t_i) = \frac{CR_{RN}(t_i) - CR_{RN}(t_{i-1})}{t_i - t_{i-1}} \quad (\text{Eq. 2})$$

where  $rate_{RN}(t_i)$  = release rate (g/yr) at time  $t_i$

$CR_{RN}(t_i)$  = cumulative release (g) at current time step

$CR_{RN}(t_{i-1})$  = cumulative release (g) at previous time step

$t_i$  = time (yr) of current time step

$t_{i-1}$  = time (yr) of previous time step.

Cumulative releases and average release rates from the saturated zone were determined using the same methods described for the unsaturated zone analysis.

The technique used to provide the reduced set of time steps was based on the 5% quantiles of the cumulative release curve for each radionuclide. In particular, for each radionuclide a normalized cumulative release curve was calculated by dividing the original cumulative release history (i.e., the 2000-point history from the GoldSim output file) with the cumulative release at 1,000,000 years. Then, the chosen 20 time steps from the cumulative release history for each

radionuclide were points that fall just prior to each 5% quantile of the fractional cumulative release curve. The values of the 20 time steps were generally different for each radionuclide. The 20 instantaneous annual mass release rates that correspond to the 20 reported cumulative release values were derived by averaging the release over each 5% quantile. For example, the instantaneous or annual mass release rate reported for the cumulative curve between the 5% and 10% quantile was equal to (the cumulative release at the 10% quantile minus the cumulative release at the 5% quantile)/(time step length). The value of this “average” annual release rate was applied at the upper end of the interval (in this example at the time step corresponding to the 10% quantile).

To verify the results, calculations for  $^{14}\text{C}$  were performed using three different techniques. MS Excel was used to report the final results. Calculations were also performed using GoldSim (see *EIS\_TimeStep\_Resolution.gsm*) for mean release results, and MathCad (see *EIS\_UZ\_Time\_Resolution\_C14.xmcd*) for the statistics data. The GoldSim and MathCad implementations were only used for verifying the MS Excel calculations (see *Compare\_Techniques\_C14.xls*).

Analysis of  $^{14}\text{C}$  for the Igneous Intrusion case shows that while EXDOC\_LA v2.0 can correctly process rate information, the calculation may not be accurate for cumulative release histories. When the cumulative release histories from the unsaturated zone were processed through EXDOC\_LA v2.0, the expected cumulative unsaturated zone release data that include probability weighting for  $^{14}\text{C}$  results shows an increase at times beyond 950,000 years (Figure 2a), whereas which is inconsistent with the cumulative release histories data directly out of the GoldSim model (Figure 2b), which data remain flat during this time period (Figure 2b). Note, that the scale for the Y-axis is different in Figures 2a and 2b because the data in Figure 2a are probability weighted and the data in Figure 2b are not probability weighted. Therefore, despite exporting a significant amount of cumulative release data from the GoldSim models, these data are not used in this analysis. Instead, expected release rates are calculated and integrated to yield expected cumulative release histories.

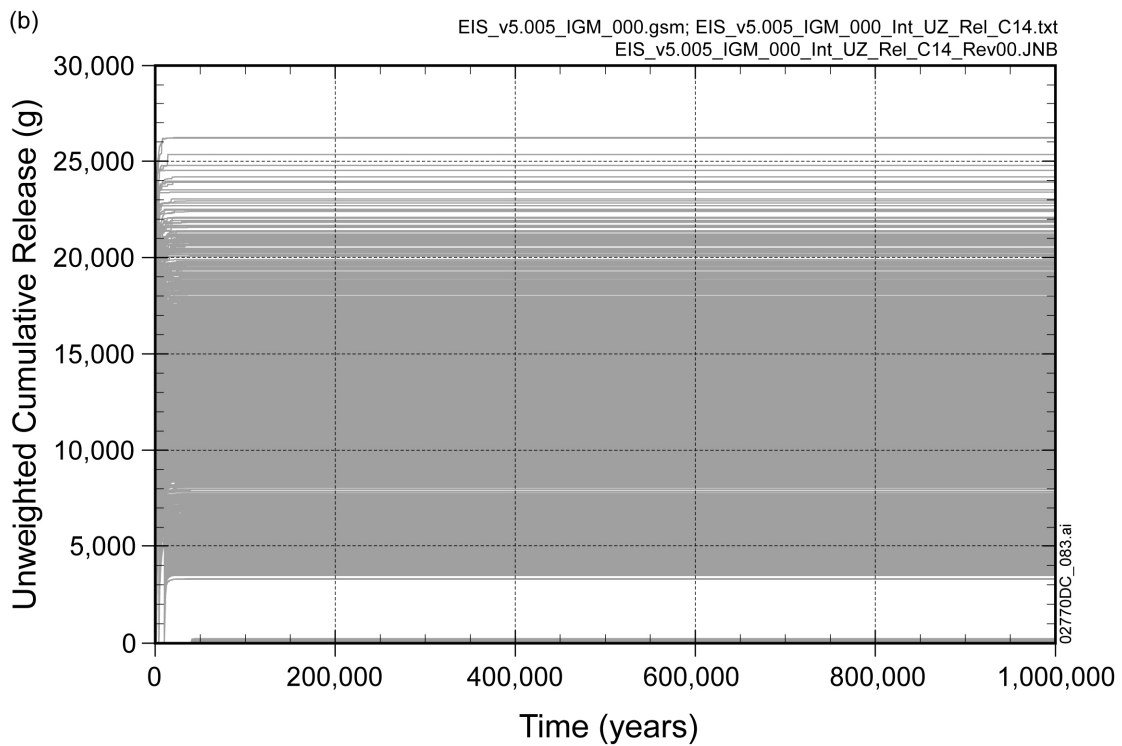
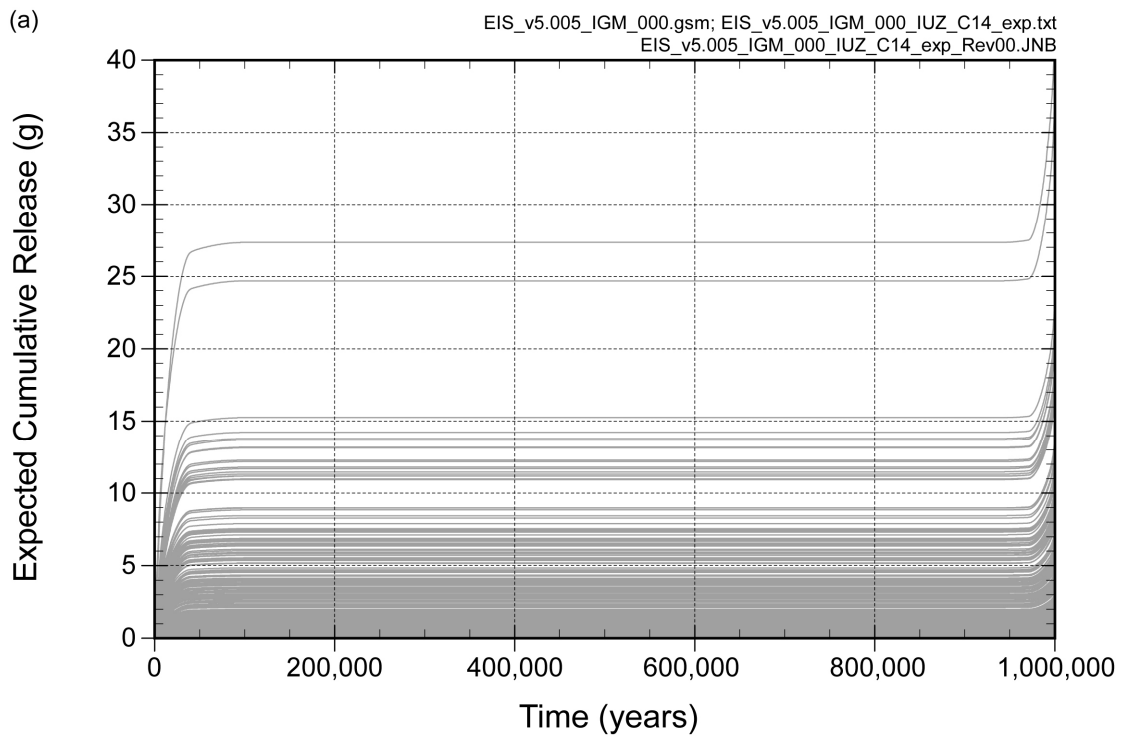


Figure 2. Cumulative Releases of  $^{14}\text{C}$  from the Unsaturated Zone: (a) Expected Values Calculated by EXDOC\_LA; and (b) Unweighted Values Calculated by GoldSim

### **3.6 EVALUATION OF BREAKTHROUGH CURVES FOR NONRADIOLOGICAL CONTAMINANTS**

The SEIS Supplementations require an analysis of the transport of nonradiological contaminants in the saturated zone from beneath the repository to the boundary of the accessible environment and beyond. Contaminants of concern include nickel, molybdenum, and vanadium, which originate from the degradation of Alloy 22 and Stainless Steel Type 316 in the repository (David Lester, Jason and Associates Corporation, personal communication, December, 2008). Sorption of these metals during transport in the saturated zone may be an important process and representative values of sorption coefficients must be defined. However, additional transport simulations with the saturated zone flow and transport abstraction model will not be performed for these metals. Instead, results from the existing radionuclide breakthrough curves will be used by choosing the most representative radioelements for these metals, based on similar values of sorption coefficients.

The most representative radioelements for which there are existing breakthrough curves are identified by comparing the uncertainty distributions for sorption coefficients of radioelements with the recommended single values of sorption coefficients for nickel, molybdenum, and vanadium. Specifically, the median values from the uncertainty distributions of sorption coefficients for all radioelements (SNL 2008 [DIRS 183750], Tables 6-8 and 6-7[a]) are compared to the recommended values for the metals and the full distribution of sampled values are also plotted for comparison to the recommended values. Recommended values of sorption coefficients for nickel, molybdenum, and vanadium in volcanic rocks and alluvium are 15, 0, and 8 mL/g, respectively (David Lester, Jason and Associates Corporation, personal communication, December, 2008).

An alternative approach was also used for the evaluation in which a single SZ transport simulation is performed for each of the nonradiological contaminants. This approach utilizes the SZ flow and transport abstraction model (SNL 2008 [DIRS 183750]) and expected values for input parameters to produce expected breakthrough curves in the saturated zone under glacial-transition climatic conditions for nickel, molybdenum, and vanadium. The expected values of other parameters used to simulate the saturated zone breakthrough curves for the nonradiological contaminants are those defined for the median case in the SZ transport model validation (SNL 2008 [DIRS 183750], Table 7-1[a]).

### **3.7 NOTE ON ANALYSIS FOR COMPARISON TO GROUNDWATER PROTECTION STANDARD**

A detailed explanation of the analysis of radionuclide releases for comparison to the groundwater protection standards is provided in the TSPA model report (SNL 2008 [DIRS 183478], Sections 6.3.11, 8.1.2, and 8.1.2[a]). A summary of the approach is provided in Section 4.7, with detailed citations of the technical basis to the TSPA model report and other sources.

## 4 ANALYSIS RESULTS AND CONCLUSIONS

This section summarizes the results of the analyses described in Section 3.

### 4.1 SIMULATED FLOW FIELDS

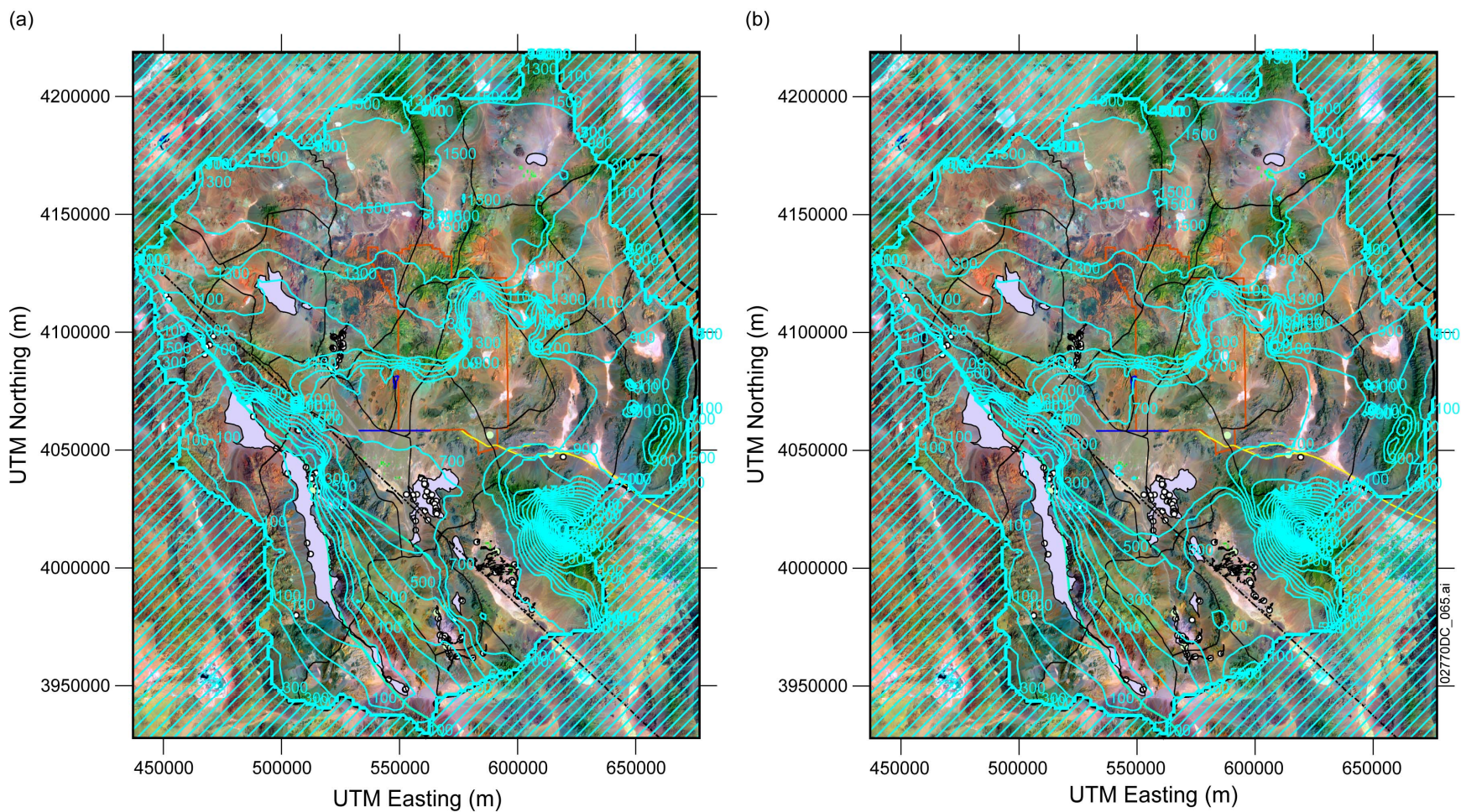
Contours of simulated hydraulic heads for layers 1, 2, 3, and 4 are shown below for Cases 1 (left, pre-pumping conditions) and Case 2 (right, initial estimate of long-term pumping conditions) (Figures 3 through 6). Layers 1 through 4 were selected because these are the DVRFS model layers that represent the alluvial aquifer and the upper volcanic aquifer through which particles released from the 18 km accessible environment boundary are expected to travel.

The simulated hydraulic heads for pre-pumping conditions (Case 1) are similar to those presented by Belcher (2004 [DIRS 173179], Figure F-46). For any given layer, simulated heads for Case 2 (2003 pumping conditions) differ from those for Case 1 in several areas, indicating effects of pumping. In addition, a comparison of Figures 3 through 6 showed that the hydraulic heads in layers 1 through 4 are similar, indicating little vertical hydraulic gradient within the alluvial aquifer (this observation is specific for Case 1 and Case 2).

Figures 3 through 6 also show that under continued pumping at the 2003 level, hydraulic heads near Devils Hole (UTM Northing 4,031,154 m and Easting 563,596 m) are approximately 613.3 m. An examination of the 2004 DVRFS model output showed that the simulated hydraulic head at this location is 691.7 m for year 1998. Therefore, continued pumping at the 2003 level yields a model-simulated drawdown of 78.4 m (691.7 m – 613.3 m) (257.2 ft) from the 1998 water level. Because the 1998 measured pool stage in Devils Hole was about 0.6 m (2 ft) below the “copper washer” datum (Figure 1b), a 78.4-m (257.2-ft) drawdown would bring the pool stage well below the threshold of 0.2 m (0.7 ft) above the datum as set forth by the Supreme Court (*Cappaert v. United States* 1976; *United States v. Cappaert* 1978). These court-imposed limitations guide the Case 3 simulations.

Note that simulated hydraulic heads near Devils Hole differ by about 30 m from the measured water levels due to model and data uncertainties associated with the 2004 DVRFS model (Belcher 2004 [DIRS 173179], p. 345). Therefore, model simulation results from the modified models should be used with caution. Despite limitations inherent in the 2004 DVRFS model, it is reasonable to use the model to perform a comparative study to evaluate the differences in modeled water levels resulting from different levels of groundwater withdrawal.

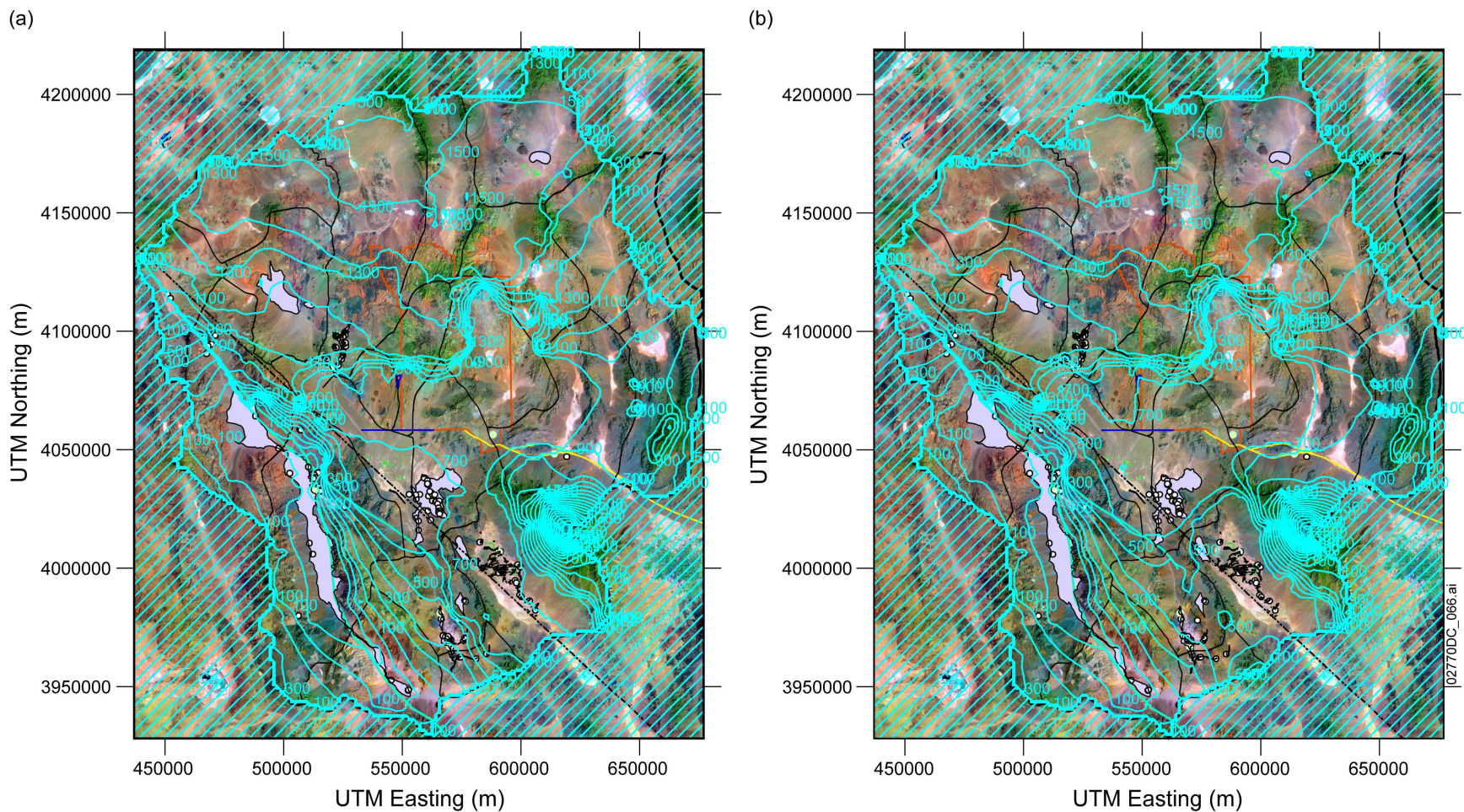




Source: *HeadContours.srf* in *FigureFiles.zip*.

NOTES Hydraulic heads are in meters. Datum is NAVD88. Hydraulic head contours shown were generated using MODPATH V5.0, post-processed using procedures described in Appendix C, and then overlaid on the base map (contained in file *Basemap\_full.srf*).

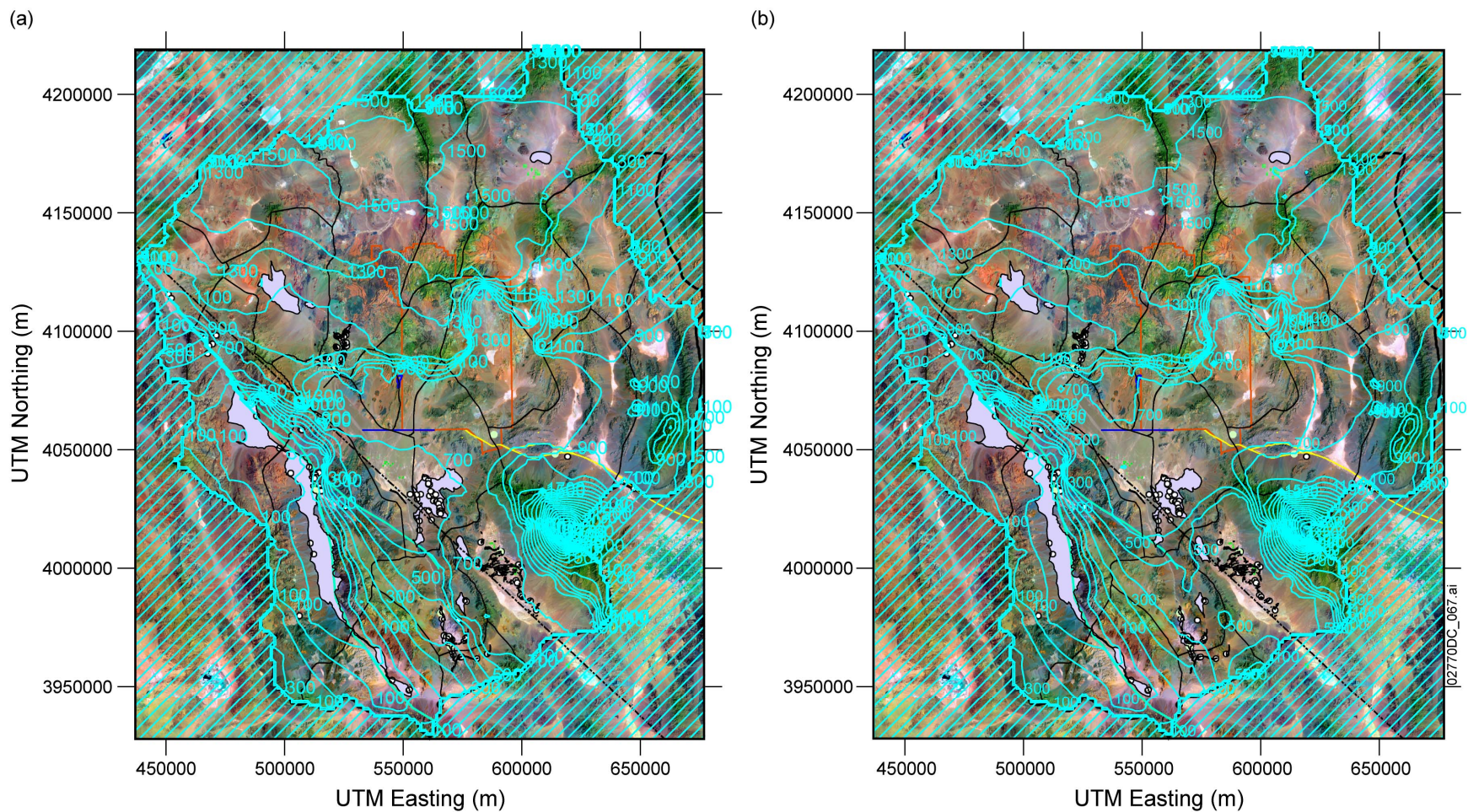
Figure 4. Layer 2 Hydraulic Heads for (a) Case 1 (pre-pumping) and (b) Case 2 (pumping)



Source: *HeadContours.srf* in *FigureFiles.zip*.

NOTES: Hydraulic heads are in meters. Datum is NAVD88. Hydraulic head contours shown were generated using MODPATH V5.0, post-processed using procedures described in Appendix C, and then overlaid on the base map (contained in file *Basemap\_full.srf*).

Figure 5. Layer 3 Hydraulic Heads for (a) Case 1 (pre-pumping) and (b) Case 2 (pumping)

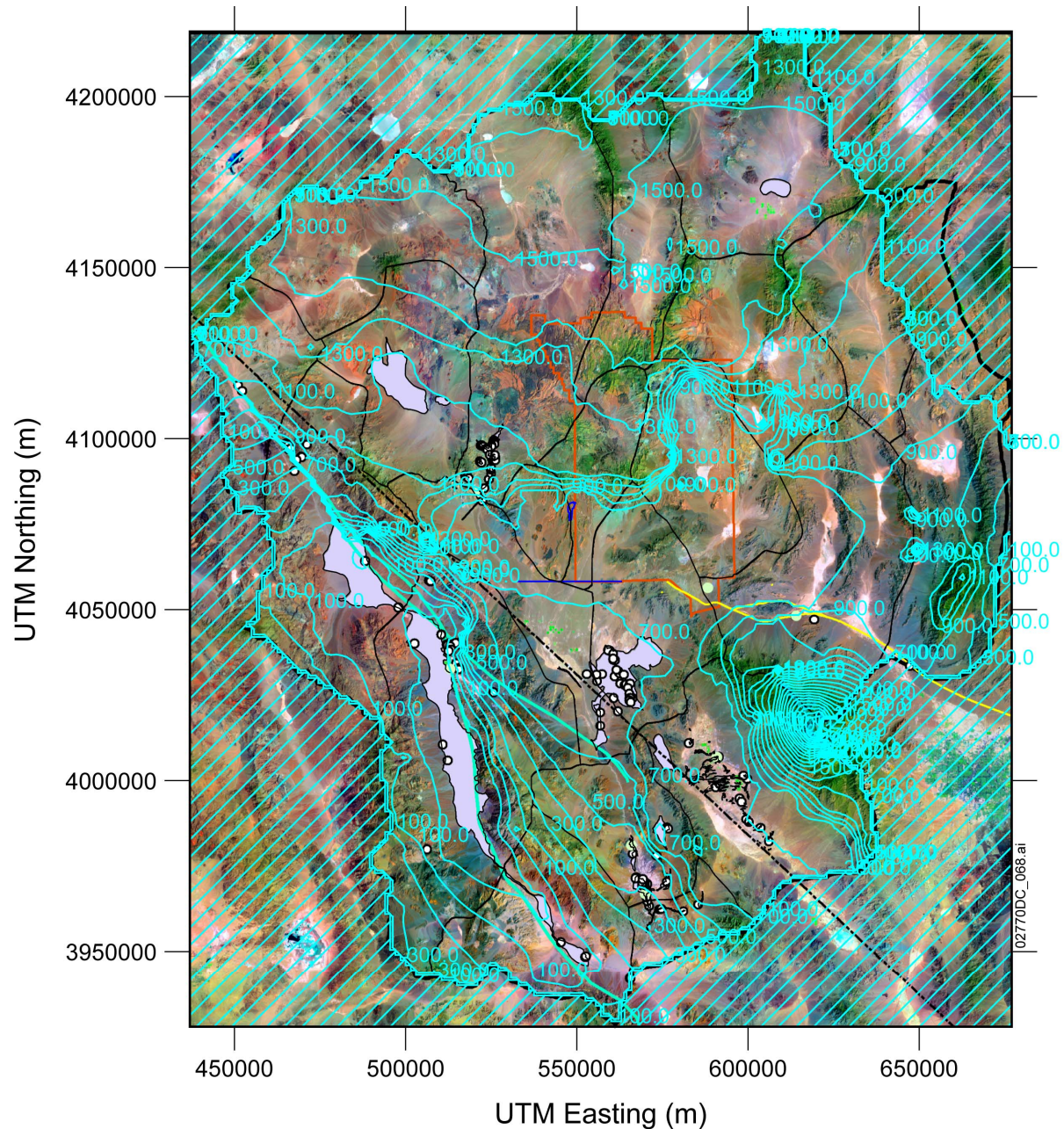


Source: *HeadContours.srf* in *FigureFiles.zip*.

NOTES: Hydraulic heads are in meters. Datum is NAVD88. Hydraulic head contours shown were generated using MODPATH V5.0, post-processed using procedures described in Appendix C, and then overlaid on the base map (contained in file *Basemap\_full.srf*).

Figure 6. Layer 4 Hydraulic Heads for (a) Case 1 (pre-pumping) and (b) Case 2 (pumping)

Hydraulic heads simulated for the reduced level of long-term pumping (Case 3) for layer 1 are shown in Figure 7. Heads for layers 2 through 4 are similar to those shown in the figure. With the reduced pumping, the modeled steady-state hydraulic head at Devils Hole is 691.5 m, which represents a drawdown of about 0.2 m (0.7 ft) from the current pool stage of about 0.6 m (2 ft) below the “copper washer” datum. Thus, the modeled drawdown is now within the threshold set by the Supreme Court (Cappaert v. United States 1976; United States v. Cappaert 1978).



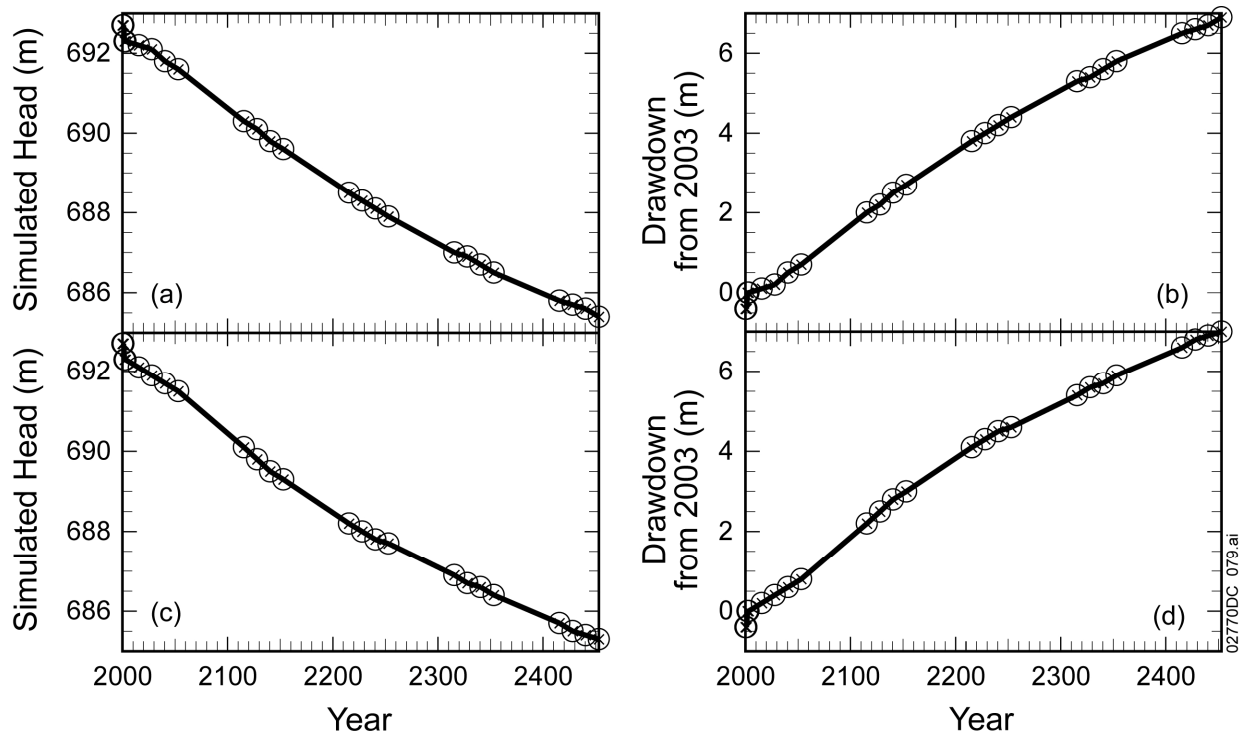
Source: *HeadContours.srf* in *FigureFiles.zip*.

NOTES: Hydraulic heads are in meters. Datum is NAVD88. Hydraulic head contours shown were generated using MODPATH V5.0, post-processed using procedures described in Appendix C, and then overlaid on the base map (contained in file *Basemap\_full.srf*).

Figure 7. Simulated Layer 1 Hydraulic Heads for Case 3 (reduced pumping conditions)

Next, hydraulic heads at Devils Hole were examined for Cases 4 and 5 by running the utility code *DH\_head.F90* with MODFLOW output file *HEADSOUT.txt*. Output from this examination include file *DevilsHole.hed*. These input and output files are contained in files: *pdt1\_mf2005\_inp.zip* and *pdt2\_mf2005\_inp.zip* for Cases 4 and 5, respectively. Figure 8a shows the simulated heads for the copper washer datum (Column 85, Row 126 in the model,

which includes UTM 563,596 m Easting and 4,031,154 m Northing) for Case 4. The heads are identical in Layers 1 through 4, indicating no vertical gradient at this location. Figure 8b shows the corresponding drawdowns from the simulated head at the “copper washer” for year 2003 (approximately 692.3 m, see file: *pdt1\_DevilsHole\_head.xls* contained in *pdt1\_mf2005\_inp.zip*). The water level in 2003 represents the current water level (see Figure 1b). This simulation shows that at approximately year 2016, the drawdown of 0.2 m is reached at Devils Hole (Figure 8b; see also file: *pdt1\_DevilsHole\_head.xls* contained in *pdt1\_mf2005\_inp.zip*). At the end of year 2453, the drawdown from the 2003 water level at Devils Hole has reached about 7 m.



Source: *pdt2\_DevilsHole\_Head.xlsx* in *pdt2\_mf2005\_inp.zip*.

NOTES: Hydraulic heads are in meters. Datum is NAVD88. Case 4 drawdown was calculated from the simulated hydraulic head for year 1998, and Case 5 drawdown was calculated from the simulated hydraulic head for year 2003. Figures present the simulated heads and drawdowns for layers 1 through 4; however, simulated heads for layers 1 through 4 are identical.

Figure 8. Simulated Hydraulic Heads and Drawdowns at the Devils Hole “Copper Washer” Datum: (a) Case 4 Hydraulic Head; (b) Case 4 Drawdown; (c) Case 5 Hydraulic Head; and (d) Case 5 Drawdown

Figures 8c and 8d present the simulated hydraulic heads and drawdowns for Case 5. As can be seen, the simulated heads and drawdowns at Devils Hole are similar to those shown in Figures 8a and 8b. The simulation indicates that the additional pumping from the proposed wells in Indian Springs, Three lakes, and Tikaboo Valleys east of the Nevada Test Site described in Section 3.1 would result in an increase of up to 0.3 m in drawdowns of water level at Devils Hole (*pdt2\_DevilsHole\_head.xls* contained in *pdt2\_mf2005\_inp.zip*). As a result, the water level would fall below the threshold level set in the Supreme Court decision (i.e., 2.7 ft or 0.82 m below the copper washer, see Section 3.1) before year 2016. The increase in the drawdown

would reach its maximum around year 2053, after which it would gradually decrease with time. The effect of the additional pumping would dissipate by year 2453.

Finally, we evaluate the impact of groundwater pumping on the vertical hydraulic gradient between the carbonate and overlying alluvial-volcanic aquifers. Upward vertical hydraulic gradients have been observed in individual boreholes with isolated test intervals such as those between the regional Paleozoic carbonate aquifer and the overlying volcanic or alluvial aquifers as observed at UE-25 p#1 and NC-EWDP-2D/2DB (BSC 2004 [DIRS 170009], Section 6.3.2, Table 6-4). At UE-25 p#1, water levels in the Paleozoic carbonate rocks are about 20 m higher than those in the overlying volcanic rocks. Water levels measured within the carbonate aquifer at NC-EWDP-2DB are about 7 m higher than levels measured in overlying volcanic rocks. The generally upward gradients effectively limit the downward potential for migration of water within the tuffs or between the tuffs and the underlying regional Paleozoic carbonate aquifer, and maintain flow paths originating from beneath the repository in the volcanic system. Although locally downward hydraulic gradients are observed, these may be attributed, in most cases, to the presence of local recharge conditions and low permeability confining units, or perched conditions (BSC 2004 [DIRS 170009], Sections 6.3.2, 6.4, and 7.1.1).

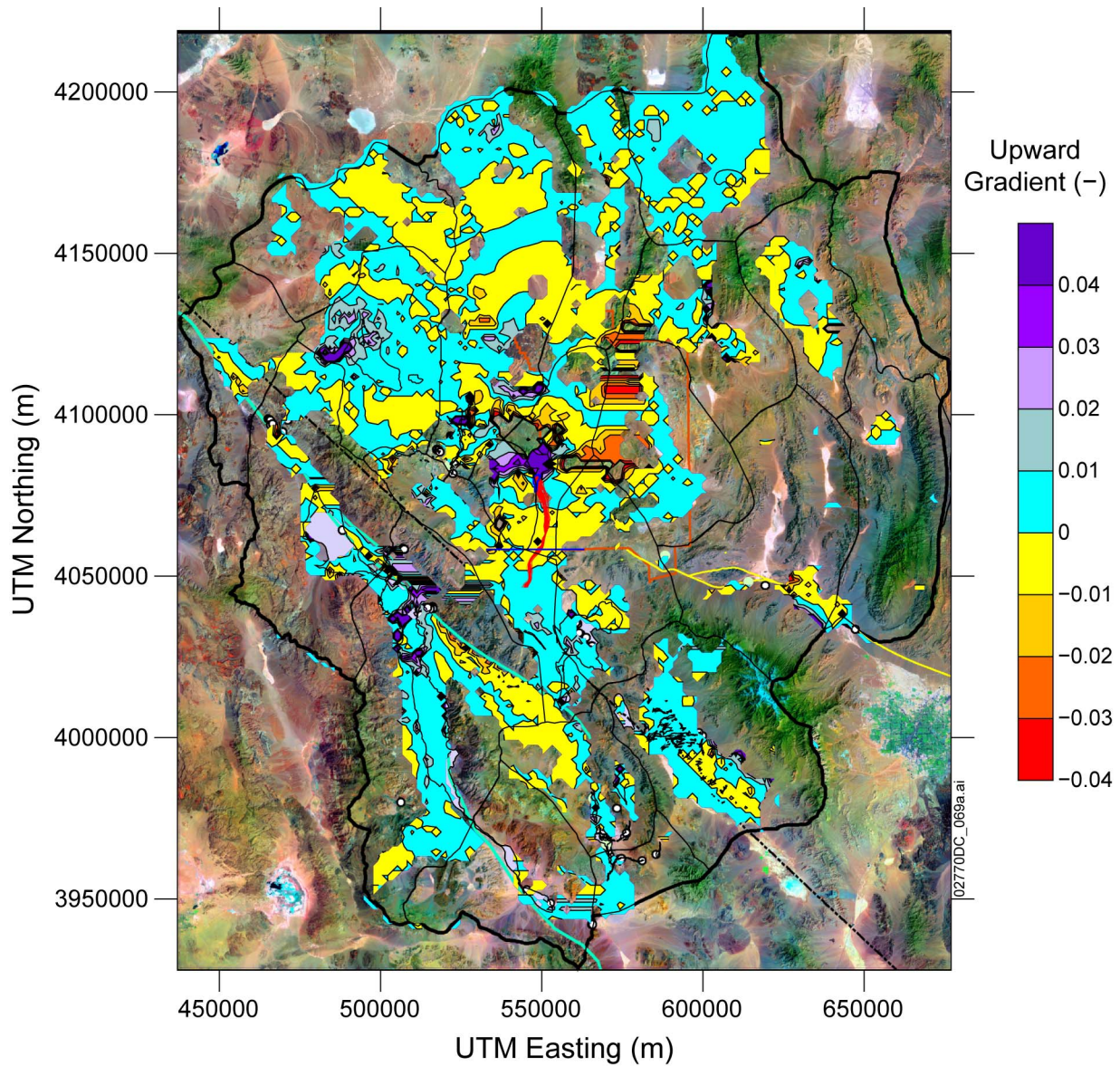
In this analysis, we extracted information from the Case 5 simulation to evaluate the impact of groundwater withdrawal on the upward vertical gradient from the carbonate aquifer. The vertical hydraulic gradient was calculated using two methods for year 2016 when the water level in Devils Hole is projected to reach the threshold of 2.7 ft (0.82 m) below the copper washer, with results illustrated in Figures 9a and 9b. In Figure 9a, the vertical hydraulic gradient was calculated using the simulated head values at the lowermost cell center of volcanic unit and the uppermost part of the lower carbonate-rock aquifer (LCA) or the lower carbonate-rock aquifer (thrusted) (LCA\_T1). The hydraulic gradient was calculated by extracting simulated hydraulic heads from the MODFLOW output file *HEADSOUT.txt* and MODFLOW input files *ibound1.asc*, *lay1\_wt\_sim.asc* and *layx\_top.asc* (where x = 1, 2, ..., 16 is the layer index number) using utility code *DVRF5-vgrad.F90* (Table 2). All these files are included in file *pdt2\_mf2005\_inp.zip*. In Figure 9b, the vertical hydraulic gradient was calculated using the simulated heads at the water table and the uppermost node in the LCA or the LCA\_T1. The upper carbonate-rock aquifer (UCA) was not used to define the Paleozoic contact because it comprises only 0.12% by volume of the site-scale saturated zone flow model (SNL 2007 [DIRS 177391], Table 6-5). The upper clastic-rock confining unit (UCCU) and lower clastic-rock confining unit (thrusted) (LCCU\_T1) were also not included because they are confining units. In both analyses, if neither the LCA nor the LCA\_T1 was present in a specific location, the upper boundary of the next lower unit below the LCA was used in the hydraulic gradient calculation (i.e., the uppermost node of either the lower clastic confining unit (LCCU), the crystalline confining unit (XCU) or the intrusive confining unit (ICU)). Vertical gradient was not calculated for areas where the carbonate aquifer is absent or the Paleozoic units outcrop.

Contour maps of the vertical hydraulic gradient from the Case 5 simulation, generated as defined above are shown in Figures 9a and 9b. A positive value indicates an upward gradient and a negative value indicates a downward gradient. Figures 9a and 9b show that there is an upward vertical gradient from the Paleozoic carbonate aquifer near the Yucca Mountain repository. This is consistent with the observed head differences in the vicinity of wells UE-25 p#1 and NC-EWDP-2D/2DB as discussed above and with the simulation result from the site-scale SZ flow model presented in the DOE responses to RAI 3.2.1.3.8-003. After the predominant

groundwater flowpaths originating from Yucca Mountain enter Amargosa Desert, the vertical gradient is changed to be slightly downward, before recovering to be moderately upward further south along the flow paths. The location of this transition zone is somewhat different from that estimated from the site-scale flow model (see Figure 1.2 of the DOE responses to RAI 3.2.1.3.8-003) due to the differences between the site-scale SZ flow model and the Death Valley regional flow model discussed in *Saturated Zone Site-Scale Flow Model* (SNL 2007 [DIRS 177391], Section 6.5.2.2) and SAR Section 2.3.9.2.2.3, pp. 2.3.9-21 and 2.3.9-22. Similar patterns of vertical gradients are shown for the two methods of calculating the vertical gradient (carbonate to volcanic and carbonate to water table). In comparison with Figure 9a, Figure 9b shows that the vertical gradient between the carbonate aquifer and the overlying volcanic aquifer is generally similar to that between the carbonate aquifer and the water table (i.e. the combined alluvial-volcanic aquifers), although there are some differences where the volcanic aquifer units are absent (most noticeably east and northeast of Yucca Mountain).

In addition, Figures 9c and 9d present simulated vertical hydraulic gradients for the pre-pumping condition. Similar to Figure 9a, Figure 9c plots the vertical hydraulic gradient that was calculated using the simulated head values at the lowermost volcanic unit in the Crater Flat Group and the uppermost part of LCA or LCA\_T1. Similar to Figure 9b, Figure 9d presents the vertical hydraulic gradient that was calculated using the simulated head values at the water table and the uppermost node in the LCA or the LCA\_T1. When compared to Figures 9a and 9b, respectively, Figures 9c and 9d show that post-development pumping in, for example, Amargosa Desert, Specter Range, and Pahrump Valley since year 1912 has resulted in slight changes of the upward gradient between the carbonate aquifer and overlying alluvial-carbonate aquifers. In areas of Pahrump Valley southeast of Yucca Mountain and away from the flow paths, pumping causes the reversal of the vertical hydraulic gradient from slightly upward to slightly downward. In the Amargosa Desert along the flow paths south and southwest of Yucca Mountain, the opposite effect is noticed—pumping from the shallow alluvial aquifer actually helps to change the gradient from slightly downward to slightly upward. Elsewhere, and including in the immediate vicinity of the Yucca Mountain, however, the upward hydraulic gradient is not significantly impacted.

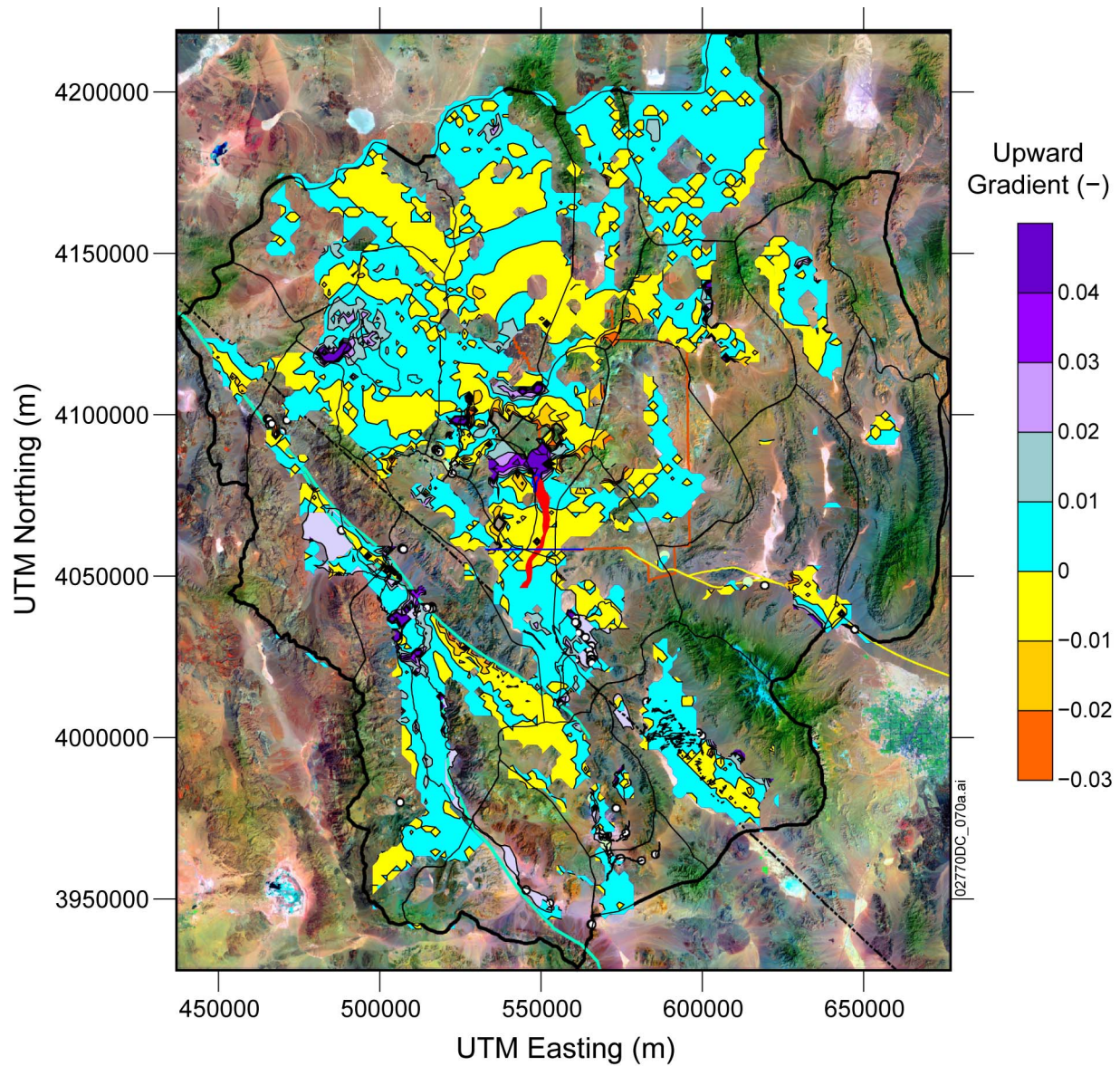
Figures 9e and 9f show the vertical gradients calculated for year 2453. The figures indicate that continuous pumping would result in a nearly complete reversal of the downward gradient in the Amargosa Desert, and some localized expansion or contraction of areas of downward gradient in Pahrump Valley. For years 2016 and 2453, there are no significant changes to the hydraulic gradient in the Death Valley area. This trend can also be clearly seen in Figure 9g which presents the change of vertical gradient with time at Amargosa Desert (an area of heavy pumping) and near wells UE-25 p#1 and NC-EWDP-2DB (where upward gradients from the carbonate aquifer are observed). Figure 9g shows that pumping causes a decline in the vertical gradient in mid 1990s near UE-25 p#1 and NC-EWDP-2DB, after which it rebounds. Throughout the simulation period, the gradient near UE-25 p#1 remains upward from the carbonate aquifer to the water table. Although the DVRFS model simulated a slightly downward vertical gradient in the cell containing NC-EWDP-2DB, which is explained below, the gradient also trends up with time as influenced by pumping. The effect of pumping is most pronounced in the heart of pumping wells at Amargosa Desert. In Row 117, Column 72, for example, heavy pumping from the shallow production wells actually helps to increase the gradient from slightly downward to moderately upward.



Source: *vgrad-carb2wt.png* in *Vgrad-Surfer.zip*.

NOTES: Hydraulic gradient is upward if positive and downward if negative. Red curves are particle tracks from the repository simulated with the site-scale saturated zone flow model.

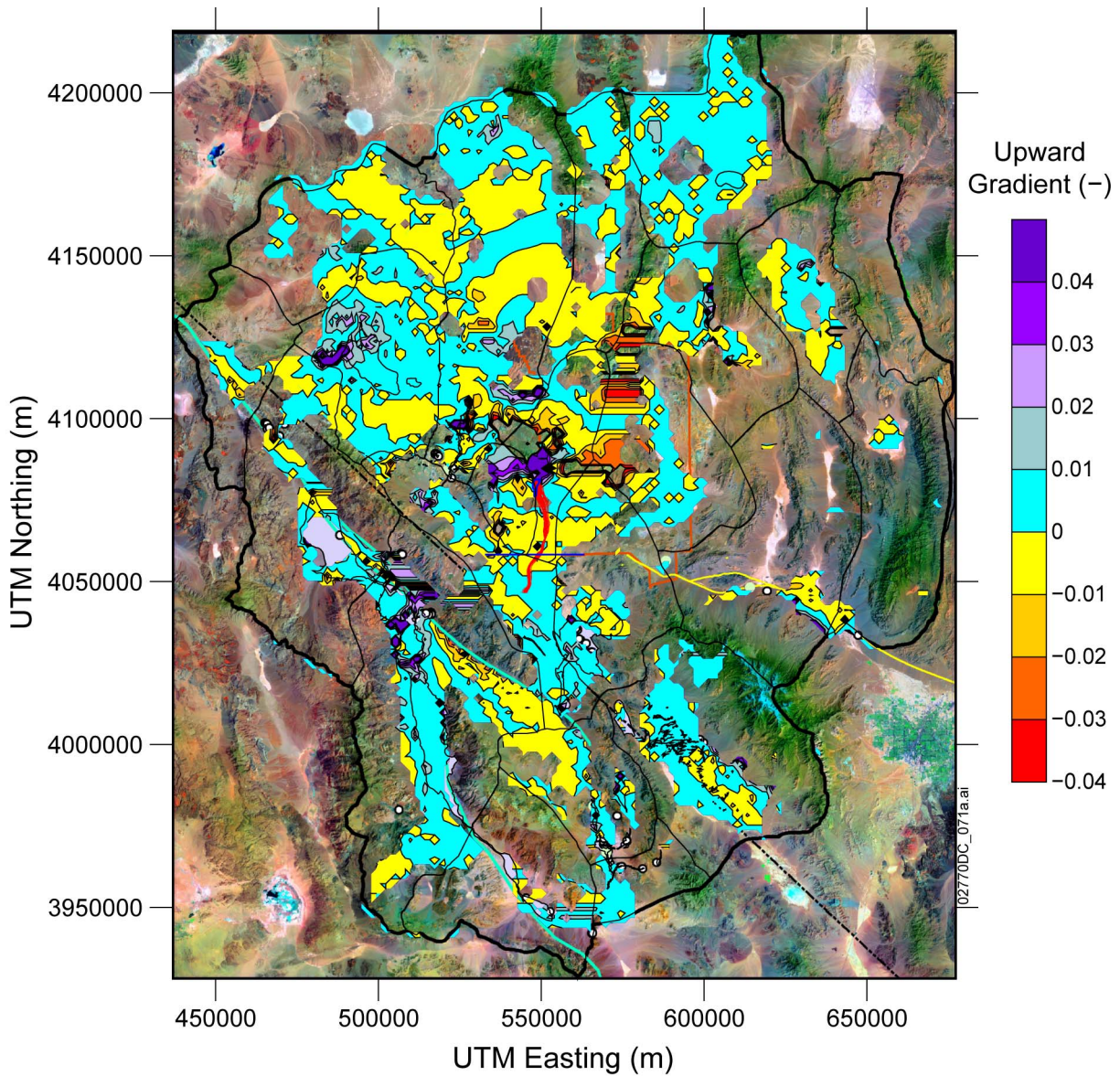
Figure 9a. Simulated Vertical Hydraulic Gradient between the Carbonate Aquifer (or Deeper Crystalline Units) and the Water Table for Case 5 for Year 2016



Source: *vgrad-carb2volc.png* in *Vgrad-Surfer.zip*.

NOTES: Hydraulic gradient is upward if positive and downward if negative. Red curves are particle tracks from the repository simulated with the site-scale saturated zone flow model.

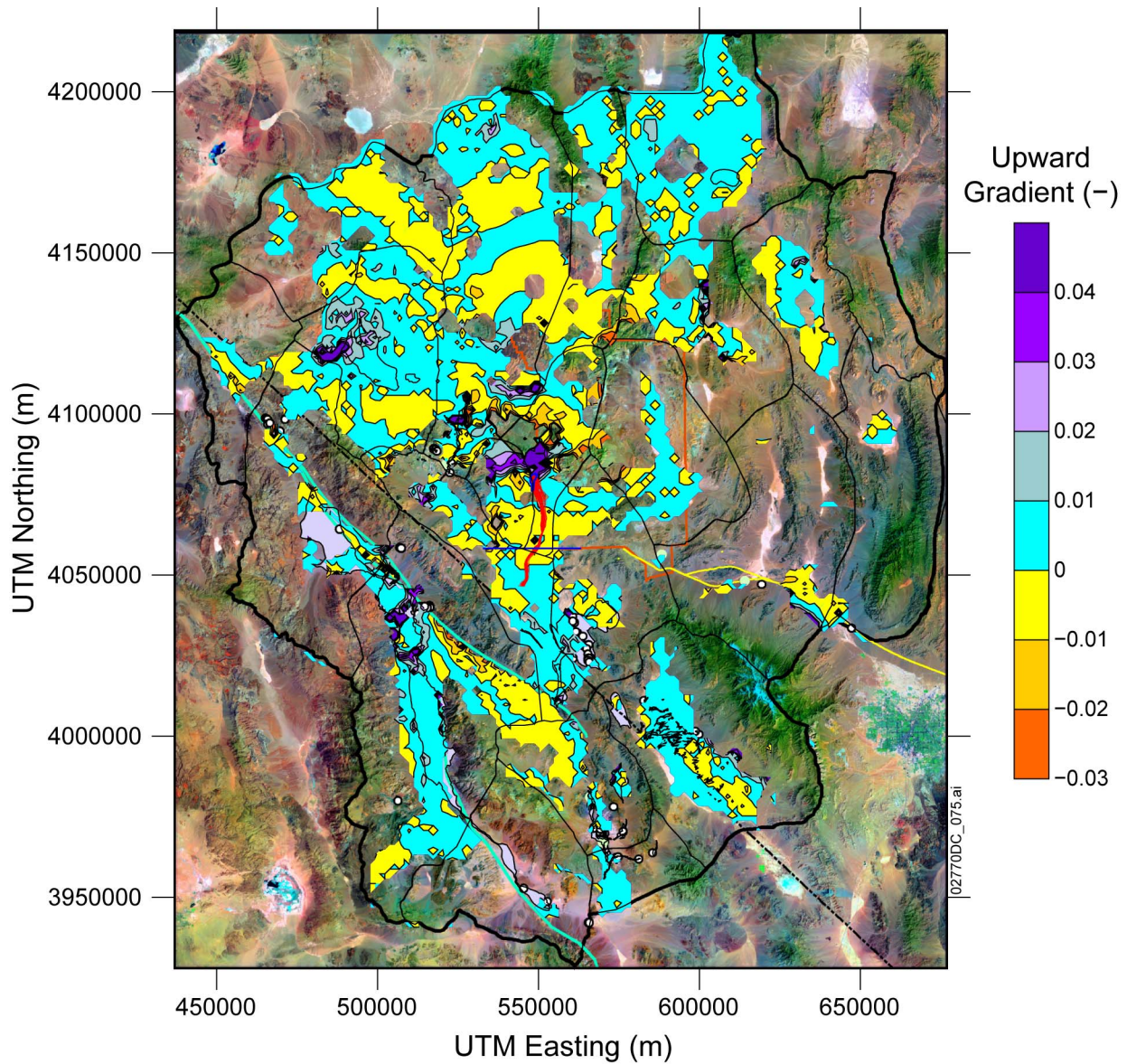
Figure 9b. Simulated Vertical Hydraulic Gradient between the Carbonate Aquifer (or Deeper Crystalline Units) and the Overlying Volcanic Aquifer for Case 5 for Year 2016



Source: *vgrad-carb2wt-t0.png* in *Vgrad-Surfer.zip*.

NOTES: Hydraulic gradient is upward if positive and downward if negative. Red curves are particle tracks from the repository simulated with the site-scale saturated zone flow model.

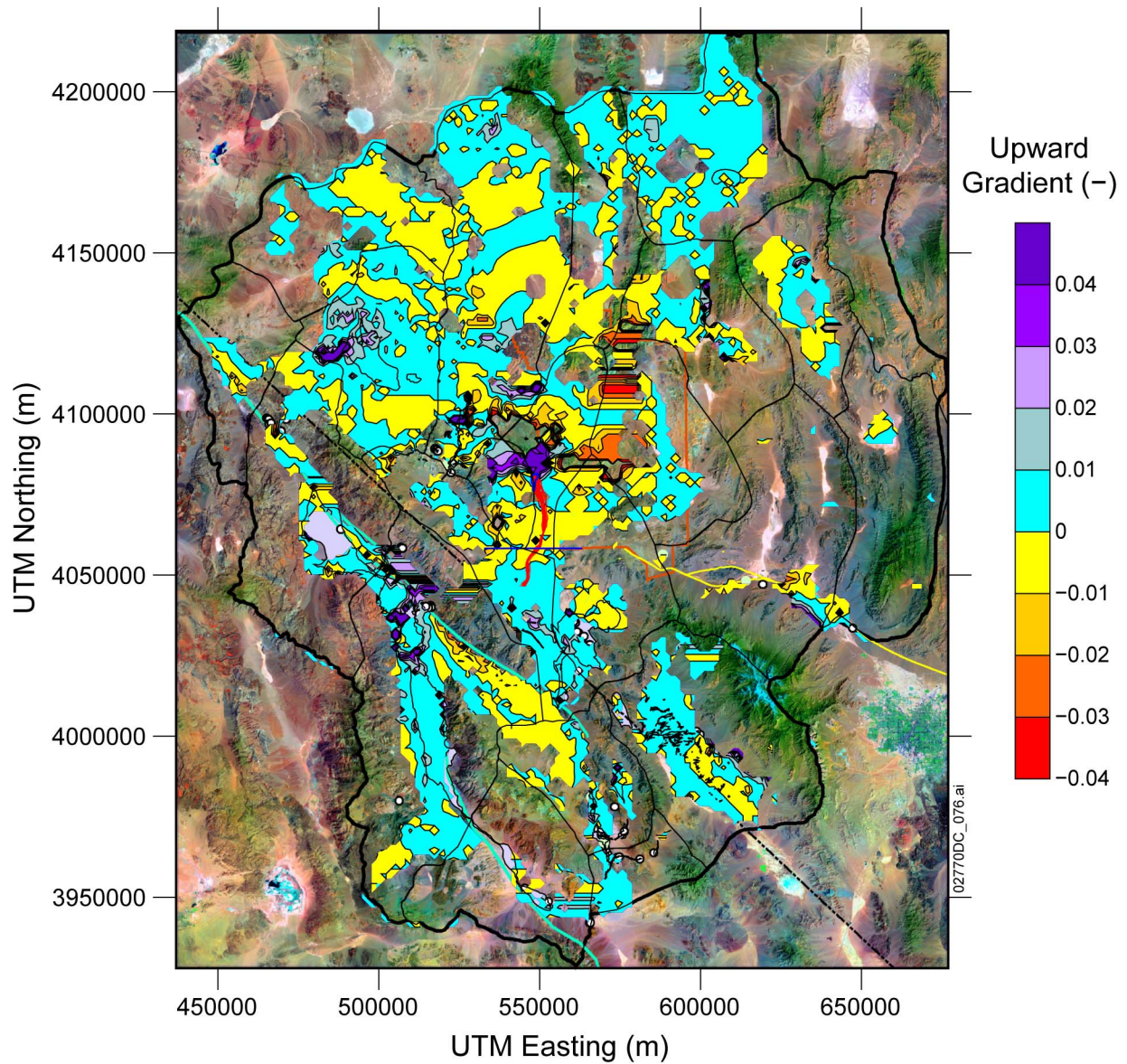
Figure 9c. Simulated Vertical Hydraulic Gradient between the Carbonate Aquifer (or Deeper Crystalline Units) and the Water Table for the Pre-pumping Condition (Stress Period 1 from Case 5)



Source: *vgrad-carb2volc-t0.png* in *Vgrad-Surfer.zip*.

NOTES: Hydraulic gradient is upward if positive and downward if negative. Red curves are particle tracks from the repository simulated with the site-scale saturated zone flow model.

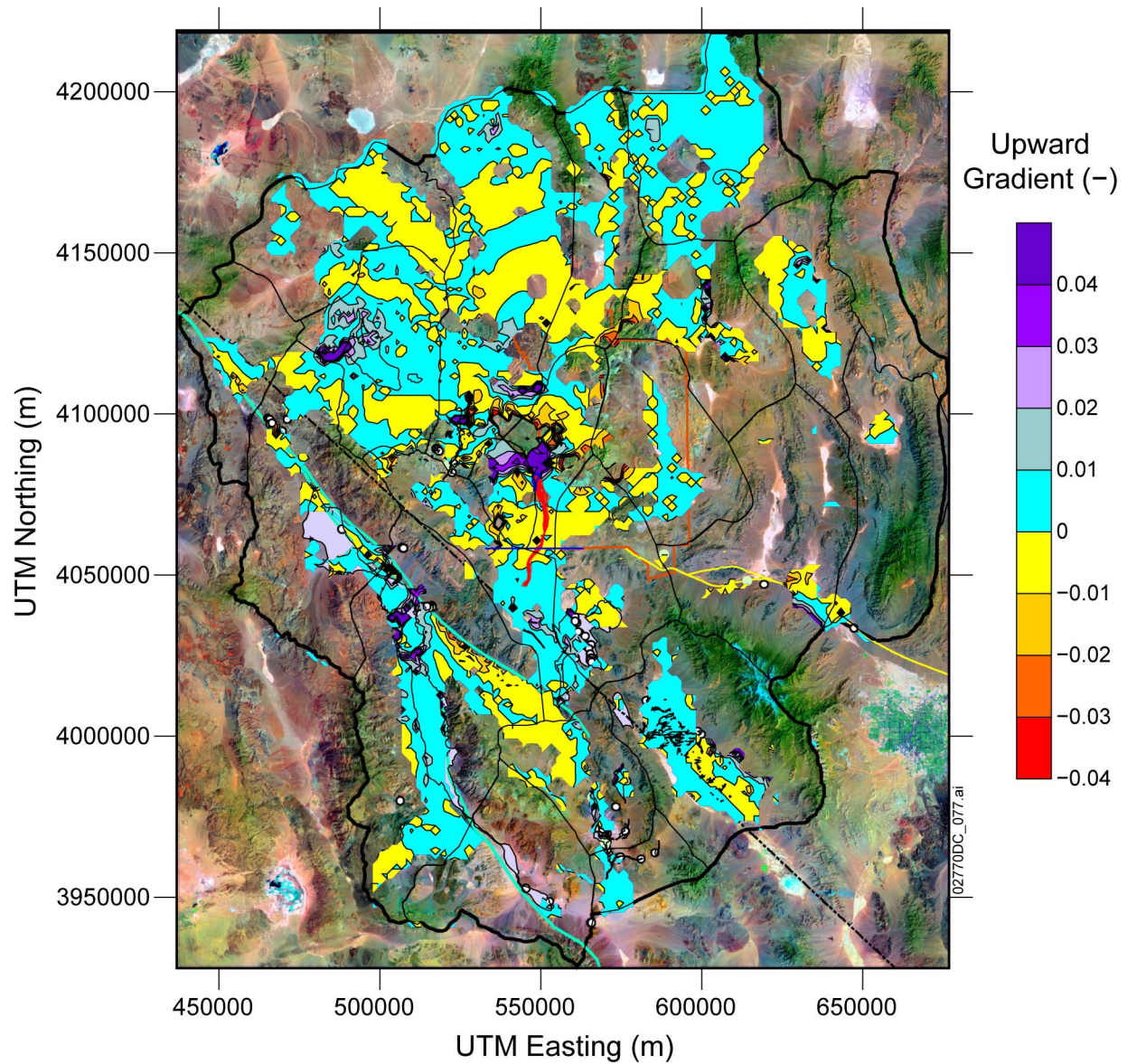
Figure 9d. Simulated Vertical Hydraulic Gradient between the Carbonate Aquifer (or Deeper Crystalline Units) and the Overlying Volcanic Aquifer for the Pre-pumping Condition (Stress Period 1 from Case 5)



Source: *vgrad-carb2wt-2453.png* in *Vgrad-Surfer.zip*.

NOTES: Hydraulic gradient is upward if positive and downward if negative. Red curves are particle tracks from the repository simulated with the site-scale saturated zone flow model.

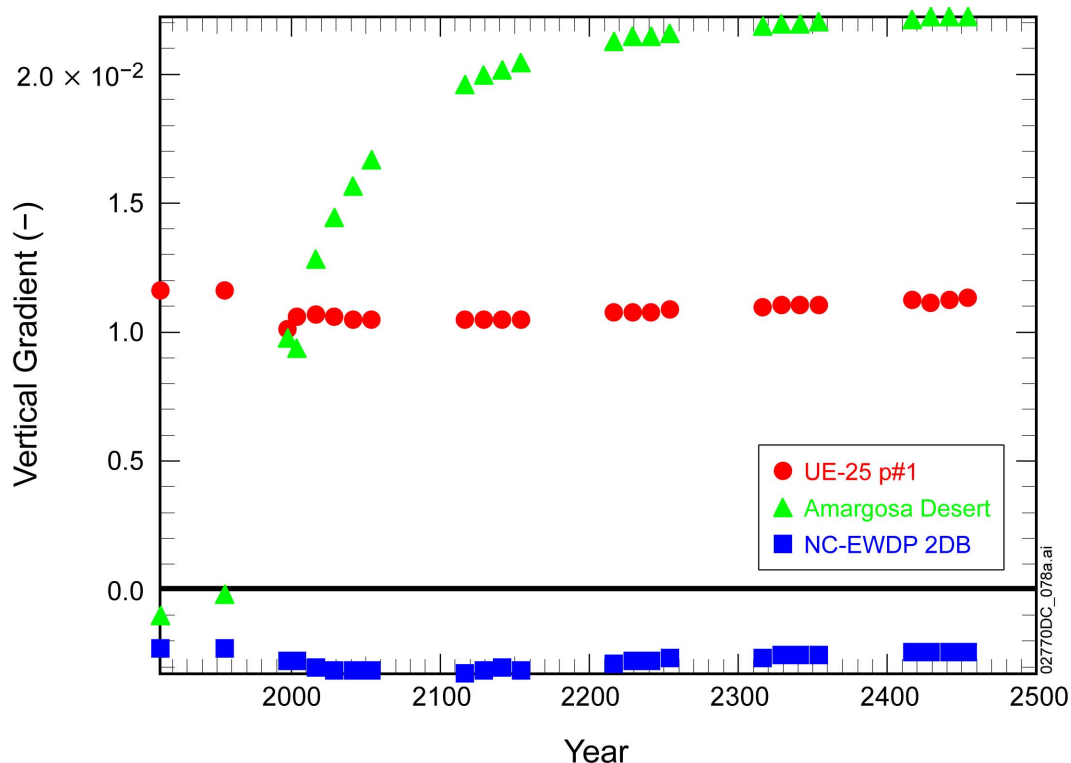
Figure 9e. Simulated Vertical Hydraulic Gradient between the Carbonate Aquifer (or Deeper Crystalline Units) and the Water Table for Case 5 for Year 2453



Source: *vgrad-carb2volc-2453.png* in *pdt2\_mf2005\_inp.zip*.

NOTES: Hydraulic gradient is upward if positive and downward if negative. Red curves are particle tracks from the repository simulated with the site-scale saturated zone flow model.

Figure 9f. Simulated Vertical Hydraulic Gradient between the Carbonate Aquifer (or Deeper Crystalline Units) and the Overlying Volcanic Aquifer for Case 5 for Year 2453



Source: *Vgrad\_local.xlsx* in *pdt2\_mf2005\_inp.zip*.

NOTES: Hydraulic gradient is upward if positive and downward if negative.

Figure 9g. Vertical Hydraulic Gradient between the Carbonate Aquifer (or Deeper Crystalline Units) and the Water Table as a Function of Time (Case 5)

Simulated hydraulic head, drawdown, and hydraulic gradients are also evaluated at the key locations of wells UE-25 p#1 and NC-EWDP-19D with the DVRFS model for Cases 1 to 5. Well UE-25 p#1 is located approximately 3 km downgradient of the repository and is a location at which the vertical hydraulic gradient between the regional Paleozoic carbonate aquifer and the overlying volcanic units has been measured. Well NC-EWDP-19D is approximately located where the inferred flow paths from beneath the repository in the saturated zone cross the 18-km boundary of the accessible environment. Simulated values of head are given for all five modeling cases in Table 6. The simulated values of drawdown in head relative to Case 1 are given in Table 7 for Cases 2 to 5. The values of average simulated vertical hydraulic gradient between the carbonate aquifer and the volcanic unit at the location of well p#1 for all cases is given in Table 8. The values of average horizontal gradient near the water table between the locations of well p#1 and 19D are also given in Table 8. Values of simulated vertical hydraulic gradient are calculated based on a vertical distance of about 1,078 m between layers 1 and 12 of the DVRFS model. Values of horizontal hydraulic gradient are calculated based on a horizontal distance of 18,248 m between the model cell centers for the cells containing wells p#1 and 19D.

Table 6. Simulated Hydraulic Head at the Approximate Locations of Well UE-25 p#1 and Well NC-EWDP-19D

Location	Simulated Head (m)				
	Case 1 (steady state) <sup>a</sup>	Case 2 (steady state) <sup>b</sup>	Case 3 (steady state) <sup>c</sup>	Case 4 (500 years of pumping) <sup>d</sup>	Case 5 (500 years of pumping) <sup>e</sup>
Well p#1 (volcanics)	729.2	685.2	727.0	724.3	724.2
Well p#1 (carbonate)	741.7	697.6	738.7	736.5	736.4
Well 19D (alluvium)	713.0	664.3	711.1	703.1	703.0

Sources: <sup>a</sup>file: test1.LIS in pdss1\_mf2k.zip

<sup>b</sup>file: test5.LIS in pdss5\_mf2k.zip

<sup>c</sup>file: test6.LIS in pdss6.zip

<sup>d</sup>file: HEADSOUT.txt in pdt1\_HEADSOUT.zip

<sup>e</sup>file: HEADSOUT.txt in pdt2\_HEADSOUT.zip

Table 7. Simulated Drawdown Relative to Pre-pumping Conditions at the Approximate Locations of Well UE-25 p#1 and Well NC-EWDP-19D

Location	Simulated Drawdown (m)			
	Case 2 (steady state)	Case 3 (steady state)	Case 4 (500 years of pumping)	Case 5 (500 years of pumping)
Well p#1 (volcanics)	44.0	2.2	4.9	5.0
Well p#1 (carbonate)	44.1	3.0	5.2	5.3
Well 19D (alluvium)	48.7	1.9	9.9	9.9

Table 8. Simulated Hydraulic Gradients at the Approximate Location of Well UE-25 p#1 and between the Location of Well UE-25 p#1 and Well NC-EWDP-19D

Location	Average Hydraulic Gradient				
	Case 1 (steady state)	Case 2 (steady state)	Case 3 (steady state)	Case 4 (500 years of pumping)	Case 5 (500 years of pumping)
Vertical Gradient at Well p#1 (carbonate to volcanics)	$1.16 \times 10^{-2}$ (upward)	$1.15 \times 10^{-2}$ (upward)	$1.09 \times 10^{-2}$ (upward)	$1.13 \times 10^{-2}$ (upward)	$1.13 \times 10^{-2}$ (upward)
Horizontal Gradient Between Well p#1 and Well 19D (shallow)	$8.88 \times 10^{-4}$	$1.15 \times 10^{-3}$	$8.71 \times 10^{-4}$	$1.16 \times 10^{-3}$	$1.16 \times 10^{-3}$

The steady-state results for Case 2 show large drawdown in head, a slight decrease in the magnitude of the upward vertical gradient at p#1, and a moderate increase in the horizontal hydraulic gradient in the area between the repository and the boundary of the accessible environment. A drawdown of about 40 to 50 m is simulated to occur for all locations, with a somewhat greater drawdown in the carbonate aquifer at well p#1. The upward vertical gradient is maintained at well p#1 and it is decreased in magnitude by about 1%, relative to Case 1. The average horizontal hydraulic gradient near the water table between the locations of well p#1 and well 19D is increased by about 30%.

The steady-state results for Case 3 show patterns of drawdown and hydraulic gradients similar to those from Case 2, but with diminished impacts. Simulated drawdown in head relative to Case 1 ranges from about 2 m to about 3 m for these locations. The upward vertical gradient at p#1 is decreased by about 6% and the horizontal gradient is decreased by about 2%.

Results for Case 4 and Case 5 indicate moderate drawdown in head at these locations, a minor decrease in the upward vertical hydraulic gradient at p#1, and a modest increase in the horizontal hydraulic gradient between the repository and the 18-km boundary. Simulated drawdown of about 5 m after 500 years of pumping occurs at the location of well p#1, with slightly greater drawdown in the carbonate aquifer versus the volcanic aquifer (4.9 m versus 5.2 m drawdown in Case 4). Drawdown at the location of well 19D is about 10 m and is greater than at well p#1, as expected given that well 19D is located closer to pumping wells in the Amargosa Desert than well p#1. The upward vertical gradient at well p#1 is maintained after more than 500 years of pumping in Case 4 and Case 5, but is decreased in magnitude by only about 3%. The average horizontal hydraulic gradient near the water table between the locations of well p#1 and well 19D is increased by about 31% relative to Case 1 because of the greater drawdown in the area of well 19D. The additional pumping in Case 5 has no significant impact on the drawdown or changes in hydraulic gradients, relative to Case 4.

Overall, these results from the DVRFS model indicate that the upward vertical hydraulic gradient between the carbonate aquifer and the overlying volcanic aquifer in the area of Yucca Mountain is maintained even for long periods of pumping from the regional groundwater flow system. Decreases in the magnitude of the upward vertical gradient with long-term pumping are small. Increases in the horizontal hydraulic gradient along the inferred flow paths in the saturated zone from beneath Yucca Mountain are modest and well within the envelope of uncertainty in the groundwater specific discharge multiplier used in radionuclide transport simulations for the TSPA model (SNL 2008 [DIRS 183750], Section 6.5.2.1[a]). Case 2 likely overestimates the impacts of pumping given the long time required to achieve the steady-state conditions represented in this model and the intolerably large drawdowns in groundwater levels on a regional basis.

### **Limitations of the DVRFS Model**

When interpreting DVRFS model results, several caveats are noted. While overall the model does a good job of simulating water levels, flow paths, and specific discharges, it must be noted that this is a “regional” model and only regional conclusions should be drawn. That is, flow paths may be representative of general flow directions, but it would be inappropriate to query the model for the deepest penetration of a particle and suggest that flow paths reach exactly this

depth (at least not with any known certainty). Moreover, the coarseness of the DVRFS model grid (1,500 × 1,500 m in the horizontal and 16 layers in the vertical direction, as compared to 250 × 250 m in the horizontal and 26 layers in the vertical direction in the site-scale SZ flow model) suggests that results should not be interpreted at a scale finer than a single cell. Also, while the global water budget has been conserved across the model domain, locally, it is expected that perhaps significant differences in recharge and discharge will exist. For example, in the middle of Death Valley, the model-estimated evapotranspiration rate from the middle basin (in model cell OBS-DV-MIDDLE) is more than three times that estimated with observation data (Belcher 2004 [DIRS 173179], Table F-4), suggesting that modeled flow paths might be preferentially drawn to this discharge point.

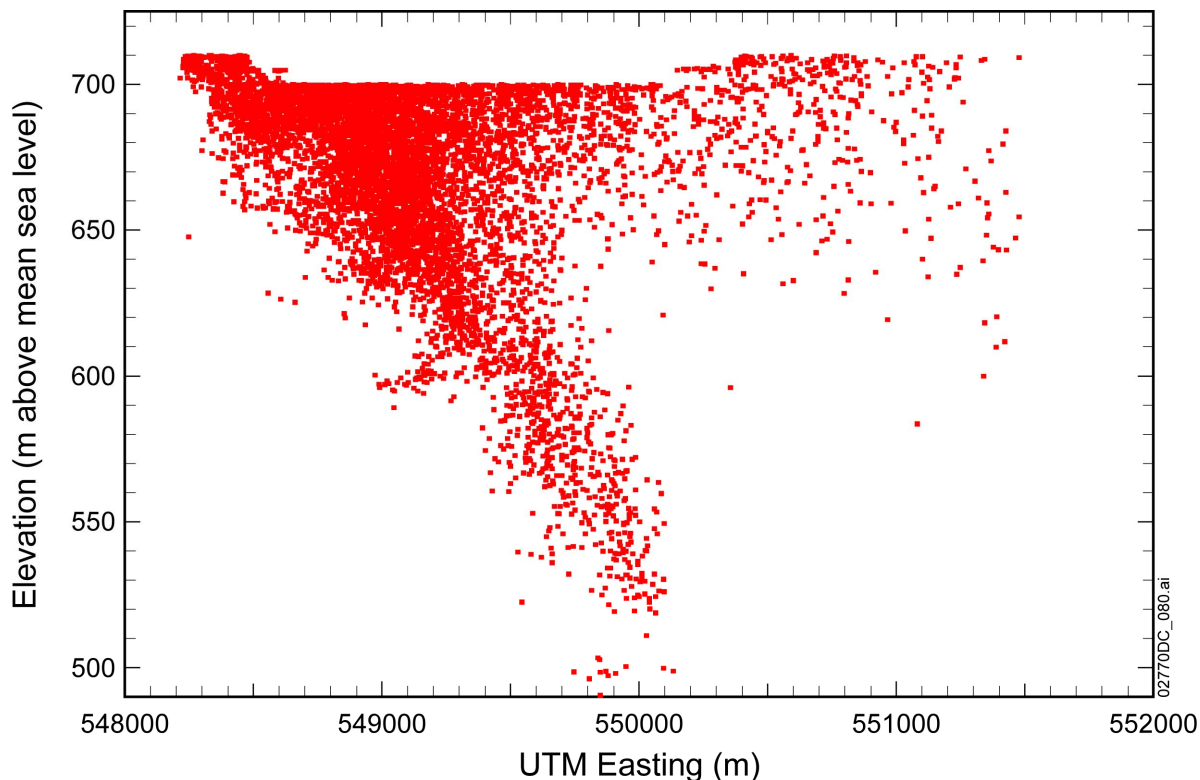
Nevertheless, while it is noted that each individual modeled scenario may not be globally accurate in space and time because of the approximations and assumptions built into the DVRFS model, much higher confidence can be placed in the relative differences between two modeled scenarios. For example, while the prediction of local water level might indicate a notable disparity from the observed water table (especially if no calibration data are available nearby), changes in predicted water levels due to various pumping scenarios can be estimated with more confidence. That is, relative differences between model results can be assessed with more confidence.

Overall, while using the DVRFS to draw conclusions about regional groundwater flow is appropriate, querying the model for detailed/local predictions should yield estimates that are considered with an appropriate level of uncertainty. For example, Figure 9g shows that the model-estimated vertical gradient for well NC-EWDP-2DB is nearly a constant downward gradient of  $-0.002$ , while an observed increase in head of 7.2 m at depth suggests an upward gradient of about 0.02 (BSC 2004 [DIRS 170009], Table 6-4 and Table A-6; SNL 2007 [DIRS 177391], Table 6-8). Because each model cell in the DVRFS model occupies an area of 2.25 km<sup>2</sup>, the model estimates only indicate, at best, results generalized to this scale. Moreover, an observation from a single well within this model cell should not be extrapolated to such a broad scale just as the model results should not be considered accurate at highly localized scales. An examination of model outputs also suggests other differences between the site-scale saturated zone flow model and the DVRFS model are due to differences in spatial discretization, the underlying hydrogeological framework model, and calibration of hydrologic properties. For instance, these differences are also responsible for the differences in simulated vertical gradients discussed earlier and seen in Figure 1.2 of the RAI 3.2.1.3.8-003 responses and Figures 9a and 9c presented herein. For the area of UTM Northing  $\sim 4075000$  m and  $\sim 4055000$  m, the DVRFS model predicts a larger area of downward gradient (Figures 9a and 9c) and nearly all of the particle tracks penetrating the lower carbonate aquifer in or near the Amargosa Desert before reemerging in the overlying volcanic and discharging into the alluvial unit into the floor of Death Valley (files: *ptrack-unit\_pdss1.dat* in *ptrack-unit\_pdss1.zip* and *ptrack-unit\_pdss5.dat* in *ptrack-unit\_pdss5.zip*), while Figure 1.2 of the RAI 3.2.1.3.8-003 responses show that the site-scale model predicts the particles would stay within the overlying units between the accessible environment and the Amargosa Desert.

For these reasons, this analysis places an emphasis on interpreting the DVRFS model results in terms of relative changes between the pumping and non-pumping conditions.

## 4.2 ESTIMATED RADIONUCLIDE PLUME AT THE ACCESSIBLE ENVIRONMENT

Of the 10,000 particles released from below the repository, 8,024 particles cross the accessible environment boundary. Figure 10 shows the locations of these particles at the accessible environment boundary. The “plume” at the access environment boundary is approximately 3,300 m wide (from 548,200 m to 551,500 m Easting UTM). At this boundary, the particle locations are dispersed through DVRFS model layers 1 through 4, to a depth of about 220 m below the current water table.



Source: *InjectionPoints.pxp (Igor) in FigureFiles.zip.*

Figure 10. Locations of Particles Released from below the Repository and Tracked with FEHM's SPTR Routine at the Accessible Environment Boundary

## 4.3 RESULTS OF PARTICLE TRACKING ANALYSIS FOR PRESENT-DAY CONDITIONS

Particle tracking results are presented in Figures 11 to 15 for Case 1 (pre-pumping), Case 2 (2003 estimate of long-term pumping rates), and Case 3 (reduced estimate of long-term pumping). Particles were released in the alluvial units in the DVRFS model as described in Section 4.2. Figure 10 is an estimate of the cross section of the plume at the 18-km accessible environment.

Figure 11a shows that without pumping (Case 1), particle tracks that originate from the plume at the accessible environment boundary would flow through Amargosa Desert toward the areas of

Furnace Creek springs and the floor of Death Valley, with a small fraction toward Alkali Flat (i.e., Franklin Lake Playa). Of the 8,024 particles originating at the accessible environment boundary, 8,023 particles generally follow the following flow path to first enter the volcanic aquifer, then through intervening layers travel through the lower carbonate aquifer, and then reemerge through the volcanic aquifer and discharge into cell Row 128, Column 49 in Layer 1 (see file: *ptrack-unit\_pdss1.dat* in *ptrack-unit\_pdss1.zip*). Layer 1 in this location corresponds to hydrostratigraphic unit 26 (file *ptrack-unit\_pdss1.dat* in *ptrack-unit\_pdss1.zip*), which is the YACU unit (Younger alluvial confining unit) (Belcher 2004 [DISR 173179], Table E-1). This model cell is located within the so-called middle basin of Death Valley labeled as OBS-DV-MIDDLE (see file *drb\_tr.txt* contained in *archive\_model\_tr.zip*, which is publicly released by the USGS). At this location, the DVRFS model-estimated evapotranspiration rate for the middle basin is more than three times that estimated with observation data (Belcher 2004 [DIRS 173179], Table F-4). Due to the uncertainties associated with the DVRFS model as discussed in Section 4.1, this discharge location should be generally regarded as the areas of Furnace Creek springs and the floor of Death Valley. One particle is predicted to discharge into cell Row 127, Column 82, Layer 1, which is within Alkali Flat.

Figure 11b illustrates the vertical flow paths for Case 1. Note that due to the uncertainties in the DVRFS model as discussed in Section 4.1, there are differences between this result and those simulated with the site-scale saturated zone flow model (see Figure 1.2 of the RAI 3.2.1.3.8-003 response). For example, while the result from the site-scale saturated zone flow model shows that the flow paths are relatively shallow and stay within the overlying units, the DVRFS model result indicates that some of the particle would flow downward into the lower carbonate aquifer along the flow paths in the northern Amargosa Desert area (see also file: *ptrack-unit\_pdss1.dat* in *ptrack-unit\_pdss1.zip* for details).

Detailed information about the hydrogeologic units along the simulated particle paths from the 18-km boundary are extracted from the DVRFS model for use in a simplified one-dimensional radionuclide transport model for SEIS analyses. Information on the radionuclide transport parameters of effective porosity, bulk density, and sorption coefficients for these hydrogeologic units is also provided. The average total flow path length between the 18-km boundary and discharge locations in Death Valley for particles in Case 1 is 55.9 km (see file: *jason\_dat.xls*). The percentages of the flow path length within each of the hydrogeologic units along the flow path and recommended values of radionuclide transport parameters are given in Table 9.

The information on the hydrogeologic units along the flow path for the non-pumping case (Case 1) was extracted from the particle tracking output for this case into the file *ptrack-units-pdss1.dat* using the utility code *DVRFS-vgrad.F90*. The total distance traveled in each hydrogeologic unit by each particle was extracted from the file *ptrack-units-pdss1.dat* using the utility codes *HGUloc.F90* and *HGU\_name.F90*. These data were then exported to the spreadsheet *jason\_dat.xls* for the calculation of average flow path lengths in each hydrogeologic unit. The FORTRAN utility code *xtract\_path\_LCA.for* was used to calculate the distances from the boundary of the accessible environment to each model cell in which the LCA unit was encountered by each particle using the data in the file *ptrack-units-pdss1.dat*. This output is contained in the file *LCA\_distr.dat*.

There is variation in the flow path length in the LCA (Lower Carbonate Aquifer) hydrogeologic unit and in the location where the LCA unit is encountered among the particles used in the flow path analysis. As indicated in Table 9, the average flow path length in the LCA unit is 40.4% of the total flow path length. Among all of the particles used in the analysis the 5th percentile of the total flow path length between the 18-km boundary and the discharge location in Death Valley is 35.1% and the 95th percentile is 49.2% (see file: *jason\_dat\_LCA\_range.xls*). The bulk of the flow path length in the LCA unit occurs along the flow paths beneath the Funeral Mountains. However, about 9% of the particles go deep enough beneath the northern Amargosa Desert in the first 15 km downgradient of the 18-km boundary to encounter the LCA unit in that area. Of the total percentage among all particles of about 40% of the flow path length in the LCA unit, about 39% occurs beneath the Funeral Mountains and about 1% occurs beneath the northern Amargosa Desert.

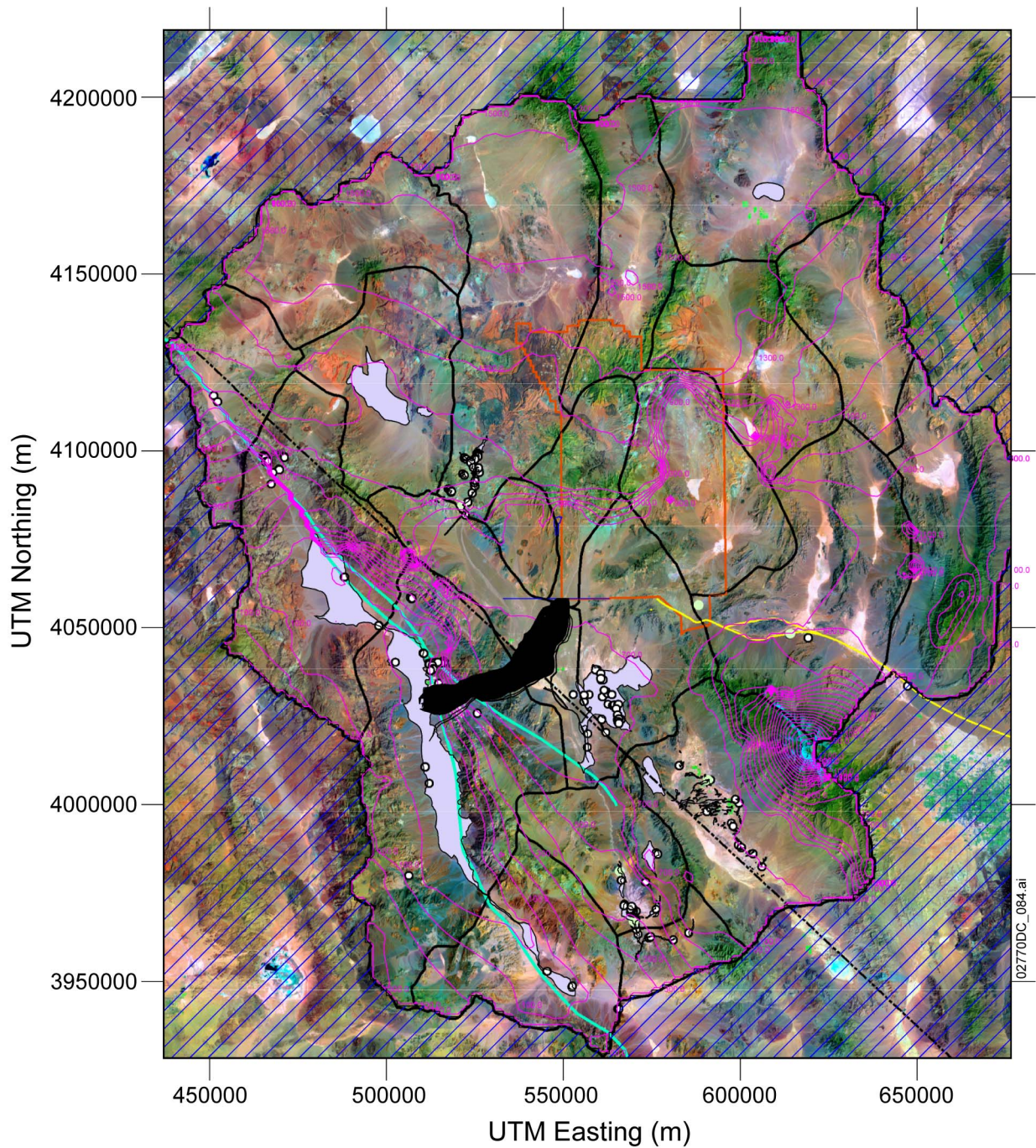
Values of effective porosity and bulk density are given for all of the hydrogeologic units for the non-pumping and the pumping cases, based on the expected values from the saturated zone flow and transport abstraction model (SNL 2008 [DIRS 183750]). Note that the Older Alluvial Aquifer (OAA), Upper Volcanic- and Sedimentary-Rock Unit (VSU), and Lower VSU hydrogeologic units consist of alluvium or basin-fill material and are assigned the median effective porosity and bulk density values of alluvium (SNL 2008 [DIRS 183750], Table 6-8, parameters NVF19, NVF7, and bulk density). The CFPPA (Crater Flat-Prow Pass Aquifer) unit is fractured tuff and assigned a value of effective porosity equal to the median of flowing interval (fracture) porosity (SNL 2008 [DIRS 183750], Table 6-8, parameter FPVO). In addition, the expected values of sorption coefficients for neptunium, uranium, plutonium, and americium for the Younger Alluvial Aquifer (YAA), Younger Alluvial Confining Unit (YACU), OAA, Upper VSU, CFPPA, and Lower VSU hydrogeologic units are also based on information from *Saturated Zone Flow and Transport Model Abstraction* (SNL 2008 [DIRS 183750]). Values of sorption coefficients for the LA and XCU hydrogeologic units are not given in Tables 9 and 10; these units constitute a minor fraction of the flow path length or, in the case of the LA unit in the pumping case, can be conservatively assumed to provide no sorption.

Expected values of sorption coefficients for the Lava-Flow Unit (LFU) and LCA hydrogeologic units are taken from evaluations of sorption data for similar rock types at the Idaho National Laboratory (INL) and the Waste Isolation Pilot Plant (WIPP), respectively. Primary sources of data on sorption coefficients were not compiled for the information presented in Tables 9 and 10. The LFU hydrogeologic unit is composed of basaltic lava flows in the area to the south of Yucca Mountain (Belcher et al. 2004 [DIRS 173179], Chapter B, p. 40) and the estimated INL performance assessment values of sorption coefficients on basalt from the report by Dicke (1997, Table 4) are assigned to this unit. The LCA hydrogeologic unit is lithologically variable, but contains significant dolomite (Belcher et al. 2004 [DIRS 173179], Chapter B, p. 63). The median values from the ranges of sorption coefficients for dolomite from the WIPP performance assessment (EPA 1998, Table 1) are assigned to the LCA unit.

One-dimensional radionuclide transport modeling along the flow paths from the 18-km boundary can be simplified by combining hydrogeologic units with identical transport parameter values and by disregarding hydrogeologic units that do not constitute a significant percentage of the flow path length. For example, in the non-pumping case the OAA, Upper VSU, and Lower VSU units are composed of alluvium along the flow path and can be combined into a single segment

that consists of about 48% of the total flow path length. Also, the Limestone Aquifer (LA), CFPPA, and Crystalline-Rock Confining Unit (XCU) hydrogeologic units are each less than 1% of the total flow path length for the non-pumping case and could reasonably be eliminated from the one-dimensional radionuclide transport model.

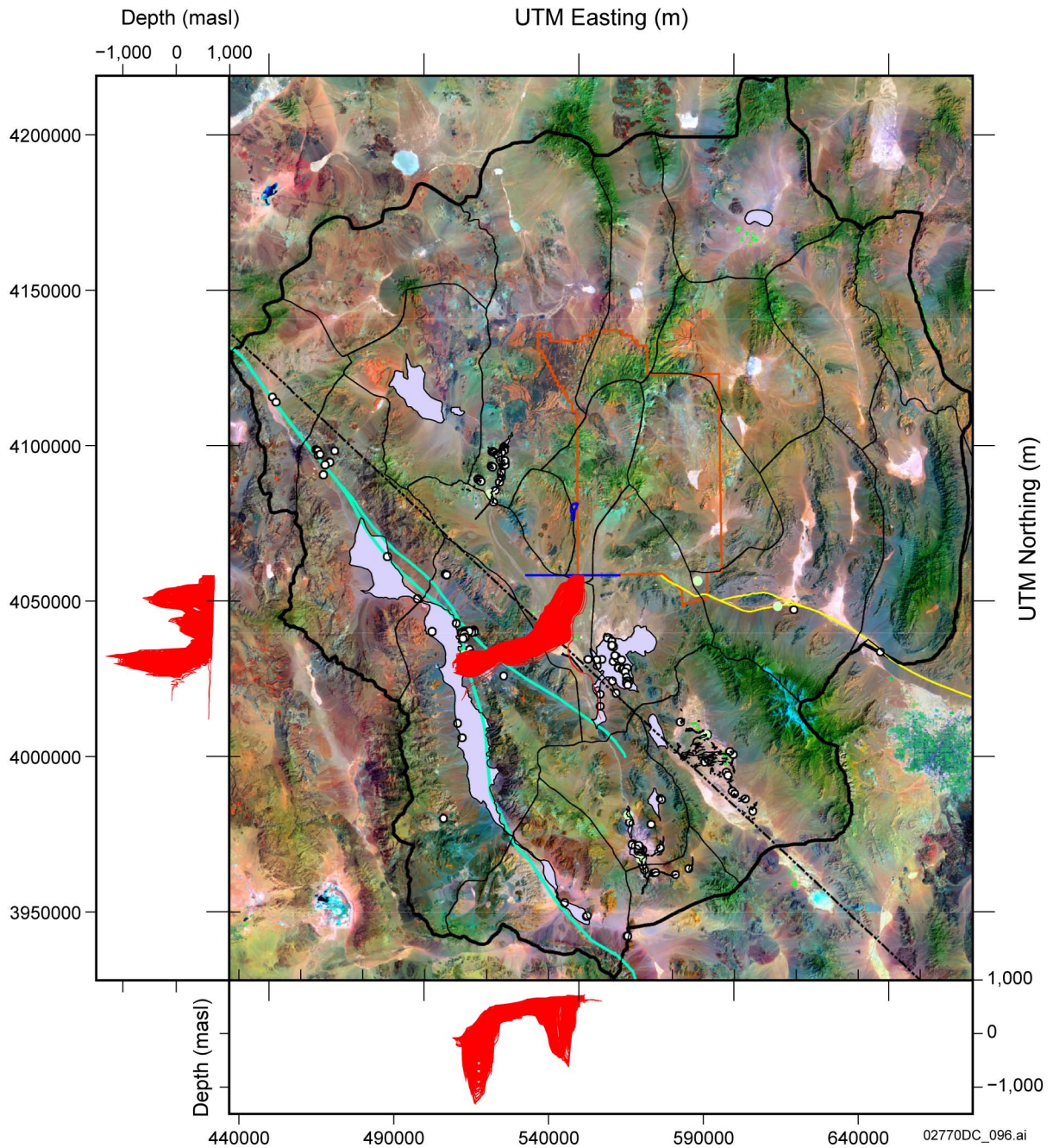
The histogram of particle specific discharges for the particle tracks for Case 1 is presented in Figure 12. Specific discharges were calculated as the average (across all particles) of the path length divided by the travel time for each particle. The minimum, average, and maximum specific discharges are  $1.04 \times 10^{-4}$ ,  $4.61 \times 10^{-4}$ , and  $1.63 \times 10^{-3}$  m/day, respectively.



Source: *PDSS1-ppaths.srf* in *PDSS1\_5-ptracks-figures.zip*.

NOTES: Purple contours are simulated heads for layer 1. Dense and thin black lines are particle tracks from 8,024 Particles that are released at the accessible environment boundary. The Nevada Test Site is outlined in red. Hatched areas outside of the Death Valley groundwater basin are treated as inactive cells in the model.

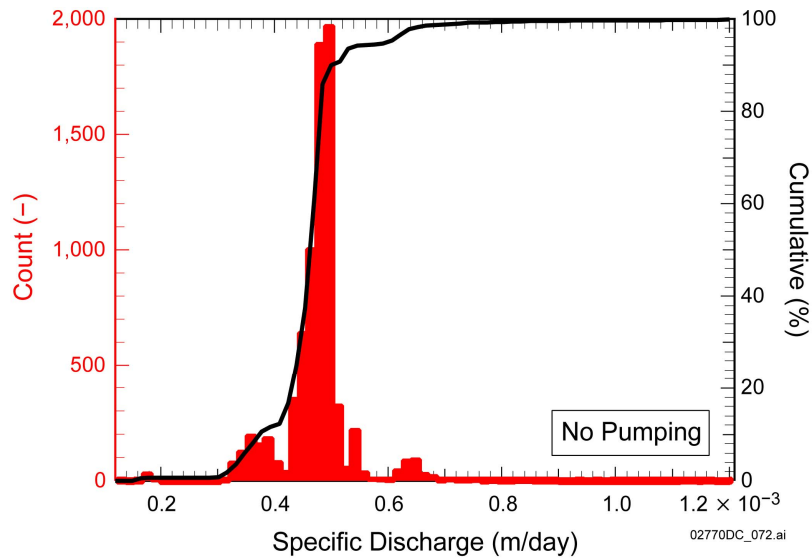
Figure 11a. Simulated Hydraulic Heads and Groundwater Flow Paths for the Pre-pumping Case (Case 1)



Source: *PDSS1-ppaths.srf* in *PDSS1\_5-ptracks-figures.zip*.

NOTES: The upper right figure shows the horizontal flow paths. The left and the lower figures show the vertical flow paths. Dense and thin red curves are particle tracks from 8,024 particles that are released at the accessible environment boundary. The Nevada Test Site is also outlined in red. The blue lines indicate the repository footprint and the accessible environment boundary.

Figure 11b. Simulated Horizontal and Vertical Groundwater Flow Paths for the Pre-pumping Case (Case 1)



Source: SPDISHist.pxp (Igor) in FigureFiles.zip.

Figure 12. Histogram of Specific Discharges for the 8,024 Particles Released at the Accessible Environment Boundary for the Pre-pumping Case (Case 1)

Table 9. Average Flow Path Lengths and Expected Transport Model Parameter Values in Hydrogeologic Units (Pre-pumping Case)

Hydrogeologic Unit Abbreviation <sup>a</sup>	Average % of Total Flow Path Length	Effective Porosity <sup>b</sup>	Bulk Density (g/cm <sup>3</sup> ) <sup>b</sup>	Np K <sub>d</sub> (mL/g)	U K <sub>d</sub> (mL/g)	Pu K <sub>d</sub> (mL/g)	Am K <sub>d</sub> (mL/g)
YACU	4.2	0.32	2.50	6.35 <sup>b</sup>	4.6 <sup>b</sup>	100. <sup>b</sup>	5500. <sup>b</sup>
OAA	1.8	0.18	1.91	6.35 <sup>b</sup>	4.6 <sup>b</sup>	100. <sup>b</sup>	5500. <sup>b</sup>
LA	0.4	0.01	2.77	-	-	-	-
LFU	6.0	0.08	2.44	8 <sup>d</sup>	3 <sup>d</sup>	100 <sup>d</sup>	70 <sup>d</sup>
Upper VSU	25.3	0.18	1.91	6.35 <sup>b</sup>	4.6 <sup>b</sup>	100. <sup>b</sup>	5500. <sup>b</sup>
CFPPA	0.2	0.001	1.84	1.435 <sup>b</sup>	6.78 <sup>b</sup>	104.2 <sup>b</sup>	5500. <sup>b</sup>
Lower VSU	21.2	0.18	1.91	6.35 <sup>b</sup>	4.6 <sup>b</sup>	100. <sup>b</sup>	5500. <sup>b</sup>
LCA	40.4	0.01	2.77	100.5 <sup>c</sup>	15.0 <sup>c</sup>	260. <sup>c</sup>	260. <sup>c</sup>
XCU	0.5	0.0001	2.65	-	-	-	-

Sources: % of total flow path length from file: jason\_dat.xls.

<sup>a</sup> Belcher et al. 2004 [DIRS 173179], Table E-1.

<sup>b</sup> SNL 2008 [DIRS 183750], Tables 6-8, 6-13, and 6-14.

<sup>c</sup> EPA 1998, Table 1.

<sup>d</sup> Dicke 1997, Table 4.

NOTE: Units that are less than 0.1% of the average total flow path length are not included in the table.

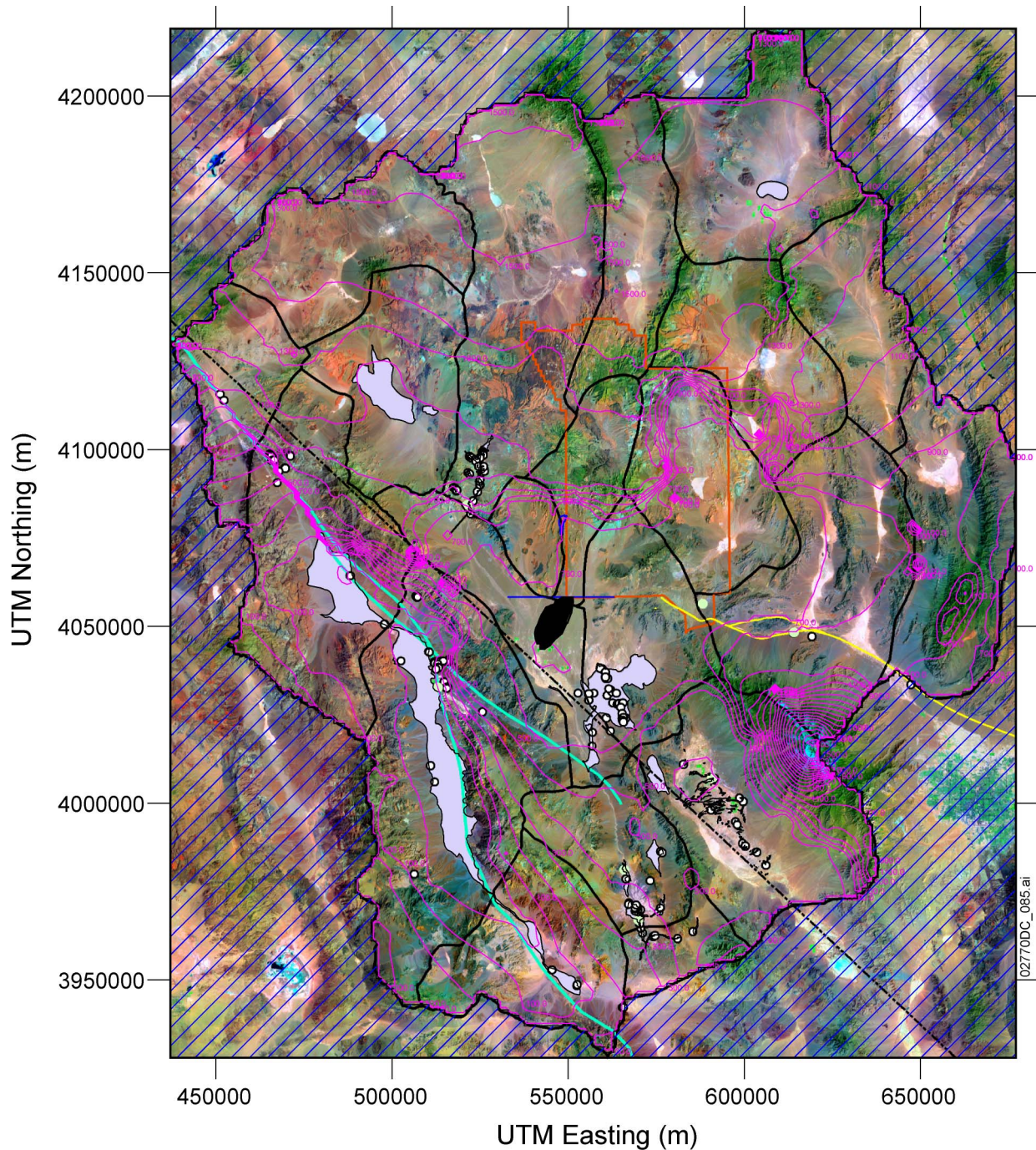
Figure 13a shows that with pumping at the 2003 level (Case 2), particle tracks originating from the plume area in alluvium layers 1 through 4 at the accessible environment boundary are fully

captured by pumping wells in Amargosa Farms. The model cell that corresponds to the discharge location is Row 117, Column 70, Layer 1 (see file: *ptrack-unit\_pdss5.dat* in *ptrack-unit\_pdss5.zip*). This result indicates that current level of pumpage would prevent further downgradient migration of dissolved contaminants to Furnace Creek, Ash Meadows, or Alkali Flat (i.e., Franklin Lake Playa).

Figure 13b illustrates the vertical flow paths for Case 2; additional details for this case can be found in file *ptrack-unit\_pdss5.dat* in *ptrack-unit\_pdss5.zip*. Similarly to Figure 11b, one should be cautioned that there are differences between this result and those simulated with the site-scale saturated zone flow model (see Figure 1.2 of the RAI 3.2.1.3.8-003 response) due to the uncertainties in the DVRFS as discussed in Section 4.1.

The average total flow path length between the 18-km boundary and discharge locations at pumping wells in Amargosa Desert for particles in Case 2 is 17.0 km. The percentages of the flow path length within each of the hydrogeologic units along the flow path and recommended values of radionuclide transport parameters are given in Table 10.

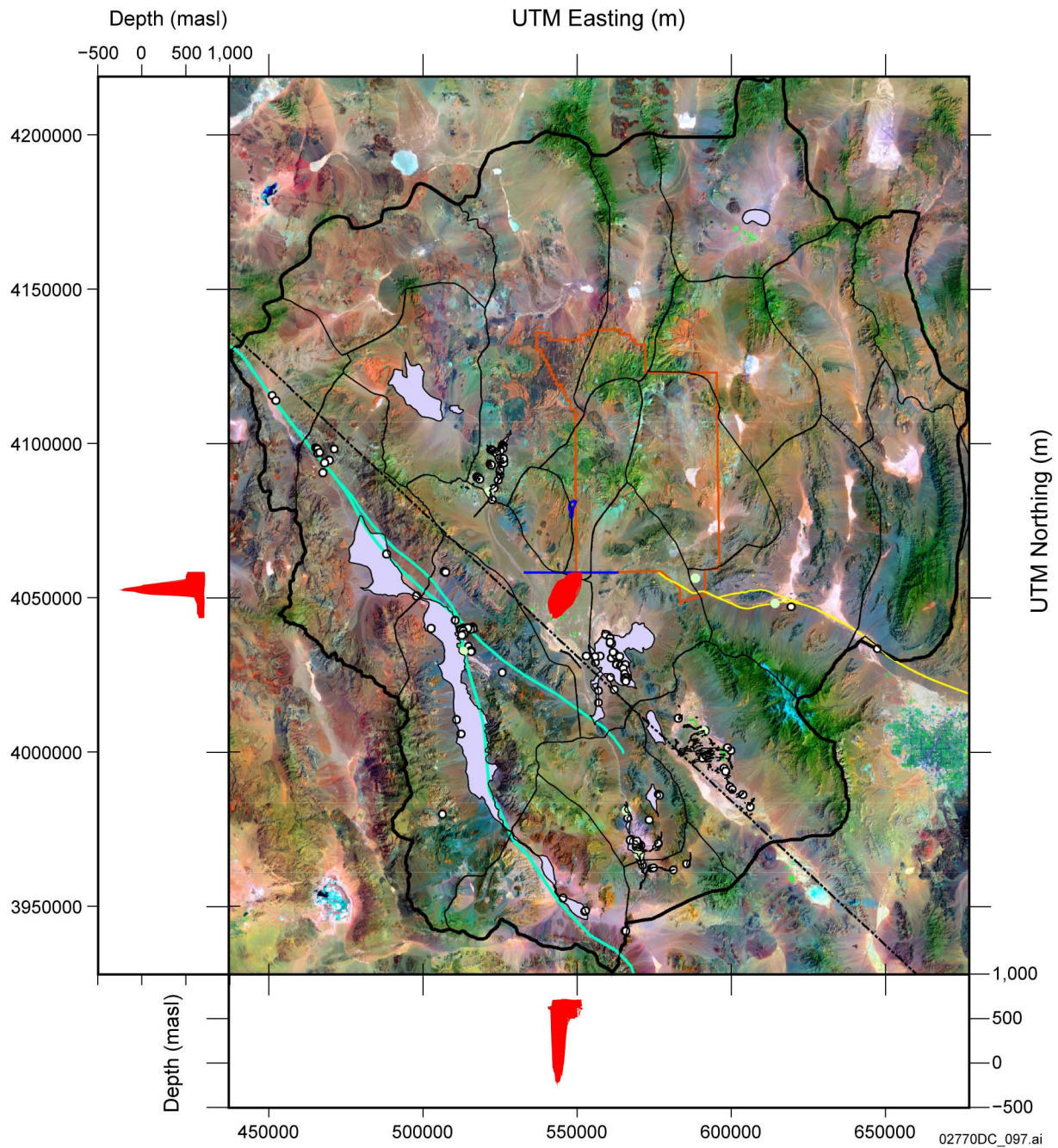
The histogram for the 8,024 particle tracks for Case 2 is shown in Figure 14. The minimum, average, and maximum specific discharges are  $2.90 \times 10^{-4}$ ,  $5.53 \times 10^{-3}$ , and  $8.38 \times 10^{-3}$  m/day, respectively. Specific discharges under the 2003 long-term pumping conditions are roughly seven times larger than those for steady-state (no pumping) conditions. Ranges for these pumping conditions are fairly broad (a factor of about 29) and this is a bit less than twice as broad as the range for steady-state conditions (whose range spans a factor of about 16).



Source: *pdss5.srf* in *pdss5\_mpath5.zip*.

NOTES: Purple contours are simulated heads for layer 1. Dense and thin black curves are particle tracks resulted from 8,024 Particles that are released at the accessible environment boundary. The Nevada Test Site is outlined in red. Hatched areas outside of the Death Valley groundwater basin are treated as inactive cells in the model.

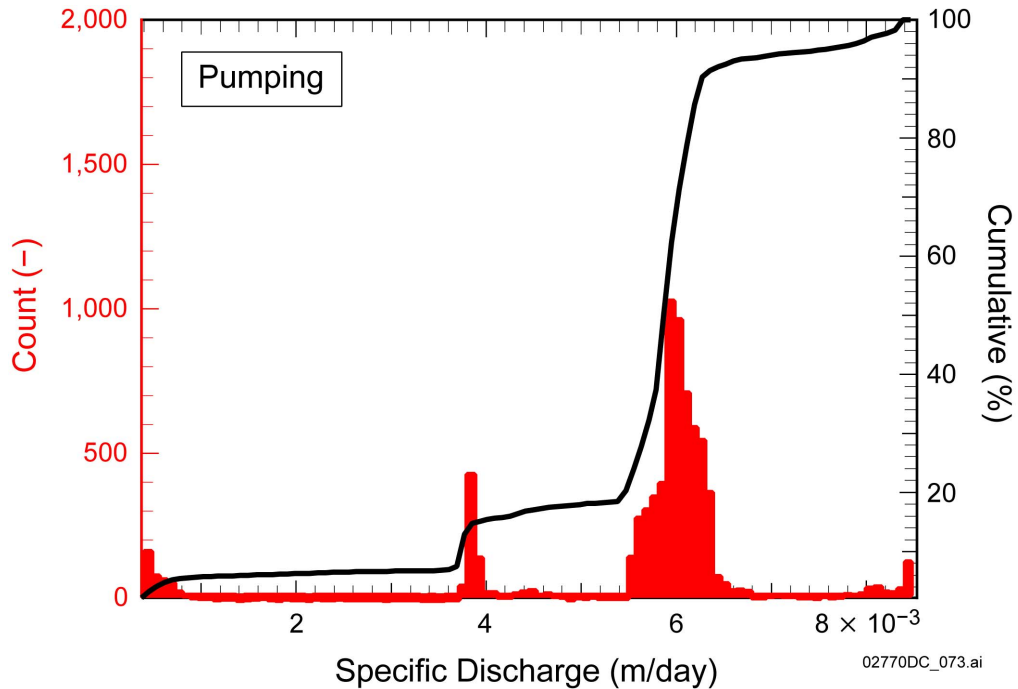
Figure 13a. Simulated Hydraulic Heads and Groundwater Flow Paths for the 2003 Estimate of Long-Term Pumping Rates (Case 2)



Source: *PDSS5-ppaths.srf* in *PDSS1\_5-ptracks-figures.zip*.

NOTES: The upper right figure shows the horizontal flow paths. The left and the lower figures show the vertical flow paths. Dense and thin red curves are particle tracks from 8,024 particles that are released at the accessible environment boundary. The Nevada Test Site is also outlined in red. The blue lines indicate the repository footprint and the accessible environment boundary.

Figure 13b. Simulated Horizontal and Vertical Groundwater Flow Paths for the 2003 Estimate of Long-Term Pumping Rates (Case 2)



Source: *SPDISHist.pxp (Igor) in FigureFiles.zip.*

Figure 14. Histogram of Specific Discharges for the 8,024 Particles Released at the Accessible Environment Boundary for the 2003 Estimate of Long-Term Pumping Rates (Case 2)

Table 10. Average Flow Path Lengths and Expected Transport Model Parameter Values in Hydrogeologic Units (Long-Term Pumping Case)

Hydrogeologic Unit Abbreviation <sup>a</sup>	Average % of Total Flow Path Length	Effective Porosity <sup>b</sup>	Bulk Density (g/cm <sup>3</sup> ) <sup>b</sup>	Np K <sub>d</sub> (mL/g)	U K <sub>d</sub> (mL/g)	Pu K <sub>d</sub> (mL/g)	Am K <sub>d</sub> (mL/g)
YAA	5.0	0.18	1.91	6.35 <sup>b</sup>	4.6 <sup>b</sup>	100 <sup>b</sup>	5,500. <sup>b</sup>
OAA	16.9	0.18	1.91	6.35 <sup>b</sup>	4.6 <sup>b</sup>	100 <sup>b</sup>	5,500. <sup>b</sup>
LA	6.9	0.01	2.77	-	-	-	-
LFU	6.6	0.08	2.44	8 <sup>c</sup>	3 <sup>c</sup>	100 <sup>c</sup>	70 <sup>c</sup>
Upper VSU	54.6	0.18	1.91	6.35 <sup>b</sup>	4.6 <sup>b</sup>	100 <sup>b</sup>	5,500. <sup>b</sup>
CFPPA	1.1	0.001	1.84	1.30 <sup>b</sup>	6.78 <sup>b</sup>	104.2 <sup>b</sup>	5,500. <sup>b</sup>
Lower VSU	8.9	0.18	1.91	6.35 <sup>b</sup>	4.6 <sup>b</sup>	100 <sup>b</sup>	5,500. <sup>b</sup>

Sources: % of total flow path length from file *jasonPump\_dat.xls*.

<sup>a</sup> Belcher et al. 2004 [DIRS 173179], Table E-1.

<sup>b</sup> SNL 2008 [DIRS 183750], Tables 6-8, 6-13, and 6-14.

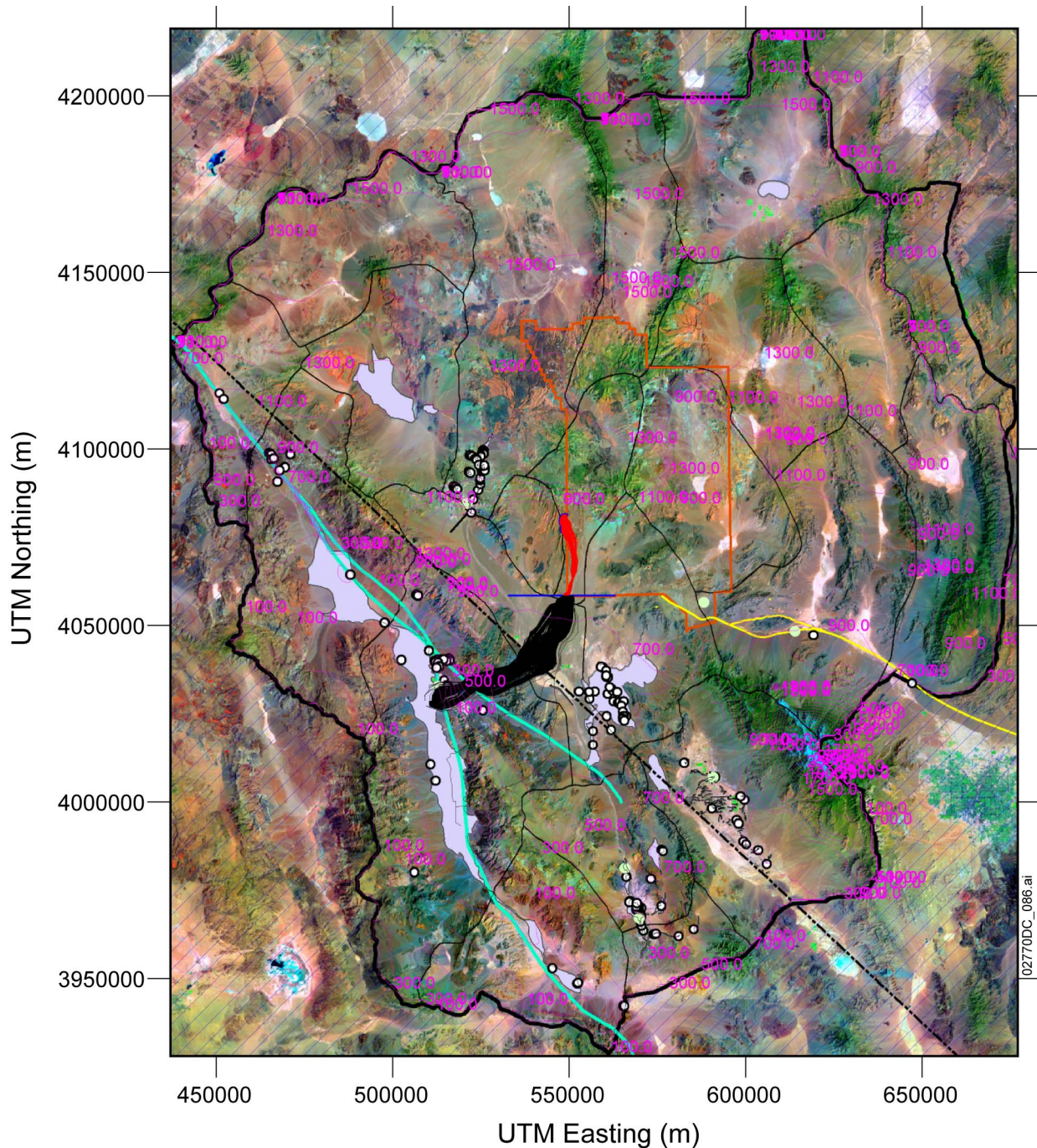
<sup>c</sup> Dicke 1997, Table 4.

NOTE: Units that are less than 0.1% of the average total flow path length are not included in the table.

Flow paths for Case 3 are presented in Figure 15a. The figure shows that flow patterns are generally similar to those shown when there is no pumping (Case 1). However, with the reduced

level of pumping, there is a component (two particles) of groundwater flow between Funeral Mountain and Alkali Flat towards the southern end of Death Valley.

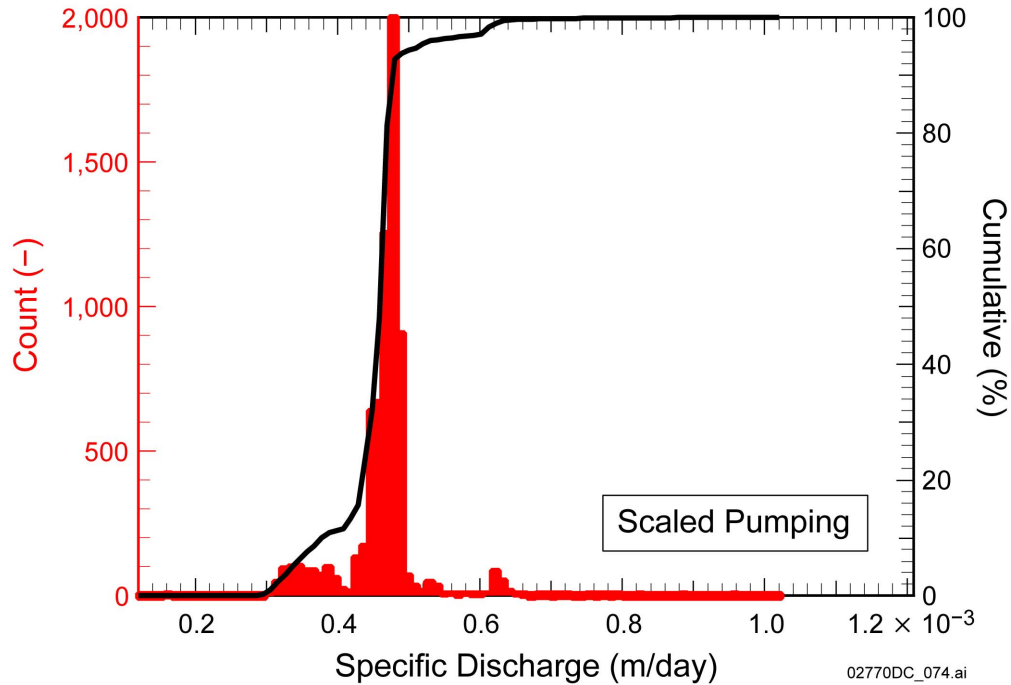
The histogram for the 8,024 particle tracks for Case 3 is shown in Figure 15b. The minimum, average, and maximum specific discharges are  $2.20 \times 10^{-7}$ ,  $4.51 \times 10^{-4}$ , and  $1.02 \times 10^{-3}$  m/day, respectively. Specific discharges under the reduced long-term pumping conditions in Case 3 (where pumping was reduced to about 2% of Case 2) are actually slowed compared to those for Case 1 (no pumping conditions). The range of specific discharges for Case 3 is much larger than for either of Cases 1 and 3 because two particles traveled very slowly (two and three orders of magnitude slower than the rest of the plume) to discharge south of Death Valley. Excluding these two flow paths in statistical analysis yields a specific discharge distribution that is similar to Case 1 (non-pumping), with a minimum specific discharge of  $1.45 \times 10^{-4}$  m/day. Why reduced pumping in Case 3 slows the flow from the 18-km compliance boundary to Death Valley may be explained by pumping effects on flow upstream and downstream of Amargosa Desert. The particles pass through the Amargosa Desert well field early on their transit to Death Valley, and once they pass the weak sinks in Amargosa Desert, their movement to Death Valley is slowed due to a smaller hydraulic gradient, reduced by pumping, along the segment of the flowpath downstream of Amargosa Desert. (In the case of continuous pumping at the year 2003 level (Case 3), this effect is actually strong enough to prevent the particles from moving further downstream and out of Amargosa Desert.) Overall, specific discharges for this reduced pumping case (Case 3) are only slightly different from the non-pumping case (Case 1) and are within the range of modeling uncertainty for both scenarios.



Source: *PDSS1-ppaths.srf* in *PDSS1\_5-ptracks-figures.zip* and *18km-no-pump.dxf*, SNL 2007 [DIRS 177391], Figure 6-17.

NOTES: Purple contours are simulated heads for layer 1. Dense and thin black curves are particle tracks from 8,024 Particles that are released at the accessible environment boundary. Red curves are particle tracks from the repository to the accessible environment boundary (SNL 2007 [DIRS 177391], Figure 6-17). The Nevada Test Site is outlined in red. Hatched areas outside of the Death Valley groundwater basin are treated as inactive cells in the model.

Figure 15a. Simulated Hydraulic Heads and Groundwater Flow Paths for the Reduced Estimate of Long-Term Pumping Rates (Case 3)



Source: *SPDISHist.pxp (Igor) in FigureFiles.zip.*

Figure 15b. Histogram of Specific Discharges for the 8,024 Particles Released at the Accessible Environment Boundary for the Reduced Estimate of Long-Term Pumping Rates (Case 3)

#### 4.4 ESTIMATED SPECIFIC DISCHARGE AND FLOW PATHS FOR FUTURE CLIMATIC CONDITIONS

The specific discharges for the future wetter climate were scaled up from those estimated for the current climate (Section 4.3). The scaling factor was chosen to be the same as the factor developed for the site-scale SZ model domain for the glacial-transition climate (3.9, see SNL 2008 [DIRS 183750], Table 6-4[a]). The results of multiplying specific discharges by the scaling factor of 3.9 for Cases 1 to 3 are summarized in Table 11.

Table 11. Specific Discharge Estimates

Case	Description	Specific Discharge (m/day)		
		Minimum	Average	Maximum
1	Pre-pumping	$4.07 \times 10^{-4}$	$1.80 \times 10^{-3}$	$5.05 \times 10^{-3}$
2	2003 estimate of long-term pumping rates	$1.30 \times 10^{-3}$	$2.39 \times 10^{-2}$	$3.61 \times 10^{-2}$
3	Reduced estimate of long-term pumping rates	$8.58 \times 10^{-7}$	$1.76 \times 10^{-3}$	$3.98 \times 10^{-3}$

There are several references that show regional springs and discharge areas within the DVRFS model domain. D’Agnese et al. (1998 [DIRS 103006]) and Belcher (2004 [DIRS 173179]) present maps showing regional springs and lakes (Figures 16 and 17). There are several discharge areas both south and southwest of the Nevada Test site as shown in Figure 17. These include discharge areas at Ash Meadows, Alkali Flat, Franklin Well area, and Death Valley.

Belcher (2004 [DIRS 173179]) also presents estimates of mean annual discharge volumes (Table 12). Forester et al. (1999 [DIRS 109425]) mention active springs at Ash Meadows and Death Valley and discharge as seepage and evapotranspiration at Alkali Flat (Figure 18).

The simulations for the pre-pumping case shown in Figure 10 indicated flowpaths to the Death Valley discharge area; whereas, for the pumping case, the flow paths go to the wells in the Amargosa Farms area. These discharge areas are consistent with the present-day discharge areas reported in the literature mentioned above.

A few scientific investigations are in disagreement with the conceptual model used in the DVRFS model that there is significant interbasin flow in the carbonate aquifer. Anderson et al. (2006 [DIRS 186108]) claims that the structural complexity of the carbonate rocks makes interbasin flow “difficult to envision.” The authors state that the majority of spring water discharging at Furnace Creek in Death Valley is locally recharged. Miner et al. (2007 [DIRS 186109]) studied fossil spring deposits in the Tecopa Basin. The authors conclude that the regional flow was from the north in a north-south trending fault region along the foot of the Resting Spring Range, as opposed to the west due to interbasin flow in carbonate rocks. Both papers note that the conceptual model of interbasin flow in the carbonate aquifer used by the DVRFS model is conservative, leading to an increase in flux through the model domain and discharge in Death Valley.

Paleodischarge sites can be used to infer potential future locations for discharge of groundwater from Yucca Mountain under future, wetter climatic conditions. By dating the paleospring deposits, they can potentially be linked to times of a wetter climate and a higher water table. The inference to the past can then be extrapolated to potential future climates. For this case, the interest is in the future glacial-transition climate that is wetter and cooler than the present-day climate. The glacial transition climate is of interest because it is this climate that the TSPA model chose to be most representative of future climatic conditions beyond 2,000 years in the future.

The climatic history in the paleodischarge sites in the DVRFS model area is complex. SAR Section 2.3.1 (p. 2.3.1-13) states:

Evidence shows that glacial periods were of limited duration, lasting from a few thousand years to as much as 35,000 years for a major glacial period that occurred from about 140,000 to 175,000 years ago. The interglacial (present-day) climates persisted for only about 20% of the documented interglacial and glacial history. Thus, much of the Yucca Mountain climate history is dominated by glacial-transition climates.

Figure 2.3.1-10 in SAR Section 2.3.1 shows that the initiation of the transition to a glacial climate occurred approximately 400, 325, 230, and 115 thousand years ago. This study assumes that any paleodischarge site older than about 10,000 years most likely occurred during a glacial transition period when the water table was higher.

Figure 18 shows areas of paleodischarge deposits shown in the report by Forester et al. (1999 [DIRS 109425], Figure 21). Paleodischarge points in the Amargosa Desert include Crater Flat

Wash deposits, Lathrop Wells diatomite, State Line deposits, and Indian Pass deposits. Of these paleospring deposits, the State Line deposits are the most likely locations for potential future discharge of groundwater from beneath Yucca Mountain, based on simulated flow paths reported in Section 4.3 (Figures 11, 13, and 15). Forester et al. (1999 [DIRS 109425]) report dates of deposits at Crater Flat deposits, Lathrop Wells diatomite and the State Line deposits to be between 40 thousand and eight thousand years old.

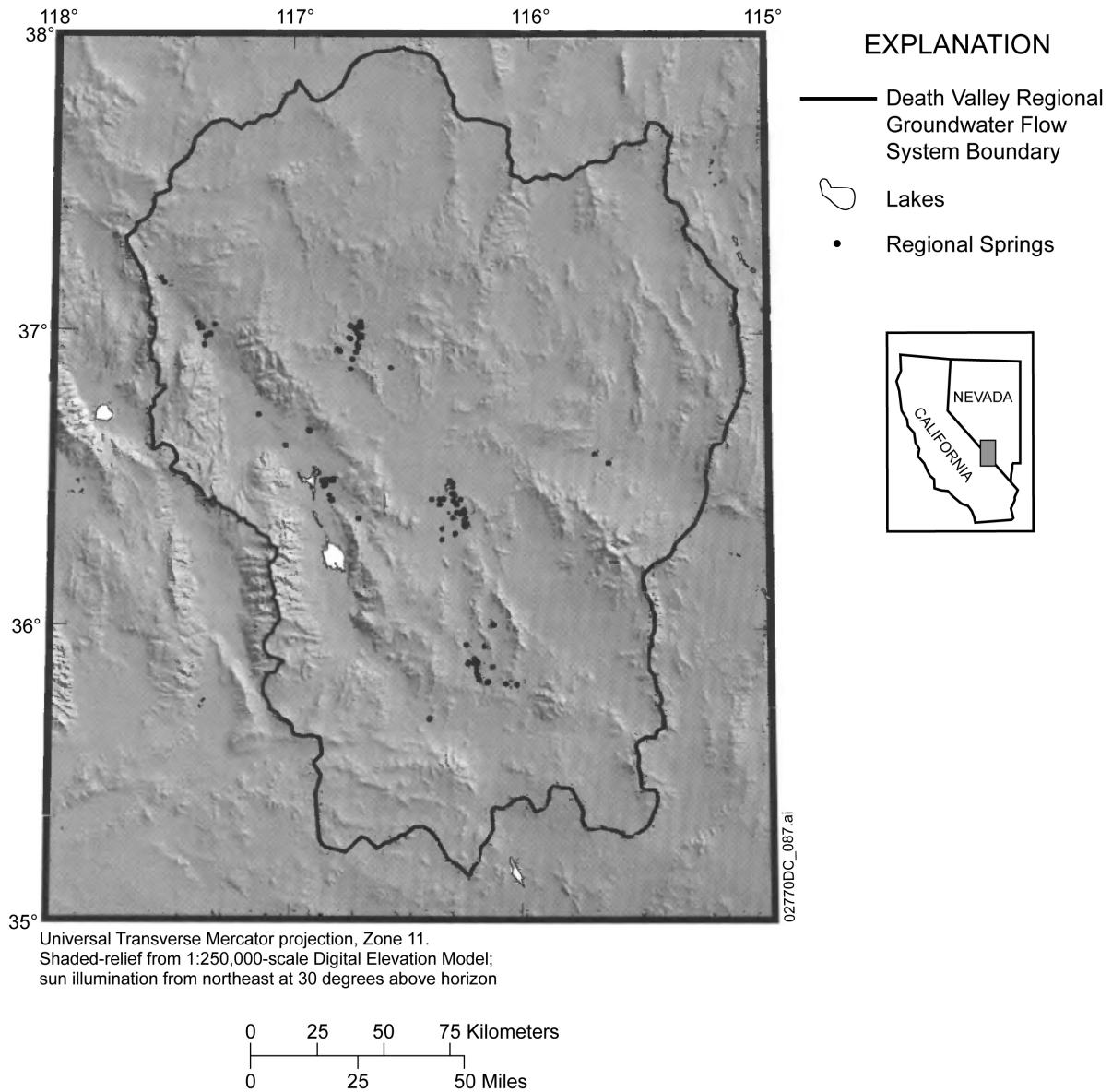
Quade et al. (1995 [DIRS 100074]) examined paleospring deposits at Lathrop Wells diatomite, Ash Meadows, Pahrump Valley, and further to the south and east. They state paleontological evidence that the Lathrop Wells diatomite deposits date to the Pleistocene. The authors also state that deposits in the Pahrump and Coyote Springs Valleys extend back to at least the early Pleistocene. They state that “most paleosprings that discharged into valley bottoms in our study area probably would plot in the “springs in limestones” field” (Quade et al. 1995 [DIRS 100074], p. 217), indicating that the waters may have originated from the carbonate system. Quade et al. (1995 [DIRS 100074]) believe that most of the paleospring deposits studied in their work were localized by faulting.

Paces (1995 [DIRS 106465]) presents studies of paleospring deposits to the south and southwest of Yucca Mountain, specifically the Crater Flat deposits and State Line deposits in the southern Amargosa Desert, and dated State Line deposits using a calibrated  $^{14}\text{C}$  age to be  $9,010 \pm 250$  to  $10,760 \pm 250$  years old. The author concludes that discharge was active at all sites during the late Pleistocene through the last glacial maximum (ages of 10,000 to 20,000 years before present) and states that “uranium and strontium isotopic compositions in past-discharge deposits are compatible with present-day ground waters in the vicinity of each of the discharge sites” (Paces 1995 [DIRS 106465]).

D’Agnese et al. (1999 [DIRS 120425]) performed simulations of groundwater flow with the DVRFS model to simulate the effects of climate change. Their study assessed the potential impacts of past (full-glacial) and future (global-warming) climate scenarios. Results for the steady-state past climatic conditions indicated significant water table rise and activation of discharge drains in the model corresponding to the State Line deposits and some model cells along the downstream reach of Fortymile Wash (Figure 19) (D’Agnese et al. 1999 [DIRS 120425]), among others. The past climate scenario evaluated by D’Agnese et al. (1999 [DIRS 120425]) is the more relevant to the glacial-transition climatic conditions that are most representative of long-term conditions at Yucca Mountain.

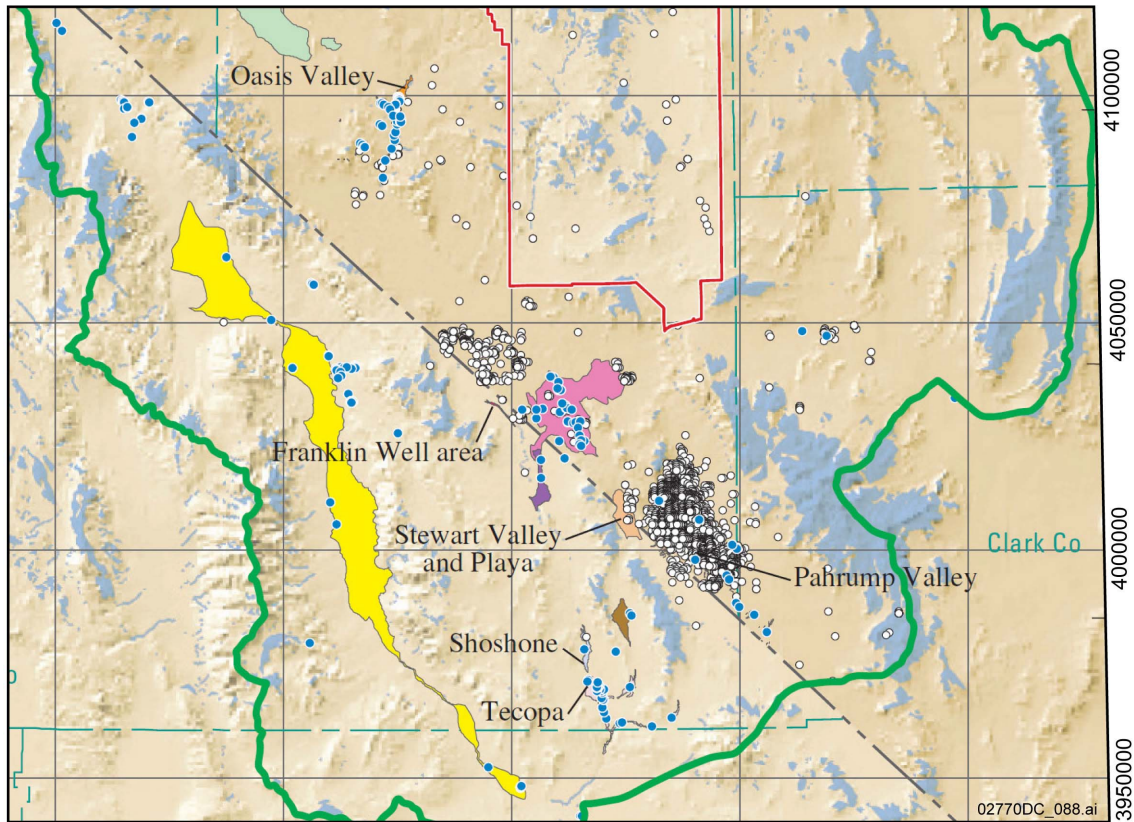
In summary, paleospring deposits in the area near Yucca Mountain indicate that groundwater from the regional flow system discharged to the surface at numerous additional locations during past glacial climatic conditions. It is reasonable to assume that many or all of these locations will be reactivated as groundwater discharge sites under future glacial-transition climatic conditions. Of these paleodischarge locations, the State Line deposits about 25 to 30 km from Yucca Mountain are the most likely sites for the potential discharge of groundwater from beneath Yucca Mountain under future glacial-transition climatic conditions. Alternatively, it is possible that groundwater flow paths from Yucca Mountain will bypass the State Line discharge locations to be discharged at the Furnace Creek springs or valley floor of Death Valley, under future glacial-transition climatic conditions. It is also possible that future groundwater pumping in the area of wells in Amargosa Farms would lower the water table, prevent surface discharge

from occurring at the State Line discharge areas, and capture groundwater originating from beneath Yucca Mountain.



Source: D'Agnese et al. 1998 [DIRS 103006], Figure 3.

Figure 16. Locations of Lakes and Regional Springs from D'Agnese et al. (1998 [DIRS 103006])



50,000-meter grid based on Universal Transverse Mercator projection, Zone 11. Shaded-relief base from 1:250,000-scale Digital Elevation Model; sun illumination from northwest at 30 degrees above horizon

0 20 40 80 Kilometers  
0 20 40 Miles

### EXPLANATION

- |   |  |   |
|---|--|---|
|  <b>Recharge area</b><br>(modified from Hevesi and others, 2003) |  <b>Death Valley regional ground-water flow system model boundary</b> |   |
| <b>Discharge area</b><br>(modified Lacznaiak and others, 2001 and DeMeo and others, 2003)   |  <b>Nevada Test Site boundary</b>                                     |   |
|  Ash Meadows   |  Franklin Well area   |  Shoshone                    |
|  Carson Slough/<br>Franklin Lake Playa                           |  Pahrump Valley   |  Oasis Valley                |
|  Chicago Valley  |  Penoyer Valley   |  Stewart Valley<br>and Playa |
|  Death Valley  |  Sarcobatus Valley  |  Tecopa                      |
|   |  <b>Regional springs</b>  |   |
|   |  <b>Pumping wells</b><br>(modified from Moreo and others, 2003)       |   |

Source: Belcher 2004 [DIRS 173179], Figure D-3.

Figure 17. Locations of Lakes and Regional Springs from Belcher (2004 [DIRS 173179])

Table 12 Estimates of Mean Annual Ground-Water Discharge from Major Evapotranspiration-Dominated Discharge Areas in Death Valley Regional Ground-Water Flow System Model Domain

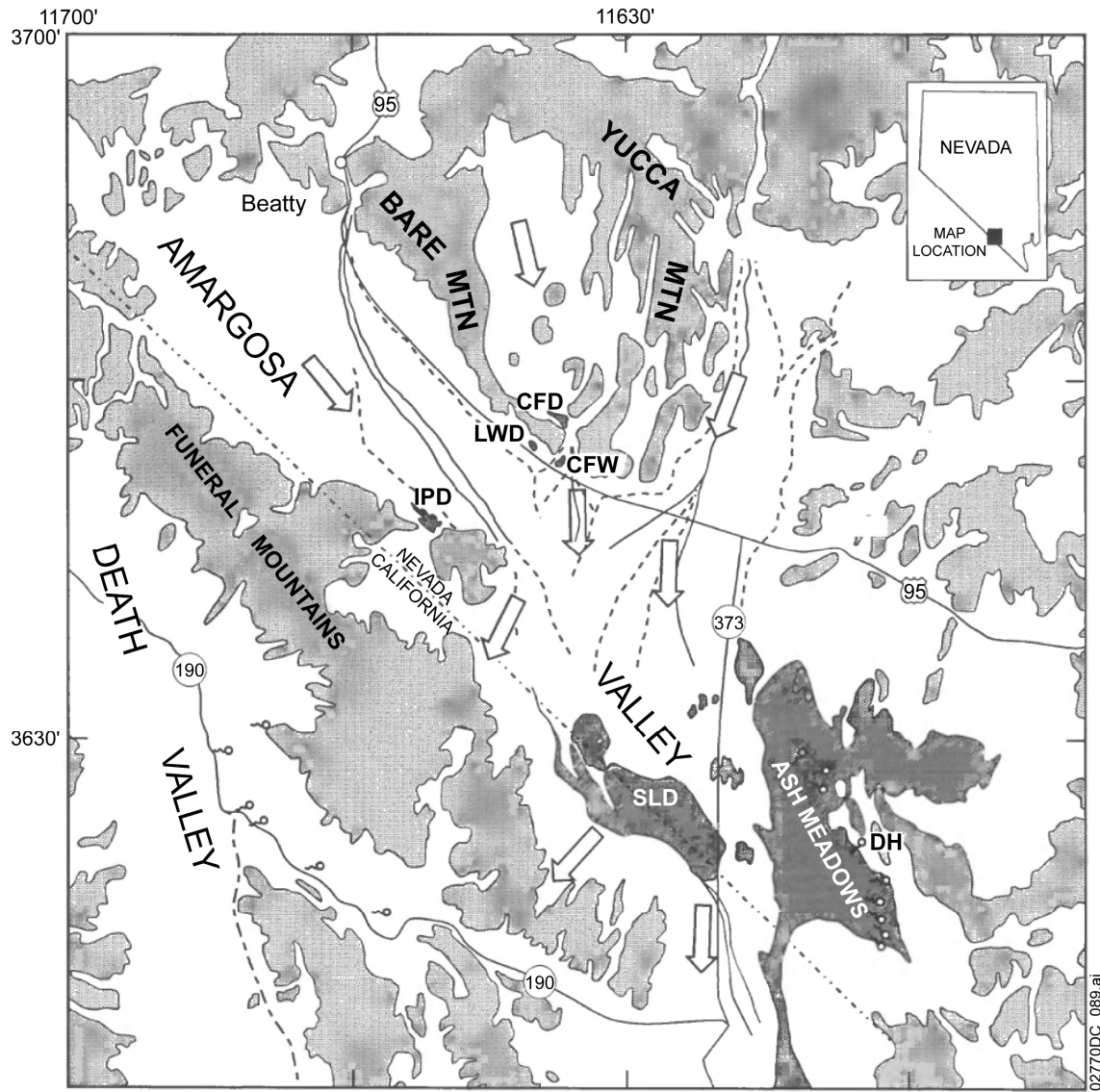
<b>Discharge Area</b>	<b>Estimated Mean Annual ET Rate (m/yr)</b>	<b>Area (km<sup>2</sup>)</b>	<b>Annual Precipitation Rate (m/yr)</b>	<b>Estimated Precipitation-Adjusted Annual Evapotranspiration Rate (m/yr)</b>	<b>Estimated Mean Annual Ground-Water Discharge (m<sup>3</sup>)</b>
Ash Meadows	0.55	50.5	0.11	0.44	22,203,000
Chicago Valley	0.34	2.48	0.11	0.23	530,000
Franklin Lake	0.23	9.43	0.10	0.13	1,234,000
Franklin Well Area	0.46	1.20	0.11	0.35	432,000
Oasis Valley	0.70	13.9	0.15	0.55	7,401,000
Pahrump Valley	0.79	12.2	0.12	0.67	8,082,000
Penoyer Valley	—	76.9	—	0.06	4,650,000
Sarcobatus Flat	0.27	138.6	0.15	0.12	16,035,000
Shoshone Area	0.55	5.62	0.09	0.46	2,590,000
Stewart Valley <sup>1</sup>	0.20	12.2	0.11	0.09	1,234,000
Tecopa/California Valley Area	0.64	14.2	0.09	0.55	7,894,000
Death Valley Floor	—	445.5	—	0.1 <sup>1</sup>	43,172,000
Total					115,457,000

Source: Belcher 2004 [DIRS 173179], Table C-1.

NOTES: Ground-water discharge rounded to the nearest thousand. Rates rounded to nearest hundredth. Mean annual ground-water discharge may not equal product of precipitation-adjusted ET rate and area because of rounding. Dash (—) indicates that no value was reported in referenced source or that the information given was insufficient to compute a value.

ET = evapotranspiration, m/yr = meters per year, km<sup>2</sup> = square kilometers, m<sup>3</sup> = cubic meters,

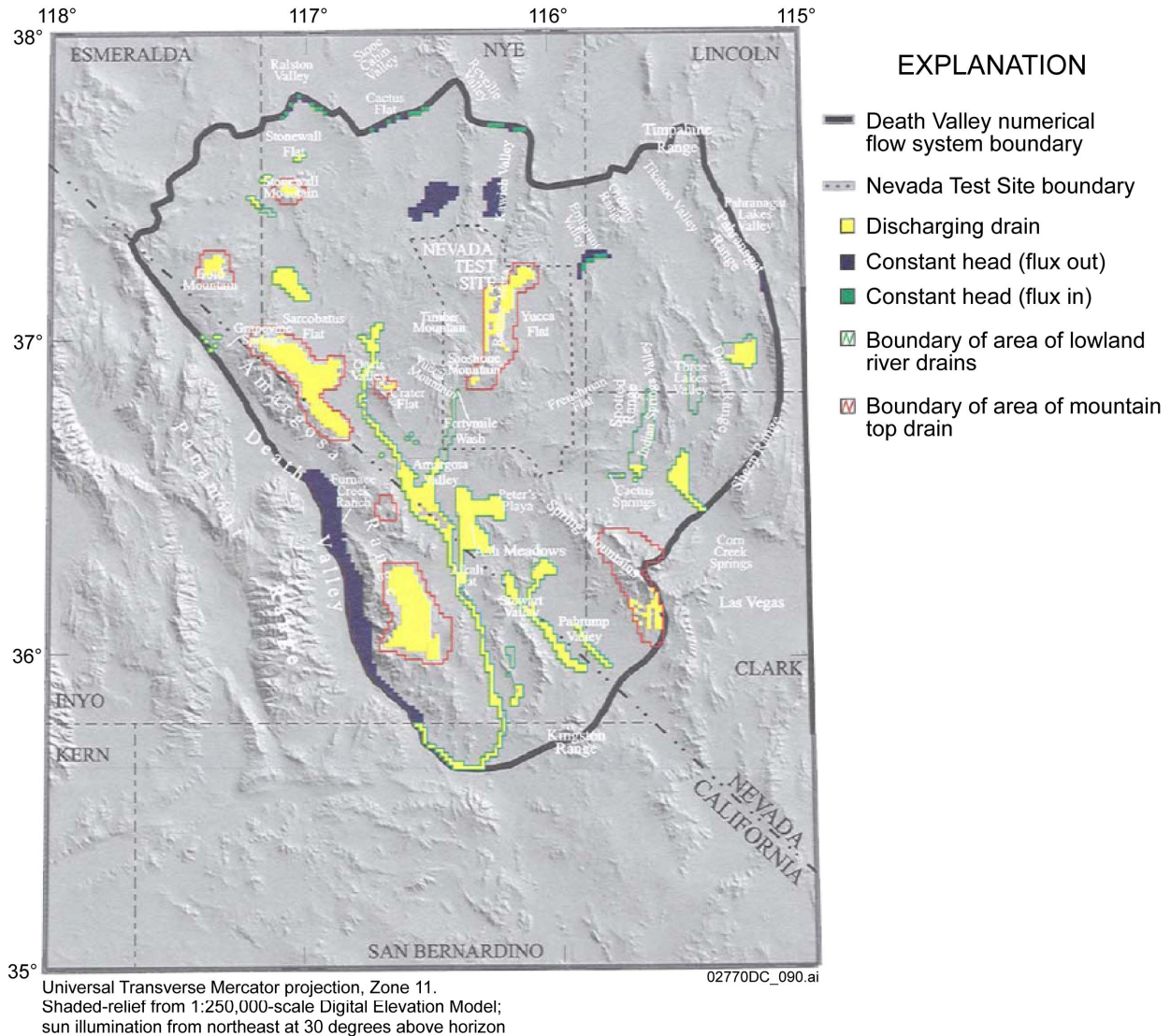
<sup>1</sup>Corrected from the original value reported in Belcher 2004 [DIRS 173179].



Source: Forester et al. 1999 [DIRS 109425], Figure 21.

NOTES: Paleodischarge deposits are shown as dark-shaded patches with CFD = Crater Flat Deposits, CFW = Crater Flat Wash, DH = Devils Hole, LWD = Latham Wells Diatomite, IPD = Indian Pass Deposits, SLD = State Line Deposits. Active springs at Ash Meadows and Death Valley are shown with spring symbols. Outlined arrows show generalized ground-water flow paths. Light-shaded polygons represent bedrock highs; intervening unpatterned areas represent alluvium-filled basins. Solid and dashed lines in basins represent fluvial channels and fan boundaries, respectively.

Figure 18. Paleodischarge Deposits and Active Springs in the Yucca Mountain Region, Nevada



Source: D’Agnese et al. 1999 [DIRS 120425], Figure 11.

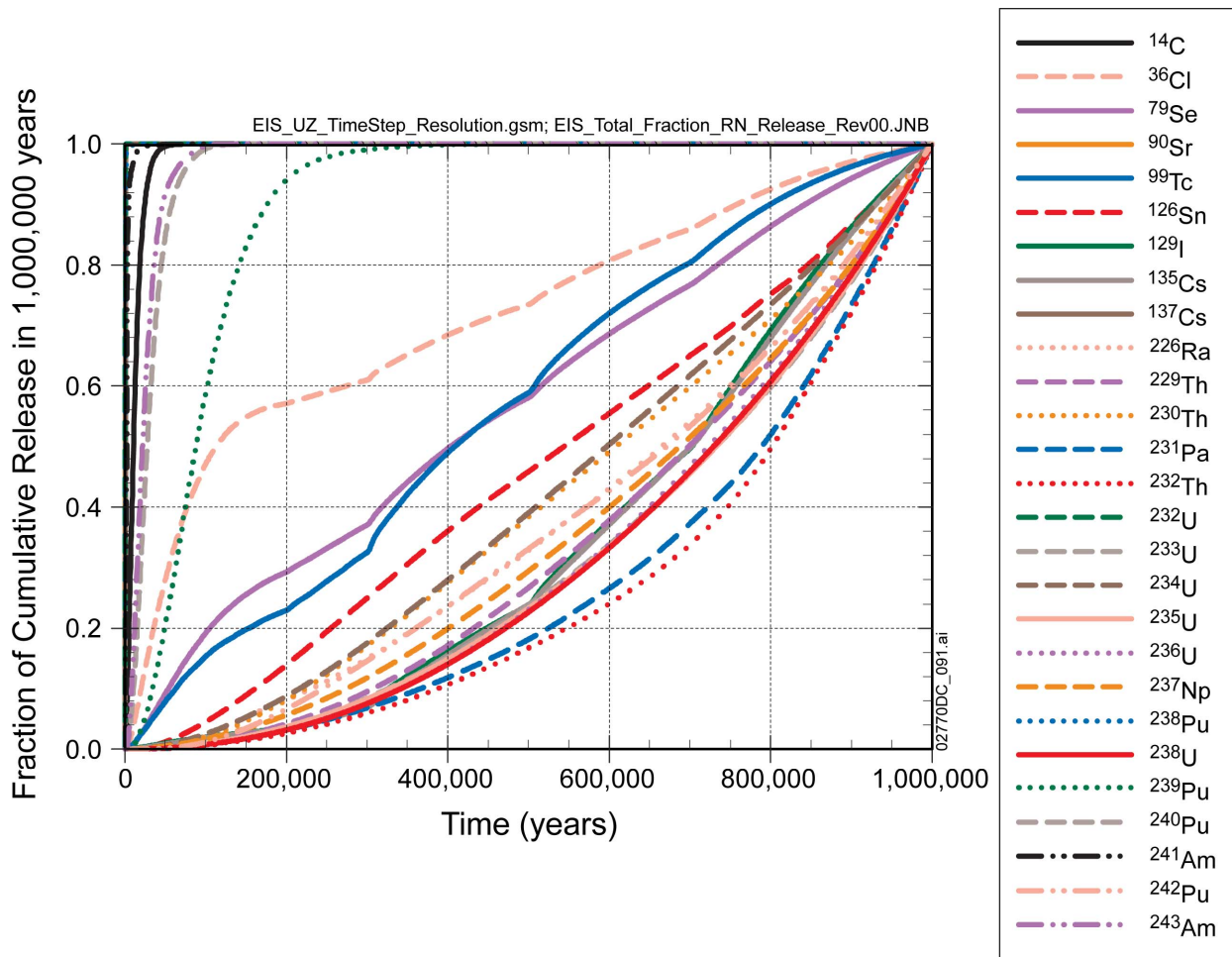
Figure 19. Distribution of Drains and Constant Head Cells Simulated as Discharging during Past Climate Conditions in the DVRFS Model

#### 4.5 CALCULATED RADIONUCLIDE MASS RELEASE RATES FROM THE TSPA-LA

The results for different radionuclides are plotted in Figure 20. This part of the analysis considers only the first 39 species tracked by the unsaturated zone model component of the TSPA-LA Model. The other 10 species tracked in the TSPA-LA model are not transported by the unsaturated zone component of the TSPA-LA model.

For cumulative unsaturated zone releases, 39 individual species are tracked by the FEHM DLL, of which four ( $^{137}\text{Cs}$ ,  $^{90}\text{Sr}$ ,  $^{232}\text{U}$ , and  $\text{I}^{238}\text{Pu}$ ) reach 100% of total cumulative release within 5,000 years.  $^{238}\text{Pu}$  and  $\text{Ic}^{238}\text{Pu}$  reach 99.7% release at this time. In addition,  $^{241}\text{Am}$  release approaches 90% of the cumulative release within 5,000 years, predominantly due to the short half-lives of these species. By 100,000 years, an additional ten species ( $^{14}\text{C}$ ,  $^{243}\text{Am}$ ,  $\text{Ic}^{243}\text{Am}$ ,  $\text{I}^{243}\text{Am}$ ,  $^{241}\text{Am}$ ,  $\text{Ic}^{241}\text{Am}$ ,  $\text{I}^{241}\text{Am}$ ,  $^{240}\text{Pu}$ ,  $\text{Ic}^{240}\text{Pu}$  and  $\text{I}^{240}\text{Pu}$ ) reach more than 99% of the cumulative release of these species. By 200,000 years  $^{239}\text{Pu}$ ,  $\text{Ic}^{239}\text{Pu}$ , and  $\text{I}^{239}\text{Pu}$  have accumulated 93% of the cumulative release and  $^{36}\text{Cl}$  has reached 58% of its cumulative release. For the other 19 species yet to be mentioned, cumulative releases are less than 30% of the final value by 200,000 years. However, it is during the period between 100,000 and 500,000 years when waste packages begin failing with a greater frequency and higher probability (seismic events or nominal corrosion processes). Because of the variation in releases, proposing a single time step schedule for all radionuclides is removed from consideration. Instead an alternate approach is proposed. The 20 time steps used in the analysis are determined by the change in the cumulative release fraction for each species. Each time the cumulative release fraction approaches a 5% increment of the total release the time is recorded and used as a value in the revised time step schedule. The cumulative release fractions, calculated by Equation 1, are calculated for the fine time step schedule that includes 2,020 time steps. The mean cumulative release history is converted to a fraction of total cumulative release. The time step that precedes a change in cumulative release by 5% of the total is reported as a time step in the revised time step schedule. Although the mean cumulative release history is used to determine the revised time step schedule, 5th-percentile, median, and 95th-percentile values are also reported at these same time steps.

Results are also reported in an Excel file (*EIS\_UZ\_TimeStep\_Resolution\_Fractional\_Basis.xls*) described in Appendix B. This workbook contains the time step refinement calculation for the radionuclides of interest, combining multiple colloidal forms of plutonium and americium.



Source: *EIS\_UZ\_TimeStep\_Resolution.gsm*.

Figure 20. Fraction of Mean Cumulative Unsaturated Zone Release in 1,000,000 Years by Radionuclide

#### 4.6 SELECTED BREAKTHROUGH CURVES FOR NONRADIOLOGICAL CONTAMINANTS

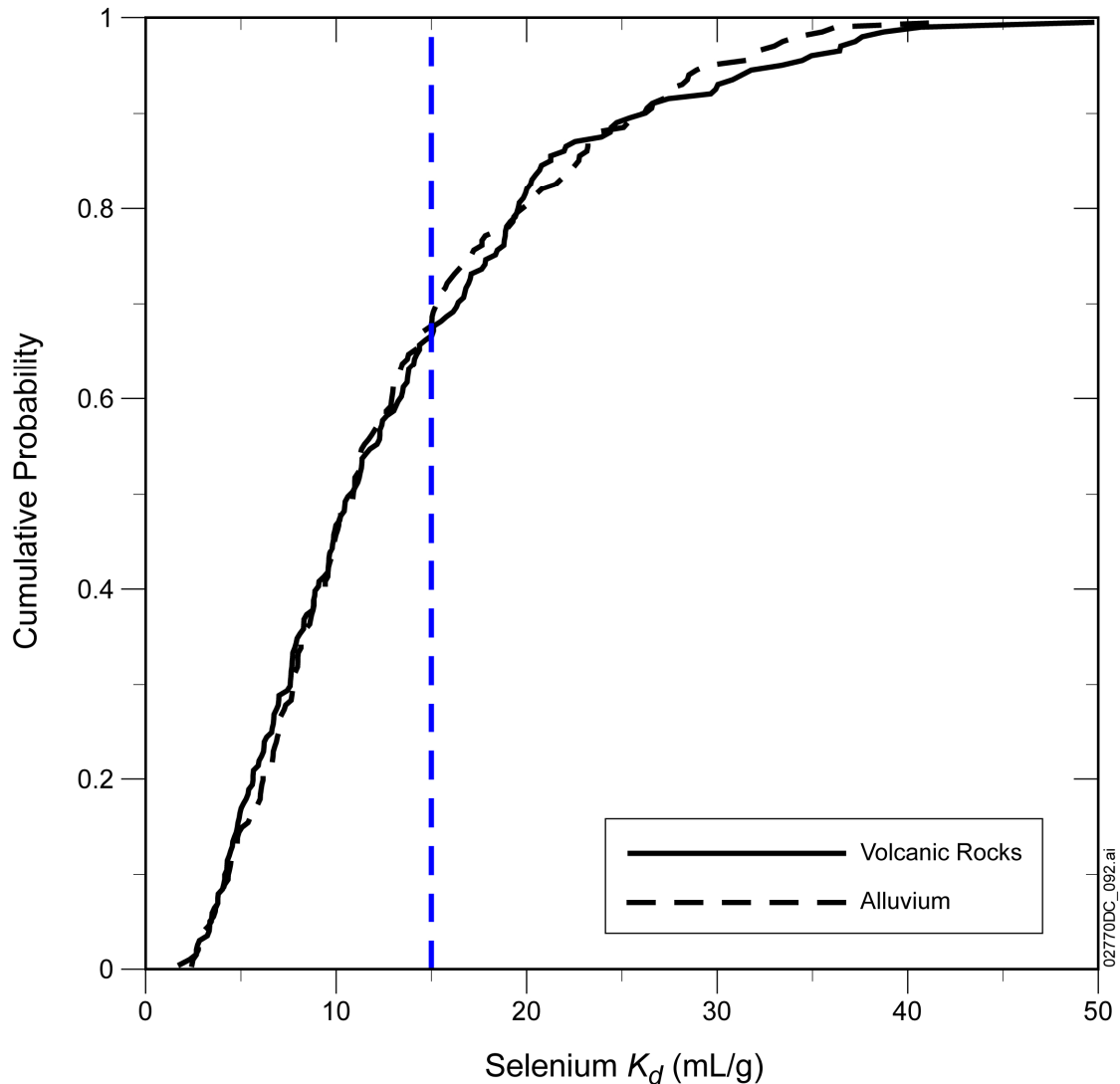
Recommended values of sorption coefficients for nickel, molybdenum, and vanadium in volcanic rocks and alluvium are 15, 0, and 8 mL/g, respectively (David Lester, Jason and Associates Corporation, personal communication, December, 2008). Table 13 shows the median values for sorption coefficients in the volcanic rocks and the alluvium from the uncertainty distributions for  $K_d$ s in the saturated zone flow and transport abstraction model (SNL 2008 [DIRS 183750], Tables 6-8 and 6-7[a]). Note that Table 13 does not contain radionuclide groups that are subject to colloid-facilitated transport because the sorption coefficients for nickel, molybdenum, and vanadium are low enough that they would not be subject to colloid-facilitated transport. The median values for  $K_d$  given in Table 13 are from the uncertainty distributions used to develop the breakthrough curves for the various radionuclide groups.

Table 13. Radioelements Transported as Solutes in the Saturated Zone Flow and Transport Abstraction Model

Radionuclide Group Number	Radioelements	Median Volcanics $K_d$ (mL/g)	Median Alluvium $K_d$ (mL/g)
1	Carbon, Technetium, Iodine, Chlorine	0.0	0.0
5	Neptunium	1.3	6.4
7	Radium	550	550
8	Strontium	210	210
9	Uranium	6.8	4.6
11	Selenium	10.8	10.8

The median values for the uncertainty distributions of  $K_d$ s are used as a reasonable metric for evaluating the most representative set of breakthrough curves to match with each of the nonradioactive contaminants. Given that the recommended value of  $K_d$  for molybdenum is 0.0 mL/g, its transport in the saturated zone clearly is associated with radionuclide group 1. The recommended value of 15 mL/g for nickel is higher than the median value of 10.8 mL/g for the uncertainty distribution for  $K_d$  of selenium, but matches this radionuclide group (Group 11) more closely than any other. The recommended value of 8 mL/g for vanadium is somewhat higher than the median values of 6.8 and 4.6 mL/g for the uncertainty distributions for  $K_d$  in volcanic rocks and alluvium of uranium, but matches this radionuclide group (Group 9) more closely than any other.

Additional comparison between the recommended values of sorption coefficients for nickel and vanadium and the uncertainty distributions for the corresponding radionuclide groups is shown in Figures 21 and 22. Figure 21 shows the truncated log-normal sampled cumulative distribution function for selenium  $K_d$  that was used to simulate the breakthrough curves for radionuclide group 11. Comparing the recommended value of 15 mL/g for the nickel sorption coefficient indicates that some of the realizations for the breakthrough curves use smaller values of  $K_d$  and some realizations use larger values of  $K_d$ . Overall, there is a satisfactory match between the recommended value for the nickel sorption coefficient and the distribution of  $K_d$  values used for the saturated zone breakthrough curves.

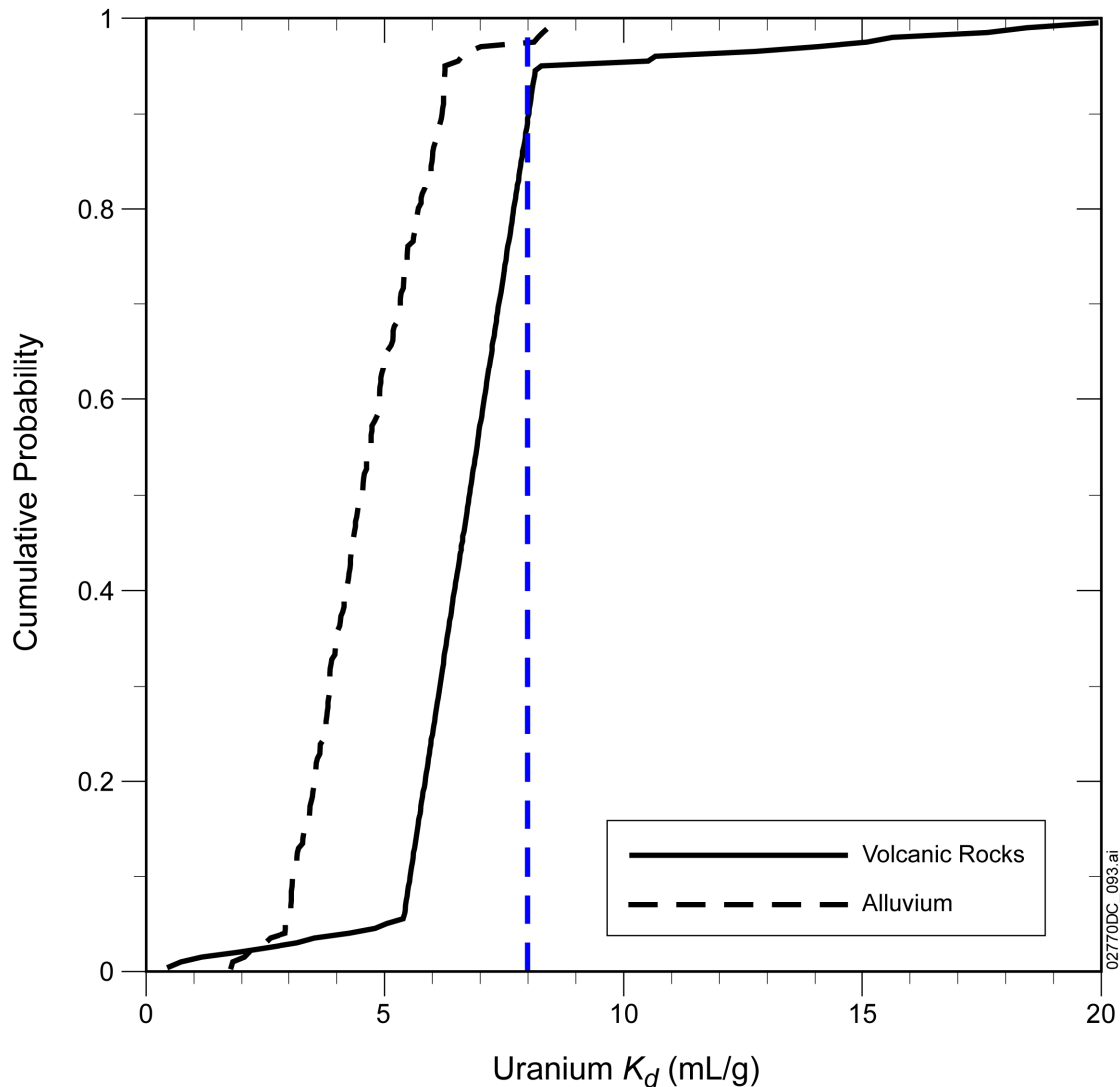


Source: SNL 2008 [DIRS 183750], Table A-1[b].

NOTE: Recommended value of sorption coefficient for nickel of 15 mL/g shown by the vertical dashed blue line.

Figure 21. Cumulative Distribution Function of Sampled  $K_d$  for Selenium in Volcanic Rocks and Alluvium

Figure 22 shows the sampled cumulative distribution function for uranium  $K_d$  that was used to simulate the breakthrough curves for radionuclide group 9. The majority of the sampled values of uranium  $K_d$  are lower than the recommended value of 8 mL/g for the vanadium sorption coefficient. The simulated breakthrough curves for uranium thus underestimate the transport times in the saturated zone relative to the expected transport times for vanadium. Overall, using the uranium breakthrough curves for the transport of vanadium in the saturated zone is a satisfactory, but conservative, approximation.



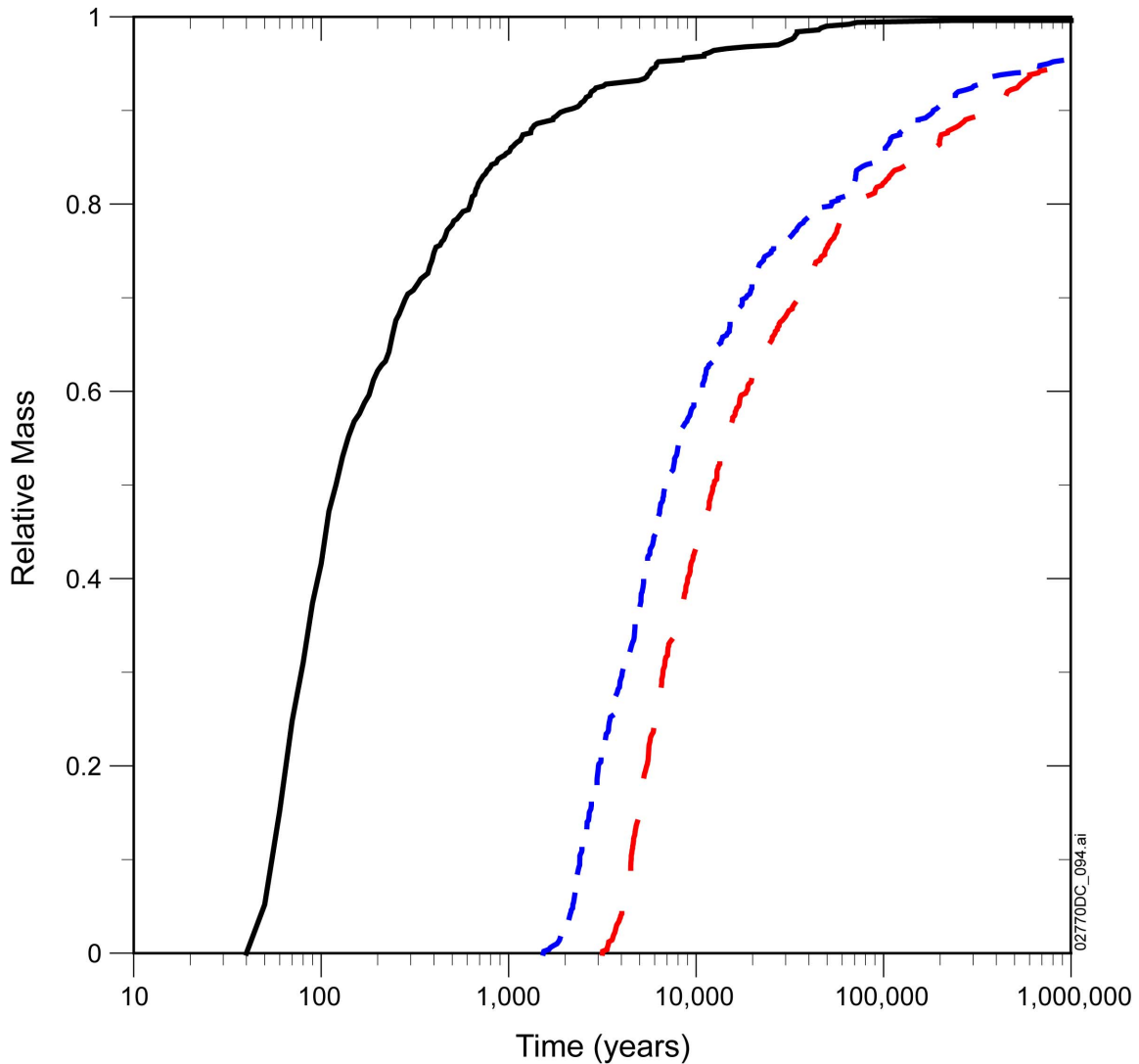
Source: SNL 2008 [DIRS 183750], Table A-1[b].

NOTE: Recommended value of sorption coefficient of 8 mL/g for vanadium shown by the vertical dashed blue line.

Figure 22. Cumulative Distribution Function of Sampled  $K_d$  for Uranium in Volcanic Rocks and Alluvium from the Saturated Zone Flow and Transport Abstraction Model

The alternative approach to providing information on transport of nonradiological contaminants uses the SZ flow and transport abstraction model (SNL 2008 [DIRS 183750]) to simulate the transport of these contaminants to produce a set of expected breakthrough curves. These simulations use the recommended values of sorption coefficients for molybdenum, vanadium, and nickel, along with the values of other uncertain parameters taken from the median case for validation of the SZ flow and transport abstraction model (SNL 2008 [DIRS 183750], Table 7-1[a]). The resulting modeled saturated zone breakthrough curves represent the expected transport behavior of these contaminants in the saturated zone from beneath the repository to the boundary of the accessible environment for the higher groundwater flow rates corresponding to glacial-transition climatic conditions.

The resulting breakthrough curves from this alternative approach are shown in Figure 23. Molybdenum, with a sorption coefficient of 0 mL/g, has an expected breakthrough curve corresponding to the nonsorbing radionuclides. Vanadium, with a sorption coefficient of 8 mL/g, experiences significant retardation and median transport times of about 7,000 years. Nickel, with a sorption coefficient of 15 mL/g, has a simulated breakthrough curve with greater retardation and a median transport time of greater than 10,000 years. The breakthrough curves for vanadium and nickel display long tails that are characteristic of diffusion and sorption onto the rock matrix in the fractured volcanic units of the saturated zone.



Source: Files: *btc\_Mo\_01\_median.dat*, *btc\_Ni\_01-median.dat*, and *btc\_V\_01\_median.dat* in *btc\_non\_rad.zip*.

NOTE: Breakthrough curve for molybdenum shown with the solid black line, for vanadium with the short-dashed blue line, and for nickel with the long-dashed red line.

Figure 23. Simulated Breakthrough Curves in the Saturated Zone for Molybdenum, Vanadium, and Nickel

## 4.7 RESULTS OF ANALYSIS TO COMPARE TO GROUNDWATER PROTECTION STANDARD

This section presents a summary and synthesis of the methods used to calculate radioactivity in groundwater with the TSPA model for comparison to groundwater protection standards. Information from the TSPA model report (SNL 2008 [DIRS 183478]) and the documentation of the SZ flow and transport abstraction model (SNL 2008 [DIRS 183750]) is used in the summary and synthesis.

The repository performance related to the groundwater protection standard is subject to the NRC requirements of 10 CFR 63.331 [DIRS 180319]. This standard requires that there be a reasonable expectation that the radionuclide releases from Yucca Mountain into the accessible environment will not exceed the specified levels of radioactivity in the representative volume of groundwater for 10,000 years of undisturbed performance after disposal. The regulated levels of radioactivity in groundwater are for three categories: (1) combined  $^{226}\text{Ra}$  and  $^{228}\text{Ra}$ , (2) gross alpha activity (including  $^{226}\text{Ra}$  but excluding radon and uranium), and (3) combined beta and photon emitting radionuclides. The regulatory limits for the three categories are, respectively: (1) 5 picocuries per liter, including natural background in groundwater, (2) 15 picocuries per liter, including natural background in groundwater, and (3) 0.04 mSv (4 mrem) per year to whole body or any organ from drinking two liters per day, respectively from the categories listed above. These regulatory requirements are summarized in Table 14 and these represent the 95% upper limit for natural background concentrations (SNL 2008 [DIRS 183750], Table 6-18).

Table 14. Groundwater Protection Regulation Limits and Radionuclides Used in Analyses

Type of Limit <sup>a</sup>	Limit <sup>a</sup>	Include Natural Background? <sup>a</sup>	Natural Background <sup>b</sup>	Primary Radionuclides Included in the Analysis <sup>c</sup>
Combined $^{226}\text{Ra}$ and $^{228}\text{Ra}$ Activity	5 pCi/L	Yes	0.5 pCi/L	$^{226}\text{Ra}$ and $^{228}\text{Ra}$
Gross Alpha Activity	15 pCi/L	Yes	0.5 pCi/L	$^{226}\text{Ra}$ , $^{227}\text{Ac}$ , $^{229}\text{Th}$ , $^{230}\text{Th}$ , $^{232}\text{Th}$ <sup>d</sup> , $^{231}\text{Pa}$ , $^{237}\text{Np}$ , $^{238}\text{Pu}$ , $^{239}\text{Pu}$ , $^{240}\text{Pu}$ , $^{242}\text{Pu}$ , $^{241}\text{Am}$ , $^{243}\text{Am}$
Combined Dose from Beta and Photon Emitting Radionuclides	4 mrem/yr	No	NA	$^{14}\text{C}$ , $^{36}\text{Cl}$ , $^{79}\text{Se}$ , $^{90}\text{Sr}$ and daughter, $^{99}\text{Tc}$ , $^{126}\text{Sn}$ and daughters, $^{129}\text{I}$ , $^{135}\text{Cs}$ , $^{137}\text{Cs}$ and daughter, $^{228}\text{Ra}$ and daughter, $^{228}\text{Th}$ daughters, $^{237}\text{Np}$ daughter, $^{229}\text{Th}$ daughters, $^{238}\text{U}$ daughters, $^{226}\text{Ra}$ daughters, $^{210}\text{Pb}$ and daughter, $^{243}\text{Am}$ daughter, $^{235}\text{U}$ daughter, $^{227}\text{Ac}$ and daughters

Sources: <sup>a</sup> 10 CFR 63.331 [DIRS 180319];

<sup>b</sup> SNL 2008 [DIRS 183750], Section 6.8.5, Table 6-18;

<sup>c</sup> SNL 2007 [DIRS 177399], Table 6.15-2 and SNL 2008 [DIRS 183478], Sections 8.1.2.2[a] and 8.1.2.3[a].

<sup>d</sup> Although  $^{228}\text{Th}$  transport is not tracked in the TSPA-LA Model, the alpha particle contribution from  $^{228}\text{Th}$  is accounted for by assuming secular equilibrium of the short-lived decay chain products of  $^{232}\text{Th}$  ( $^{232}\text{Th} \rightarrow ^{228}\text{Ra} \rightarrow ^{228}\text{Ac} \rightarrow ^{228}\text{Th}$ ). By assuming secular equilibrium among  $^{232}\text{Th}$ ,  $^{228}\text{Ra}$ ,  $^{228}\text{Ac}$ , and  $^{228}\text{Th}$ , the number of alpha particles emitted per decay of one atom of  $^{228}\text{Th}$ , which is 4 (DTN: MO0702PAGWPROS.001 [DIRS 179328]), can be added to that for  $^{232}\text{Th}$ , for a total of 5 (SNL 2007 [DIRS 177399], Section 6.15.1.1). This alternative number of alpha particles emitted per decay of one atom of  $^{232}\text{Th}$  is used in conjunction with the  $^{232}\text{Th}$  concentration in curies at the 18-km accessible environment boundary to determine the combined contribution of  $^{232}\text{Th}$  and  $^{228}\text{Th}$  to gross alpha activity. Note also that  $^{228}\text{Ra}$  and  $^{228}\text{Ac}$  are not alpha particle emitters.

The TSPA model calculations of activity concentrations in groundwater were performed in the following way. The combined  $^{226}\text{Ra}$  and  $^{228}\text{Ra}$  activity concentration was calculated by summing the alpha activity concentrations for these two radionuclides in the representative groundwater volume of 3,000 acre-ft, as indicated in the TSPA model report (SNL 2008 [DIRS 183478], Equation 6.3.11-2). Because of its relatively short half-life of 5.8 years and retarded transport in the saturated zone,  $^{228}\text{Ra}$  is conservatively assumed to be in secular equilibrium with its parent,  $^{232}\text{Th}$ , at the boundary of the accessible environment, and its activity concentration is calculated accordingly. The sum of  $^{226}\text{Ra}$  and  $^{228}\text{Ra}$  activity concentrations is added to the estimated natural background concentration of 0.5 pCi/L (SNL 2008 [DIRS 183750], Section 6.8.5, Table 6-18) for comparison to the regulatory limit of 5 pCi/L.

The gross alpha activity concentration was calculated by summing the activity concentrations of all of the primary radionuclides listed in Table 14 and SNL 2008 [DIRS 183478], Section 8.1.2.2[a] in the representative groundwater volume of 3,000 acre-ft, as indicated in the TSPA model report (SNL 2008 [DIRS 183478], Equation 6.3.11-2). Several of the primary radionuclides listed in Table 14 have several alpha emissions associated with them because of short-lived alpha-emitting daughter products (other than radon and uranium) (SNL 2008 [DIRS 183478], Section 8.1.2.2[a]). Note that there are four alpha decays (other than radon) counted for each  $^{226}\text{Ra}$  decay in the calculation of activity concentrations to account for the alpha emissions from its short-lived daughter products  $^{218}\text{Po}$ ,  $^{218}\text{At}$ ,  $^{214}\text{Po}$ , and  $^{210}\text{Po}$ .  $^{227}\text{Ac}$  has six decays,  $^{232}\text{Th}$  has five decays (including  $^{228}\text{Th}$ ), and  $^{229}\text{Th}$  has six decays. These relationships among the primary radionuclides and short-lived daughter products are summarized in *Biosphere Model Report* (SNL 2007 [DIRS 177399], Table 6.15-2). The sum of contributing alpha-emitting radionuclide activity concentrations is added to the estimated natural background concentration of 0.5 pCi/L (SNL 2008 [DIRS 183750], Section 6.8.5 and Table 6-18) for comparison to the regulatory limit of 15 pCi/L.

The TSPA model calculations of combined dose from beta and photon emitting radionuclides were performed in the following way. The combined dose was calculated for the whole body or for individual organs by summing the dose from individual beta and photon emitting radionuclides listed in Table 14, as indicated in the TSPA model report (SNL 2008 [DIRS 183478], Equation 6.3.11-3). The conversion factors for calculating beta-photon annual dose from daily consumption of 2 liters of water are documented in *Biosphere Model Report* (SNL 2007 [DIRS 177399], Table 6.15-6). Some of the beta and photon emitting radionuclides listed in Table 14 have short-lived daughter products that are themselves beta-photon emitters and that are not tracked in the TSPA transport simulations. For example,  $^{126}\text{Sn}$  has two daughter products,  $^{126\text{m}}\text{Sb}$  and  $^{126}\text{Sb}$ , that are also beta emitters and have half-lives of minutes to days. Some of the other primary radionuclides are not themselves beta or photon emitters, but they have short-lived daughter products that are beta or photon emitters. For example,  $^{226}\text{Ra}$  experiences alpha decay, but the decay chain from  $^{226}\text{Ra}$  contains  $^{214}\text{Pb}$ ,  $^{214}\text{Bi}$ ,  $^{210}\text{Tl}$ ,  $^{210}\text{Pb}$ , and  $^{210}\text{Bi}$ , all of which are beta emitters. The impacts of these daughter products on beta-photon dose are implicitly included in the groundwater protection analysis by assuming equilibrium with the primary radionuclide parent in the biosphere and including their effects in the conversion factors used to calculate annual whole body and individual organ dose (SNL 2008 [DIRS 183478], Section 8.1.2.3[a]).

Finally, the TSPA analyses for comparison to the groundwater protection standard were limited to some of the scenario classes and to the first 10,000 years following closure of the repository for consistency with the standard (10 CFR 63.331 [DIRS 180319]). The scenario classes included in the groundwater protection analyses were the nominal modeling case, the waste package early failure modeling case, the drip shield early failure modeling case, and the seismic ground motion modeling case (for peak ground velocities with annual frequency greater than  $10^{-5}$  per year only) (SNL 2008 [DIRS 183478], Section 8.1.2).

INTENTIONALLY LEFT BLANK

## 5 REFERENCES

### 5.1 DOCUMENTS CITED

- 186108 Anderson, K.; Nelson, S.; Mayo, A.; and Tingey, D. 2006. "Interbasin Flow Revisited: The Contribution of Local Recharge to High-Discharge Springs, Death Valley, CA." *Journal of Hydrology*, 323, 276-302. Amsterdam, The Netherlands: Elsevier.
- 173179 Belcher, W.R. 2004. *Death Valley Regional Ground-Water Flow System, Nevada and California - Hydrogeologic Framework and Transient Ground-Water Flow Model. Scientific Investigations Report 2004-5205*. Reston, Virginia: U.S. Geological Survey. ACC: MOL.20050323.0070.
- 186071 Blainey, Joan B.; Faunt, Claudia C. and Hill Mary C. 2006. *A Guide for Using the Transient Ground-Water Flow Model of the Death Valley Regional Ground-Water Flow System, Nevada and California*. Open-File Report 2006-1104- US Geological Survey (USGS). Denver, Co: U.S. Geological Survey.
- 170009 BSC (Bechtel SAIC Company) 2004. *Water-Level Data Analysis for the Saturated Zone Site-Scale Flow and Transport Model*. ANL-NBS-HS-000034 REV 02. Las Vegas, Nevada: Bechtel SAIC Company. ACC: DOC.20041012.0002; DOC.20050214.0002.
- N/A Cappaert v. United States. 1976. 426 U.S. 128, 147 (1976).
- 162809 CWD V. 2.0. 2003. WINDOWS 2000. STN: 10363-2.0-00.
- 181037 CWD V. 2.0. 2007. WINDOWS 2003. STN: 10363-2.0-01.
- 103006 D'Agnesse, F.A.; Faunt, C.C.; and Turner, A.K. 1998. An Estimated Potentiometric Surface of the Death Valley Region, Nevada and California, Developed Using Geographic Information System and Automated Interpolation Techniques. Water-Resources Investigations Report 97-4052. Denver, Colorado: U.S. Geological Survey. TIC: 237331.
- 120425 D'Agnesse, F.A.; O'Brien, G.M.; Faunt, C.C.; and San Juan, C.A. 1999. *Simulated Effects of Climate Change on the Death Valley Regional Ground-Water Flow System, Nevada and California*. Water-Resources Investigations Report 98-4041. Denver, Colorado: U.S. Geological Survey. TIC: 243555.
- Dicke, C.A. 1997. *Distribution Coefficients and Contaminant Solubilities for the Waste Area 7 Baseline Risk Assessment*. INEL/EXT-97-00201. Idaho Falls, Idaho: Idaho National Engineering and Environmental Laboratory.

- 180751 DOE (U.S. Department of Energy) 2008. *Final Supplemental Environmental Impact Statement for a Geologic Repository for the Disposal of Spent Nuclear Fuel and High-Level Radioactive Waste at Yucca Mountain, Nye County, Nevada*. DOE/EIS-0250F-S1. Las Vegas, Nevada: U.S. Department of Energy, Office of Civilian Radioactive Waste Management. ACC: MOL.20080606.0001.
- 186100 Eastman Whipstock 1983. Report of Sub-Surface Directional Survey, 00 UE25P1, May 1, 1983. Job Number P0583-G-1250. Las Vegas, Nevada: Fenix & Scisson. ACC: NNA.19890728.0159.
- EPA (U.S. Environmental Protection Agency) 1998. *Technical Support Document for Section 194.14: Assessment of  $K_{ds}$  Used in the CCA*. Washington, DC: U.S. Environmental Protection Agency.
- 182102 EXDOC\_LA V. 2.0. 2007. WINDOWS XP, WINDOWS 2000 & WINDOWS 2003. STN: 11193-2.0-00.
- 185792 FEHM V. 2.26. 2008. WIN 2003. STN: 10086-2.26-00.
- 109425 Forester, R.M.; Bradbury, J.P.; Carter, C.; Elvidge-Tuma, A.B.; Hemphill, M.L.; Lundstrom, S.C.; Mahan, S.A.; Marshall, B.D.; Neymark, L.A.; Paces, J.B.; Sharpe, S.E.; Whelan, J.F.; and Wigand, P.E. 1999. *The Climatic and Hydrologic History of Southern Nevada During the Late Quaternary*. Open-File Report 98-635. Denver, Colorado: U.S. Geological Survey. TIC: 245717.
- 181040 GetThk\_LA V. 1.0. 2006. WINDOWS 2000 & WINDOWS 2003. STN: 11229-1.0-00.
- 184387 GoldSim V. 9.60.300. 2008. WIN 2000, WINXP, WIN2003. STN: 10344-9.60-03.
- 186107 Halford, K.J. and Hanson, R.T. 2002. *User Guide for the Drawdown-Limited, Multi-Node Well (MNW) Package for the U.S. Geological Survey's Modular Three-Dimensional Finite-Difference Ground-Water Flow Model, Versions MODFLOW-96 and MODFLOW-2000*. Open-File Report 02-293. Sacramento, California: U.S. Geological Survey. '
- 155197 Harbaugh, A.W.; Banta, E.R.; Hill, M.C.; and McDonald, M.G. 2000. *MODFLOW-2000, The U.S. Geological Survey Modular Ground-Water Model—User Guide to Modularization Concepts and the Ground-Water Flow Process*. Open-File Report 00-92. Reston, Virginia: U.S. Geological Survey. TIC: 250197.
- 186106 Harbaugh, A.W. 2005. "MODFLOW-2005, The U.S. Geological Survey Modular Ground-Water Model--the Ground-Water Flow Process." Chapter 16 of *Book 6. Modeling Techniques, Section A. Ground Water*. U.S. Geological Survey Techniques and Methods 6-A16. Reston, Virginia: U.S. Geological Survey.
- 167885 InterpZdll\_LA V. 1.0. 2004. WINDOWS 2000. STN: 11107-1.0-00.

- 181043 InterpZdll\_LA V. 1.0. 2007. WINDOWS 2003. STN: 11107-1.0-01.
- 167884 MFCP\_LA V. 1.0. 2003. WINDOWS 2000. STN: 11071-1.0-00.
- 181045 MFCP\_LA V. 1.0. 2006. WINDOWS 2003. STN: 11071-1.0-01.
- 181047 MkTable\_LA V. 1.0. 2006. WINDOWS 2000. STN: 11217-1.0-00.
- 181048 MkTable\_LA V. 1.0. 2007. WINDOWS 2003. STN: 11217-1.0-01.
- 186109 Miner, R.E.; Nelson, S.T.; Tingey, D.G.; and Murrell, M.T. 2007. "Using Fossil Spring Deposits in the Death Valley Region, USA to Evaluate Palaeoflowpaths." *Journal of Quaternary Science*, 22, (4), 373-386. New York, New York: John Wiley & Sons. TIC: 260318.
- 183751 MO0710ADTSPAWI.000. TSPA-LA Addendum Groundwater Modeling Cases (V5.005) and Eruptive Model (V1.004) with Final Documentation. Submittal date: 10/30/2007.
- 179328 MO0702PAGWPROS.001. Groundwater Protection Standards Conversion Factors. Submittal date: 02/06/2007.
- 185968 Moreo, M.T. and Justet, L. 2008. Update to the Ground-Water Withdrawals Database for the Death Valley Regional Ground-Water Flow System, Nevada and California, 1913–2003, USGS Data Series 340. Reston, Virginia: U.S. Geological Survey. ACC: TBD.
- 186113 NRC (U.S. Nuclear Regulatory Commission) 2008. *U.S. Nuclear Regulatory Commission Staff's Adoption Determination Report for the U.S. Department of Energy's Environmental Impact Statements for the Proposed Geologic Repository at Yucca Mountain*. Washington, D.C.: U.S. Nuclear Regulatory Commission. ACC: LLR.20090203.0020.
- 106465 Paces, J. 1995. "Letter Report on FY1995 Studies of Paleodischarge Deposits." Internal memorandum from J. Paces (USGS) to Chief, Yucca Mountain Project Branch (USGS), June 26, 1995. ACC: MOL.19960702.0134.
- 181051 PassTable1D\_LA V. 2.0. 2007. WINDOWS 2000 & WINDOWS 2003. STN: 11142-2.0-00.
- 100074 Quade, J.; Mifflin, M.D.; Pratt, W.L.; McCoy, W.; and Burckle, L. 1995. "Fossil Spring Deposits in the Southern Great Basin and Their Implications for Changes in Water-Table Levels Near Yucca Mountain, Nevada, During Quaternary Time." *Geological Society of America Bulletin*, 107, (2), 213-230. Boulder, Colorado: Geological Society of America. TIC: 234256.
- 181054 SCCD V. 2.01. 2007. WINDOWS 2003. STN: 10343-2.01-01.

- 181157 SCCD V. 2.01. 2003. WINDOWS 2000. STN: 10343-2.01-00.
- 180318 SEEPAGEDLL\_LA V. 1.3. 2006. WINDOWS 2000. STN: 11076-1.3-00.
- 181058 SEEPAGEDLL\_LA V. 1.3. 2007. WINDOWS 2003. STN: 11076-1.3-01.
- 177399 SNL (Sandia National Laboratories) 2007. *Biosphere Model Report*. MDL-MGR-MD-000001 REV 02. Las Vegas, Nevada: Sandia National Laboratories. ACC: DOC.20070830.0007; LLR.20080328.0002.
- 177391 SNL 2007. *Saturated Zone Site-Scale Flow Model*. MDL-NBS-HS-000011 REV 03. Las Vegas, Nevada: Sandia National Laboratories. ACC: DOC.20070626.0004; DOC.20071001.0013.
- 183750 SNL 2008. *Saturated Zone Flow and Transport Model Abstraction*. MDL-NBS-HS-000021 REV 03 AD 02. Las Vegas, Nevada: Sandia National Laboratories. ACC: DOC.20080107.0006; LLR.20080408.0256.
- 184806 SNL 2008. *Site-Scale Saturated Zone Transport*. MDL-NBS-HS-000010 REV 03 AD 01. Las Vegas, Nevada: Sandia National Laboratories. ACC: DOC.20080121.0003; DOC.20080117.0002
- 183478 SNL 2008. *Total System Performance Assessment Model /Analysis for the License Application*. MDL-WIS-PA-000005 REV 00 AD 01. Las Vegas, Nevada: Sandia National Laboratories. ACC: DOC.20080312.0001; LLR.20080414.0037; LLR.20080507.0002; LLR.20080522.0113; DOC.20080724.0005.
- 181060 SZ\_CONVOLUTE V. 3.10.01. 2007. WINDOWS 2000 & WINDOWS 2003. STN: 10207-3.10.01-00.
- 181061 TSPA\_Input\_DB V. 2.2. 2006. WINDOWS 2000. STN: 10931-2.2-00.
- 181062 TSPA\_Input\_DB V. 2.2. 2006. WINDOWS 2003. STN: 10931-2.2-01.
- 183752 TSPA-LA Addendum Groundwater Modeling Cases (V5.005) without Final Documentation (Used for Regulatory Compliance). Submittal date: 10/30/2007.
- N/A United States v. Cappaert. 1977. United States District Court for the District of Nevada: Unpublished Order, Civil LV\_1687 (December 22, 1977).
- 181064 WAPDEG V. 4.07. 2007. WINDOWS SERVER 2003. STN: 10000-4.07-01.
- 181774 WAPDEG V. 4.07. 2003. Windows 2000. STN: 10000-4.07-00.

## 5.2 REGULATIONS CITED

- 180319 10 CFR 63. 2007. Energy: Disposal of High-Level Radioactive Wastes in a Geologic Repository at Yucca Mountain, Nevada. Internet Accessible.

**APPENDIX A**  
**MEMORANDUM FROM CLAUDIA FAUNT**





United States Department of the Interior  
U.S. GEOLOGICAL SURVEY  
California Water Science Center  
4165 Spruance Road, Suite 200  
San Diego, CA 92101-0812  
(619) 225-6142



February 24, 2009

## Memorandum

**To:** Ming Zhu, Sandia National Laboratories, Las Vegas, NV  
**From:** Claudia Faunt, USGS-WRD/WR/CAWSC, San Diego, CA  
**CC:** Mike Chornack, Dan Bright, Wayne Belcher, Bob MacKinnon  
**Subject:** Documentation of the comparison of DVRFS model files utilized by Ming Zhu

The purpose of this memo is to document the comparison of model files that Ming Zhu asked me to review on 12/10/2008. The comparison can be summarized in three parts:

- (1) Update to model files with new pumping data from Moreo and Justet (2008)  
<http://pubs.usgs.gov/ds/340/>
- (2) Examining Ming's updated model files to be used for a flow path analysis; and
- (3) Conversion of DVRFS model from MODFLOW-2000 to MODFLOW-2005

I've organized more detailed summaries of the analysis in this memo according to the three aspects of the review.

In summary, my review finds two steady-state DVRFS model runs set up properly for MODFLOW in comparison to the original DVRFS model (Faunt and others, 2004). One model run represents the first stress-period of the original published model: pre-development with no pumping. The second model run represents pumping at 2003 rates with irrigation returns based on 20% of seven years prior pumping (if this WEL is activated) to steady-state conditions. This basically represents continued pumping at 2003 rates and a small irrigation return flow "forever." Particle paths were started at what appears to be the edge of the site-scale model and allowed to run forward at steady-state conditions. The model is run at steady-state and porosity values of 1.0 were used so no realistic time frames can be calculated. Not surprisingly, the pre-pumping conditions show particles moving south and then southwest, predominantly towards Death Valley and some going toward Alkali Flat. Likewise, pumping conditions show the particles being captured by pumping wells in the Amargosa Valley.

Two things to consider would be: (1) More detailed simulations planned with some embedded modeling (SAMM Project) using more comprehensive stratigraphy in the Amargosa Valley may serve to help refine these flow paths in the future. (2) From my understanding a new version of "MODPATH" has been developed and might be useful. I am not sure of the release status, but I think it will allow nesting of models, more accurate transition of particles from one grid-scale to the next, and some ability to allow particles to be observations.

If you have any questions, feel free to contact Claudia Faunt at (619) 225-6142 or by email at [ccfaunt@usgs.gov](mailto:ccfaunt@usgs.gov).

### **Update of Pumping Data through 2003**

Originally I provided Ming with a preliminary MODFLOW-2000 multi-node well (MNW) file and irrigation return flow MODFLOW-2000 well (WEL) file based on preliminary files from Mike Moreo. To support the documentation Ming's flow path analysis, he asked Elena to compare the MNW file I provided him with the 2003 groundwater withdrawal data as contained in Moreo and Justet (2008) (<http://pubs.usgs.gov/ds/340/>). She noticed some differences. Based on these differences, we updated the MNW file with the released version of the dataset and sent the new file on 12/19/2008 (mnw\_dvrfb\_pub\_03.txt). The update included some changes in the database in the released version, some addition of pumpage to wells where more than one use was specified in the database, and addition of location of wells based on locations that weren't provided in the public release of the database. In the new MNW file (mnw\_dvrfb\_pub\_03.txt), there are 92 stress periods. The initial stress period represents steady-state pre-pumping conditions and is not labeled with a stress period number. The subsequent pumping stress periods are labeled SP 1 through SP 91 and correspond to years 1913 through 2003 during the pumping period. Ming had some problems running the updated file after he modified it to only include pumping for 2003 on 12/22/2003. I tested his new MNW file with MODFLOW-2005 and had no problems. After some review I found an update to the file and provided Ming with the change (a leading space was necessary before the number of wells on the first line for MODFLOW-2000). On 12/24, Ming emailed a note from Elena that the input MNW input file matched the published database. The output file produced from MODFLOW-2000 appears to have slight differences due to rounding.

The irrigation return flow WEL file was identical pre and post-update. On December 24, I provided the information on how the irrigation return flow was calculated. Basically, for each

withdrawal point, return flow was estimated to be 20 percent of the estimated annual pumpage, lagged by 7 years.

As was described by Faunt and others (2004) and San Juan and others (2004), some return flow pumpage through subsequent infiltration of excess irrigation, lawn water, or septic tank wastewater is likely to occur. Moreo and others (2003) and Moreo and Justet (2008) did not adjust estimates of annual pumpage for water potentially returned to the flow system through subsequent infiltration of excess irrigation, lawn water, or septic tank wastewater. The magnitude and timing of these returns have not been precisely quantified. Many difficulties are associated with estimating return flows. These include uncertainties in pumpage, in the hydraulic properties of unsaturated zone sediment, and delineating the actual areas where water is or was returned to the environment. Despite these uncertainties, a San Juan and others (2004) developed a method to compute informal estimates of return flow. Return flows were computed as the product of the estimated annual pumpage and a user-defined return-flow percentage, and could be lagged in time by a user-defined value. All computed return flows were assumed to return to the water table at the location of the pumped well. In the 2004 DVRFS model, for each withdrawal point, return flow was estimated to be 20 percent of the estimated annual pumpage, lagged by 7 years (Faunt and others, 2004). The same method of calculation and values were used for the 2005 DVRFS model. However, instead of putting the return flow in layer 1 of the MNW Package, a separate WEL Package (Harbaugh, 2005) was developed to apply the irrigation return flow. Separating the pumping and irrigation return flow will allow updates to pumping and return flow separately. The separation will also aid in varying the percentage of return flow and the lag time through automated parameter estimation methods.

**Examination of updated model files to be used for a flow path analysis**

Two input data sets were provided, both pumping and pre-pumping input files. Both set up input files use the DVRFS model archive files modified to run for one steady-state stress period. One set has no pumping and represents pre-development conditions. The second set includes pumping based on calendar year 2003. The description of the 2003 pumping is in the previous section. Based on the input files provided, the input data sets appear to be successfully converted. Table 1 summarizes the comparison.

Table 1. Model file comparison.

Input Package/Files	2004 DVRFS archive	Pumping	Prepumping	Notes
arrays	*.asc	*.asc	*.asc	unchanged from archive file
BAS6	BAS_active.txt	test5.BAS	test1.BAS	identical
CHOB	CHOB_15reg.txt	test5.CHO	test1.CHO	unchecked - only used for observations for parameter estimation, not necessary for forward run
CHD	CHD_15reg_tr.txt	test5.CHD	test1.CHD	identical
DIS	DIS_WT_CONFINED.txt	test5.DIS	test1.DIS	The new discretization files include a new first stress period that is steady-state. The appropriate variable (NPER) has been modified to reflect only one stress period.
DRN	DRN_tr.txt	test5.DRN	test1.DRN	identical
DROB	DROB_tr.txt	test5.DRO	test1.DRO	unchecked - only used for observations for parameter estimation, not necessary for forward run
HFB6	HFB_final_tr.txt	test5.HFB	test1.HFB	identical
HOB	HOBs_sstr.txt	test5.HOB	test1.HOB	unchecked - only used for observations for parameter estimation,

				not necessary for forward run
HUF2	HUF2_CONFINED.txt	test5.HUF	test1.HUF	Storage properties have all been removed for both pumping and prepumping, as these are both steady-state solutions, that should be fine.
HYD	HOB5_sstr.hyd	none	none	unchecked - only used for looking at output, not necessary for forward run
KDEP	KDEP.txt	test5.KDE	test1.KDE	identical
MULT	MULT.txt	test5.MUL	test1.MUL	identical
OBS	OBS.txt	test5.OBS	test1.OBS	unchecked - only used for observations for parameter estimation, not necessary for forward run
OC	OC.txt	test5.OC	test1.OC	unchecked - only used for output of information at time points as needed
PCG	PCG.txt	test5.PCG	test1.PCG	identical
PES	PES.txt	test5.PES	test1.PES	unchecked - only used for observations for parameter estimation, not necessary for forward run
RCH	RCH_tr.txt	test5.RCH	test1.RCH	identical
SEN	SENSITIVITY.txt	test5.SEN	test1.SEN	Storage properties have all been removed for both pumping and prepumping, as these are both steady-state solutions, that should be fine.
ZONE	ZONE.txt	test5.ZON	test1.ZON	identical
MNW1	MNW_withdrawal_1_7_20.txt	test5.MNW	none	MNW file updated for pumping for 2003 (see previous section)
WEL	None	test5.WEL	none	new file for irrigation return flow for 2003 (see previous section)

In addition, on December 28, some MODPATH input and output files were provided to examine steady-state pre and post-pumping particle paths. Particle paths were started at what

appears to be the edge of the site-scale model and allowed to run forward at steady-state conditions. (I have no ability to check these starting locations. Spatially they look appropriate; particles appear to be predominantly in layer 1 (near the water table, with some particles starting deeper in the system). The model was run at steady-state and porosity values of 1.0 were used so no realistic time frames can be calculated. Not surprisingly, the pre-pumping conditions show particles moving south and then southwest, predominantly towards Death Valley and some going toward Alkali Flat, while pumping conditions show the particles being captured by pumping wells in the Amargosa Valley. Given the amount of pumping in the Amargosa Valley simulated in 2003, I am not overly surprised by capture of these particles by these pumping wells. Additional refined simulations (500 m xy spacing and much more detailed vertical spacing) are planned with some embedded modeling (SAMM Project). This new model will be using more detailed stratigraphy in the Amargosa Valley (based on Don Sweetkind and Emily Taylor's work) may serve to help refine these flow paths in the future. Currently, this work is only partially complete.

After the detailed review (documented on December 29 2008), the response files test1.rsp and test5.rsp were provided. In MODPATH, a weak sink is a model cell (representing a well, for example) that does not discharge at a sufficiently large rate to capture all of the flow entering the cell; thus, some of the flow leaves the cell across one or more of the cell faces. Because of this limitation of model discretization, flow paths to weak sink cells cannot be uniquely defined, as it is impossible to know whether a specific water particle discharges to the sink or passes through the cell. In MODPATH, the user must arbitrarily decide how particles will be treated whenever they enter cells with internal sinks: either pass through a weak sink, stop at a weak sink, or stop at a weak sink where discharge to the sink is larger than a specified fraction of the total inflow to

the cell. The response files provided show that particles are treated with the option to pass through a weak sink. For reference, Spitz (2001) has developed a method for converting weak sinks representing wells to strong sinks when using MODPATH. Recently, a new version of "MODPATH" was developed and from my understanding, it will allow nesting of models, more accurate transition of particles from one grid-scale to the next, and some ability to allow particles to be observations. I am not sure of the status of this code and I suggest Ming and others check with Randy Hanson and/or Mary Hill (both USGS) on the status of this code and whether or not it might be more helpful.

#### **Conversion of DVRFS model from MODFLOW-2000 to MODFLOW-2005**

On the afternoon of 12/22/2008, Scott James (Sandia) emailed saying that Ming had asked him to "re-run the DVRFS model with MODFLOW-2005." In order for him not to "re-invent the wheel," I provided Scott with the MODFLOW-2005 files that I had already converted later that afternoon. The biggest change is no sensitivity process, so all the parameters are in a "pval" file. I attached a zip file of all the input files (except the arrays, they haven't changed). The numerical code still requires compiling double precision or it will crash. I have attached some of the preliminary documentation of the conversion from the report documenting the conversion. This report (Li and others, in review) summarizes the model conversion as well as the update with new pumping (Moreo and Justet, 2008) and water level observation data (Pavelko, in review).

#### ***2005 DVRFS Model***

The 2004 DVRFS model was updated in two stages. First, the code was converted to the latest version of MODFLOW and inverse parameter estimation techniques. To evaluate differences resulting from the conversion, comparison simulations were conducted using the two

models with a selected group of parameters and observations from the 2004 DVRFS model. These comparisons include sensitivity analyses with a selected group of parameters. Simulated flow budgets, residuals and sensitivities of the two models were used to demonstrate the success of model conversion.

Second, the input data were updated. Three updated data sets were used: 1) pumping data, 2) water level observations, and 3) an update to the distribution of the shallow alluvium. The first two datasets update the data to include new pumping and observation data through 2003. The model was not recalibrated. This updated model, referred to here as the 2005 DVRFS model, simulates ground-water flow condition of Death Valley from 1913 to 2003 using the same set of parameter values as the 2004 DVRFS model. The 2005 DVRFS model does include simulated water-levels from 1998 to 2003 and residuals from new water-level observations.

#### **Numerical Code Updates**

The flow part of the 2004 DVRFS model was upgraded from MODFLOW-2000 (Hill and othes, 200) to MODFLOW-2005 (Harbaugh, 2005), and the parameter estimation part was replaced by UCODE\_2005 (Poeter and others, 2005), a universal inverse parameter-estimation code. Changes in MODFLOW from MODFLOW-2000 to MODFLOW-2005 include both code changes and code application (Harbaugh, 2005). The primary change in numerical code in MODFLOW-2005 is the adoption of a different approach for internal data management. Instead of subroutine arguments as previously used by MODFLOW-2000, MODFLOW-2005 makes use of FORTRAN modules for storing and sharing data. Each package includes one or more FORTRAN modules that declare the shared data for that package (Harbaugh, 2005). The modules are designed so that data for multiple model grids can be simultaneously defined.

The primary change in MODFLOW-2005 is the separation of parameter-estimation functionality from ground-water flow simulation functionality. Unlike MODFLOW-2000, MODFLOW-2005 has no internal inverse procedure. The combined use of MODFLOW-2005 and UCODE\_2005 allows parameters in any package or process to be estimated. UCODE\_2005 is also capable of non-linear uncertainty analysis, when combined with six other computer programs.

### Changes to Input Files

The update in numerical codes required changes to the input files. The 2005 DVRFS model input files are described below. The files that were changed during the update are listed in Table 1. The input changes can be divided into three groups: 1) forward processes; 2) parameter estimation, sensitivity, and observation processes; and 3) updates to existing files.

The input files associated with FORWARD process of MODFLOW may be used by MODFLOW-2005 directly without any change. Examples of these files include files for basic packages (BAS, DIS, OC, and Zon), internal flow packages (HUF and HFB), stress packages (CHD, DRN, RCH, and MNW), and solver packages (PCG).

The second group of input files is associated with the change in numerical code due to the separation of the ground-water flow processes from the parameter estimation and sensitivity processes. Although the OBSERVATION process remains in the MODFLOW-2005, the input files containing observations were slightly modified to match MODFLOW-2005 format. For each type of observation, two new extra fields were added in the first line of input file for dry cell and for saving observation output (.\_os). Fields related to weights and plot-symbols were deleted. Each type of observation is activated by the appropriate input file. In addition to the change of observations files, a new Parameter Value File (PVAL) is used to replace

MODFLOW-2000 sensitivity (SEN) file for specification of parameter values. As appropriate, the changes were made in the NAME file. For detailed input instruction on these files, the user is referred to MODFLOW-2005 documentation (Harbaugh, 2005).

In the 2005 DVRFS model, the sensitivity and parameter estimation processes are a part of UCODE\_2005. Input files related to UCODE\_2005 include main input (.in), template (tpl), instruction (.ins), observation (.obs), and parameter (params) files. For usage and format of each file, the user is referred to UCODE\_2005 documentation (Poeter and others, 2005).

The third set of changes is two updates in model input files. These updates are to values utilized during parameter estimation and sensitivity analyses and are not utilized in a forward run of the ground-water flow processes. First, the drain observation file (drob\_tr.txt, Table 1) was updated. Because MODFLOW-2005 uses a different memory allocation method; it requires consistency between array size and the number of records it stored. Although not used, this value was mis-specified in the 2004 DVRFS model input. The value was updated to 787, the total number of drain observations utilized in the 2005 DVRFS model.

Second, scale factors for the storage parameters were updated. An error was identified in the scale factors for the storage parameters in the report documenting the 2004 DVRFS model (Faunt and others, 2004). A relatively large value for a storage scale factor (1) was identified in the model input files after the report was published. A significantly smaller value ( $1.0\text{e-}10$ ) is considered more reasonable. Since publication of the report, the values were updated in the archived 2004 DVRFS model files. The values specified in the 2005 DVRFS model remain unchanged from those in the updated and archived files.

### **References**

Belcher, W.R., ed., 2004, Death Valley Regional Ground-Water Flow System, Nevada and California—Hydrogeologic Framework and Transient Ground-Water Flow: U.S. Geological

Survey Scientific Investigations Report 2004-5205, 408 p. On-line at:  
<http://water.usgs.gov/pubs/sir/2004/5205/>

Belcher, W.R., D'Agnesse, F.A., and O'Brien, G.M., 2004, A. Introduction, in Belcher, W.R., ed., Death Valley regional ground-water flow system, Nevada and California--Hydrogeologic framework and transient ground-water flow model: U.S. Geological Survey Scientific Investigations Report 2004-5205, p. 3 - 19. On-line at:  
<http://water.usgs.gov/pubs/sir/2004/5205/>

Faunt, C.C., Blainey, J.B., Hill, M.C., D'Agnesse, F.A., and O'Brien, G.M., 2004, F. Transient flow model, in Belcher, W.R., ed., Death Valley regional ground-water flow system, Nevada and California--Hydrogeologic framework and transient ground-water flow model: U.S. Geological Survey Scientific Investigations Report 2004-5205, p. 257 - 352. On-line at:  
<http://water.usgs.gov/pubs/sir/2004/5205/>

Halford, K.J. and Hanson, R.T., 2002, User guide for the drawdown-limited, Multi-Node Well (MNW) Package for the U.S. Geological Survey's modular three-dimensional finite-difference ground-water flow model, versions MODFLOW-96 and MODFLOW-2000: U.S. Geological Survey Open-File Report 02-293, 33 p. <http://water.usgs.gov/pubs/of/2002/ofr02293/>

Harbaugh, A.W., 2005, MODFLOW-2005, The U.S. Geological Survey Modular Ground-Water Model—the Ground-Water Flow: U.S. Geological Survey Techniques and Methods 6-A16, variously p. On-line at: <http://pubs.usgs.gov/tm/2005/tm6A16/>

Harbaugh, J.W., Banta, E.R., Hill, M.C., and McDonald, M.G., 2000, MODFLOW-2000, The U.S. Geological Survey's modular ground-water flow model—User guide to modularization concepts and the ground-water flow process: U.S. Geological Survey Open-File Report 00-92, 121 p.

Hill, M.C., Banta, E.R., Harbaugh, A.W., and Anderman, E.R., 2000, MODFLOW-2000, The U.S. Geological Survey's modular ground-water flow model—User guide to the observation, sensitivity, and parameter-estimation procedures and three post-processing programs: U.S. Geological Survey Open-File Report 00-184, 209 p., accessed September 1, 2004, at <http://water.usgs.gov/nrp/gwsoftware/modflow2000/modflow2000.html>

Li, Zhen, Faunt, C.C., Pavelko, M.T., Moreo, M.T., Justet, L., Belcher, W.R., and Spengler, R.W., in review, Death Valley Regional Flow System Model: Conversion from MODFLOW-2000 to MODFLOW-2005 and UCODE 2005 and Update with water-level and pumping data through 2003: U.S. Geological Survey Open-File Report xx-xx, xx p.

Mehl, S.W. and Hill, M.C., 2005, MODFLOW-2005, The U.S. Geological Survey modular ground-water model—Documentation of shared node local grid refinement (LGR) and the boundary flow and head (BFH) package: U.S. Geological Survey Techniques and Methods 6-A12, 68 p.

- Moreo, M.T., Halford, K. J., La Camera, R.J., and Lacznik, R.J., 2003, Estimated ground-water withdrawals from the Death Valley regional flow system, Nevada and California, 1913–98: U.S. Geological Survey Water-Resources Investigations Report 03–4245, 28 p.
- Moreo, M.T., and Justet, Leigh, 2008, Update to the Ground-Water Withdrawals Database for the Death Valley Regional Ground-Water Flow System, Nevada and California, 1913–2003: U.S. Geological Survey Data Series 340, 10 p.
- Pavelko, M.T., in review, Ground-Water-Level Database for the Death Valley Regional Ground-Water Flow System, 1907–2007, Nevada and California: U.S. Geological Survey Data Series xxx, xx p.
- Poeter, E.P., Hill, M.C., Banta, E.R., Mehl, Steffen, and Christensen, Steen, 2005, UCODE\_2005 and Six Other Computer Codes for Universal Sensitivity Analysis, Calibration, and Uncertainty Evaluation: U.S. Geological Survey Techniques and Methods 6-A11, 283 p.
- San Juan, C.A., Belcher, W.R., Lacznik, R.J., and Putnam, H.M., 2004, Hydrologic Components for Model Development, in Belcher, W.R., ed., Death Valley regional ground-water flow system, Nevada and California—Hydrogeologic framework and transient ground-water flow model: U.S. Geological Survey Scientific Investigations Report 2004-5205, p. 99 - 136. On-line at: <http://water.usgs.gov/pubs/sir/2004/5205/>
- Spitz, F.J., 2001, Method and computer programs to improve pathline resolution near weak sinks representing wells in MODFLOW and MODPATH ground-water-flow simulations: U.S. Geological Survey Open-File Report 00-392, 41 p. On-line at: <http://nj.usgs.gov/publications/OFR/00-392/ofr00-392.pdf>

**APPENDIX B**  
**DESCRIPTION OF *EIS\_UZ\_TIMESTEP\_RESOLUTION\_FRACTIONAL\_BASIS.XLS***  
**WORKSHEET**

INTENTIONALLY LEFT BLANK

## **WORKBOOK NOTES ARE PROVIDED IN SUBSHEET: “WORKBOOK NOTES”**

For each of the 31 species of interest, the results for downstream calculations are tabulated in cell A2:J25, with calculation notes in rows 26 through 28. An original sheet was developed for  $^{14}\text{C}$ . The calculations were verified using two other techniques and then this sheet was replicated 30 more times, each time replacing the input data with appropriate values for other radionuclides.

**A1:** Identify source model.

**H1:** Identify radionuclide.

**J1:** Identify release location.

**Cells A4 through J24:** These cells repeat calculated values that are determined elsewhere in the sheet.

Tabulated headers and footers in rows 2 and 25 are updated based on the text entered into cells A1, H1, and J1. The identifying text should be added into these cells.

**Columns P through V:** Paste GoldSim output into row 2. GoldSim output is the time history for the mean, lower bound, 5th-percentile, median, 95th-percentile, and upper bounds of cumulative release for the radionuclide specified in cell H1 for the location specified in cell J1 of the model specified in cell A1.

**Column W:** Repeats time values in time history data from Column P.

**Column X:** Calculates fraction of mean cumulative release at each time step using Equation 1.

**Column Y:** Specified list of target fractions for outputting time steps.

**Column Z:** Performs a look-up into the calculated cumulative release fraction of columns W and X. Result for each row is the time from the GoldSim input data that has a cumulative release fraction that is closest to and less than or equal to the target fraction specified on the same row.

**Column AA:** Checks to see if any time points are repeated in Column Z. Repeated time steps indicates that the input time history data increases by more than one of the specified cumulative release fraction increments between sequential time steps.

**Column AB:** Repeats look-up table results of times from Column Z.

**Column AC:** For each row, looks-ups the time value in the same row of Column AB in the pasted in GoldSim history (Column P) and reports back the mean cumulative release value for that row (Column Q).

**Columns AD through AH:** Repeats the look-up operation of Column AC for lower bound (Column R), 5th-percentile (Column S), median (Column T), 95th-percentile (Column U), and upper bound ((Column V) of cumulative releases.

**Column AI:** Calculates the duration between time steps reported in Column AB (which is from Column Z). This is the time step length over which cumulative releases increased between values reported in Columns AC through AH. The first row calculates the difference from 0 years, the start of the run.

**Column AJ through AO:** Calculates the increase in the cumulative release between time steps reported in Column AB. This is the amount of mass that exited the system over the time step length in Column AI. Columns are in sequence with the statistical quantity reported in Columns AC through AH. The first row calculates the difference from 0 grams, the cumulative release value at the start of the run.

**Column AP:** Repeats the time step value from Column Z.

**Column AQ through AV:** Calculates the average release rate over the specified time interval using Equation 2. Columns are in sequence with the statistical quantity reported in Columns AC through AH. The first row calculates the difference from 0 grams, the cumulative release value at the start of the run.

**APPENDIX C**  
**POSTPROCESSING OF MODPATH V5.0-GENERATED HYDRAULIC HEAD**  
**CONTOURS**



Hydraulic head contours were generated as DXF files for Layers 1 to 4 using MODPATH V5.0 with MODFLOW 2000-simulation results for Cases 1 and 2. The MODFLOW simulations are described in Section 3.1. These DXF files were uniformly scaled up from plotted dimensions to real world coordinates, and then moved to their position in the NAD27 UTM zone 11 coordinate system. The scaling factor is 51522.6601 for X and Y directions. The resulting files were saved as a new set of DXF files, and were used to overlay with the base map (*basemap\_full.srf*) for generating Figures 3 to 7. File: *basemap\_full.srf* was prepared with topographic information available from the USGS web site for the Death Valley regional flow model (<http://rmgsc.cr.usgs.gov/dvrfsIntro/>).

INTENTIONALLY LEFT BLANK